Aus dem Zentrum für Infektiologie-Abteilung Virologie der Universität Heidelberg

(Geschäftsführende Direktor:

Prof. Dr. med. Dr. h.c. Hans-Georg Kräusslich)

Investigation of the crosstalk of different interferon lambdas and lambda-related cytokines in the JAK/STAT pathway

Inauguraldissertation

zur Erlangung des Doctor scientiarum humanarum (Dr. sc. hum.)

an der

Medizinischen Fakultät Heidelberg

der

Ruprecht-Karls-Universität

vorgelegt von

Cuncai Guo

aus

Anhui, China

2022

Dekan: Herr Prof. Dr. med. Dr. h.c. Hans-Georg Kräusslich

Doktorvater: Herr Prof. Dr. med. Dr. h.c. Hans-Georg Kräusslich

Contents

List of Tables

List of figures

1 Introduction

1.1 Human and mouse intestine, structure and functions

1.1.1 Structure of human and mouse intestine

1.1.1.1 Human intestinal structure, components, different sections, and functions

The human intestine mainly consists of two organs, the small intestine, and the large intestine. The gastrointestinal (GI) tract or "the gut" performs all digestive functions (Figure 1-1). The human small intestine contains three sections: duodenum, jejunum, and ileum from stomach to large intestine (Figure 1-1) (Helander and Fändriks 2014). The primary functions of the small intestine are secretion and absorption. By contrast, the human large intestine contains four sections: cecum, colon, rectum, and anus (Figure 1-1). The main functions of human large intestine are absorption of nutrients and water, synthesizing of vitamins, as well as forming and eliminating feces from the body.

The cross-sectional structure of the human intestine consists of four layers: mucosa, submucosa, muscular layer, and adventitia (Figure 1-1) (Collins and Bhimji 2017). The mucosa and submucosa constitute numbers of folds called plicae, which contains microvilli and further expends the surface area and increases absorption (Turiccki 2021). The muscular layer contains two smooth muscle layers, between which the myenteric plexus lies. The adventitia is composed of loosely arranged fibroblasts and collagen and the vessels and nerves pass through the adventitia (Turiccki 2021).

The gastrointestinal tract is also home to the intestinal microbiome. The microbiome can synthesis vitamins and short chain-fatty acids (SCFAs), providing numerous nutrition to the host (Kau, Ahern et al. 2011). Moreover, the microbiome also contributes to gut development and the fulfillment of the intestinal immune system (Hooper 2004). The interaction between the intestinal immune system and the microbiome is vital in maintaining mucosal homeostasis. In general, the human intestine harbors trillions of bacteria which are from daily food. The bacteria can secret metabolites which serve as bioactive compounds. These bioactive compounds play a role in regulating the body metabolic homeostasis and organ physiology (Forkosh and Ilan 2019). The complex relationship between the host immune system and the microbiota affects body functions that relate to other organs, which serves as an "axis" between host and microbiota. The host-microbe metabolic axis acts as a

multifunctional communication system between distinct microbes and the host cellular pathways. Among the axis, various microbial species produce bile acids, choline, and short-chain fatty acids (SCFAs) to modulate metabolic reactions in human body, which is critical for the host health (Nicholson, Holmes et al. 2012). These microbial metabolites promote the host metabolic response and possibility of disease development (Clemente, Ursell et al. 2012). Additionally, the dietary changes or environmental stresses can influence the dynamic and flexible components of microbiota and change the species or composition, resulting in the change in the health or disease risk (Clemente, Ursell et al. 2012). Therefore, signals from metabolites and components of microbiota and induced by microbiota in intestinal epithelial cells (IECs) or intestinal dendritic cells play a critical role in the host physiological and pathophysiological functions (Rogler and Rosano 2014).

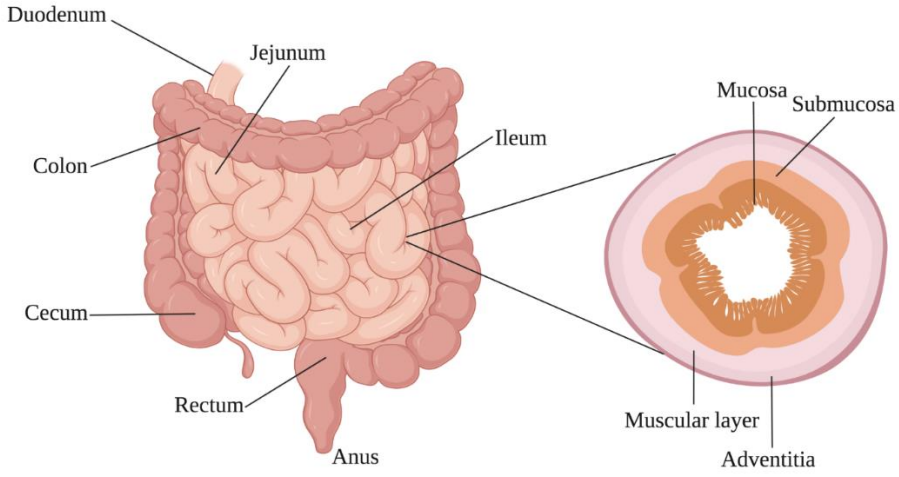

Figure 1-1. Schematic of the human small and large intestines. (left) Human intestine contains the small intestine and large intestine. The human small intestine consists of duodenum, jejunum and ileum, while the human large intestine contains colon, cecum, rectum and anus. (Right) The cross-section of human intestine contains mucosa, submucosa, muscular layer and adventitia from outside to inside.

1.1.1.2 Mouse intestine and its difference with human intestine

Mouse and human are anatomically similar in their gastrointestinal structure. Precisely, mouse and human have similar ratio of intestinal surface area: body surface area (Casteleyn, Leliaert et al. 2010). Mice intestinal villi is taller than human villi, which increases the surface area of the mouse small intestine and is considered as a compensation mechanism for the lack of mucosal folds in the mouse intestine. Additionally, the mouse cecum is relatively large to its total (GI) and is vital to ferment plant materials and produce vitamin K and B. These morphological differences allow mice to extract nutrients from indigestible food in their diet. Above all, the mammalian digestive tract is very conserved with diet driving major difference between species.

1.1.1.3 Intestinal epithelium, cellular component, immune response

The intestinal epithelium is lined by a monolayer of cells which are composed of multiple cell types (Helander and Fändriks 2014) (Figure 1-2). These cell types form a columnar shape which includes crypts and villi at multiple scale, and microvilli at the subcellular level (García-Peñalvo 2018). This columnar structure can optimize surface areas for absorbing nutrient and maintaining a barrier to the outside (Helander and Fändriks 2014), and serves as a first line of defense against invading pathogens (Stanifer, Pervolaraki et al. 2019).

The gastrointestinal tract is in constant contact with a large and varied microbial community (also called microbiota) (Vereecke, Beyaert et al. 2011), but it also harbors a large variety of immune cells and physiological formation to maintain intestinal homeostasis against microbial challenge (Abreu 2010). The microbiota set up symbiotic relationships with their hosts, playing a key role in mammalian metabolism. Regardless of the symbiotic nature, the close relationship between a dense microbiota and intestinal tissues still poses a serious threat to human health. This threat from microbiota can lead to breakdown of symbiotic host-microbiota relationship and cause pathologies like chronic inflammation or bacteraemia. Nevertheless, the fact is that inflammation and systemic diseases due to pathogens are rare in immunologically healthy individuals, suggesting that intestinal immune system effectively restricts side effects from the microbiota. The intestinal immune can directly limit bacterial contact with epithelial cell surfaces, boost quick detection and elimination of invading pathogens, establishing a stable symbiotic relationship (Hooper and Macpherson 2010).

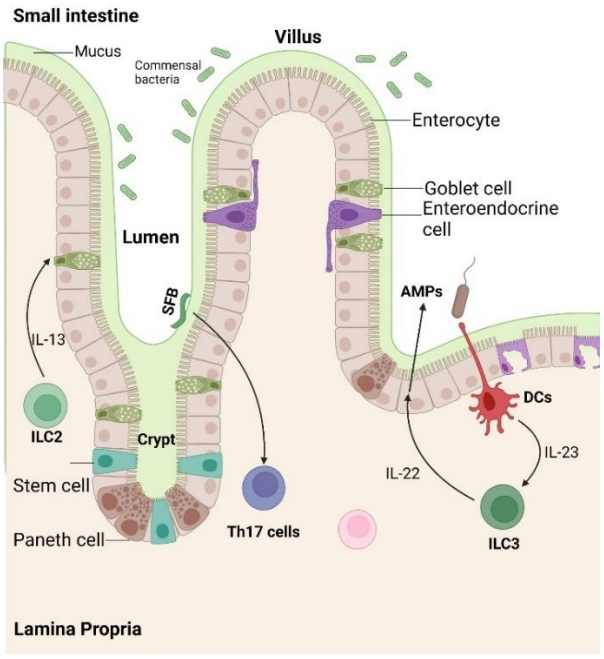

Figure 1-2. Schematic diagram of the human intestinal epithelium. The epithelium surface consists of finger-like protrusions, villi and gland-like invaginations, crypts. Several kinds of distinct cell types form the consistent monolayer of the epithelium. The epithelium separates the gut lumen from the lamina propria. Cells in the epithelium renew every three days. Adapted from (Abreu 2010)

Cell types and its functions

To better exhibit the intestinal digestion and absorption, the intestinal epithelium monolayer consists of several unique cell types: the enterocytes, goblet cells, enteroendocrine cells, tuft cells, microfold cells and Paneth cell (Figure 1-2). In addition to the monolayer, the intestinal tissue contains immune cells such as intraepithelial lymphocytes (IELs), innate lymphoid cells (ILCs), and Th17 cells.

Enterocytes

Enterocytes are the main epithelial cells in the intestine. These cells are polarized with an apical side facing the lumen of the gut and a basolateral side facing the *lamina propria*. These two sides are separated by tight junctions. Enterocytes can take up and absorb food nutrients and luminal antigens through fluid-phase endocytosis (Snoeck, Goddeeris et al. 2005). They also play a role in fighting against invading pathogens. To achieve this function, enterocytes express different pattern recognition receptors to recognize microbiota, participating in immunological surveillance and direction of host responses in the gut. Therefore, with inflammatory stimulation, enterocytes can produce chemotactic factors to stimulate both myeloid and lymphoid cells (Yang, Eckmann et al. 1997). Interleukin-17 (IL-17) stimulates epithelial cells to produce neutrophil chemokines (Awane, Andres et al. 1999). Additionally, epithelial cells can directly defend microbial populations through producing anti-microbial peptides in the gut (Iimura, Gallo et al. 2005).

Goblet cells

Goblet cells are located among the layer of absorptive enterocytes. They produce mucus which spreads above the layer of epithelial cells and contains bacterial metabolites like butyrate (Biancheri, Di Sabatino et al. 2013). Butyrate is critical in pluri-functional intestinal cells and helps to control intestinal metabolism. In addition, butyrate could promote the treatment of some gastrointestinal disorders (Leonel and Alvarez-Leite 2012). Furthermore, the mucus layer is a key barrier in the intestinal and acts to block microbial contact with epithelial cells (McDermott and Huffnagle 2014).

Tuft cells

Tufts cells are rare chemosensory epithelial cells and act as a main cell line of the small intestinal response to parasites and protists (Gerbe, Sidot et al. 2016, Howitt, Lavoie et al. 2016, Von Moltke, Ji et al. 2016). The tuft cells are the source of IL-25 which plays a critical role in intestinal immunity. In addition, they are critical for type 2 immune circuits associated

with group 2 innate lymphoid cells (ILC2s) and crypt stem cells (Gerbe, Sidot et al. 2016, Howitt, Lavoie et al. 2016, Von Moltke, Ji et al. 2016).

Enteroendocrine cells

Enteroendocrine cells are believed to derive from intestinal stem cells (Gribble and Reimann 2016). They are found in the epithelial layer of the intestinal tract and contain microvilli-covered apical surfaces which directly keep contact with the luminal constituents (Gribble and Reimann 2016). The enteroendocrine system determines how the host is responsive to the ingestion of nutrients and secrets a diversity of hormones to regulate physiological responses within and outside the gut (Gribble and Reimann 2016).

Microfold cells

Microfold (M) cells are composed of 10% of the epithelial cells within the follicle-associated epithelia (FAE) (Mabbott, Donaldson et al. 2013). They contain a reduced glycocalyx, irregular brush border and reduced microvillus which are unique morphological features for M cells. In addition, M cells are critical for the phagocytosis and transcytosis of macromolecules, antigens and pathogenic or commensal microorganisms in the gut lumen (Mabbott, Donaldson et al. 2013). Also, M cells can express receptor molecules for some pathogenic microorganisms in the gut (Mabbott, Donaldson et al. 2013).

Paneth cells

Paneth cells are a kind of specialized secretory cells which are the main source of antimicrobial peptides in the intestine (Porter, Bevins et al. 2002, Wehkamp, Fellermann et al. 2005, Ouellette 2010). Paneth cells secrete molecules to fight against enteric bacterial pathogens in the small intestine (Bevins and Salzman 2011). In addition, the products produced by paneth cells establish and maintain the intestinal microbiota for homeostasis (Salzman, Hung et al. 2010).

Intraepithelial lymphocytes (IELs)

Intraepithelial lymphocytes (IELs) reside within the epithelium. IELs adheres to IECs, which are mediated by crosstalk between E-cadherin on the epithelial cells and CD103 on IELs. IELs are activated by stimulation and express effector cytokines, like keratinocyte growth factor (KGF), interferon-γ (IFN-γ) and tumour necrosis factor-α (TNF-α) (McDermott and Huffnagle 2014). KGF is reported to promote localized epithelial cell proliferation and differentiation and protect the epithelium from damage during colitis induced by chemicals (Chen, Chou et al. 2002), whereas IFN-γ and TNF-α were reported to promote pathologic

activity related to the progress of inflammatory bowel disease (IBD) (Simpson, Holländer et al. 1997).

ILCs

Innate lymphoid cells (ILCs) are distributed in mucosal surfaces to initiate immune response, maintain mucosal integrity, and contribute to lymphoid organogenesis (Diefenbach, Colonna et al. 2014, Eberl, Colonna et al. 2015). Immature ILCs develop in bone marrow from common lymphoid progenitor, and they generally migrate to mucosal tissues, but can also be found in other lymphoid tissues such as spleen and lymphoid nodes and other non-lymphoid organs skin, liver, brain, and pancreas. ILC differentiation process is similar in humans and mice (Stojanović, Saksida et al. 2021). ILCs can be classified by the transcription factors (T-bet, GATA3, or RoRγt) and cytokines (such as IL-13, IL-22 or IFN-γ) they differently express. They have three main subtypes: ILC1, ILC2 and ILC3. Precisely, ILC1 cells are specialized for secreting interferon-γ (IFN-γ) when they are responsive to interleukin-12 (IL-12), IL-15 and IL-18 (Wang, Cao et al. 2017). ILC2 cells can produce IL-5, IL-9, and IL-13, which belong to type 2 T helper (Th2) cell cytokines, when they respond to IL-25 and IL-33 (Brestoff, Kim et al. 2015). ILC3 cells generate IFN-γ, IL-17 and IL-22 when stimulated with IL-1β and IL-23 (Klose, Kiss et al. 2013). All the cytokines play a role in immune response and mucosal integrity.

Th17 cells

Intestinal Th17 cells are generated when the host is responsive to intestinal microbes, such as segmented filamentous bacteria (SFB) and some extracellular pathogens (Ivanov, Atarashi et al. 2009). Th17 cells generate IL-17, IL-17F and IL-22, which protect the host from bacterial and fungal infections at mucosal surfaces (Ivanov, Atarashi et al. 2009).

1.1.2 Microbiota and homeostasis

Microbiota regulates the immune system. For example, a capsular polysaccharide on the surface of commensal bacterium, called polysaccharide A (PSA) can be recognized by TLR2. Activated TLR2 regulates the induction of regulatory T cells, which drives the production of anti-inflammatory cytokine IL-10 (Round and Mazmanian 2010). In addition, commensal bacteria modulate the activity of NF-κB to downregulate the production of pro-inflammatory cytokines in the gut (Kelly, Campbell et al. 2004). The microbiota also maintains the innate immunity tone of the gut by inhibiting colonization and overgrowth of pathogens. It was reported that commensal flora stimulates TLR signalling in paneth cells

and epithelial cells, inducing the production of the antimicrobial lectin regenerating islet-derived protein 3γ (REG3γ) (Vaishnava, Behrendt et al. 2008). Cytokines activated by commensal bacteria are important regulators of host mucosal response. For example, IL-23 can trigger the production of IL-17 and IL-22, which control the mucosal response to enteric pathogens. IL-17 employs two mechanisms to confer protection against enteric pathogens, maintaining intestinal barrier functions. First, IL-17 amplifies the expression of CXC-chemokines to promote the gut to recruit neutrophils. Second, IL-17 can cooperate with IL-22 to upregulate antimicrobial proteins and defensins (Blaschitz and Raffatellu 2010). IL-22 can also be highly induced upon enteric pathogen infection. IL-22 greatly induces epithelial cells to produce antimicrobial proteins in the intestinal mucosa.

1.1.3 Hypoxic environment in the intestine

Intestinal epithelial cells are located in between an anaerobic lumen (pO2 < 10%, 71 mmHg) and a highly metabolic lamina propria , leading the cells to be exposed to a steep physiologic oxygen gradient (Colgan and Taylor 2010, Singhal and Shah 2020) (Figure 1-3). For reference, breathable air at sea level has a pO_2 of 140-150 mmHg (21% pO_2) (Zheng, Kelly et al. 2015). Oxygen level in the healthy lung alveolus is about 100-110 mmHg (Schaible, Schaffer et al. 2010). By contrast, the luminal side of the healthy intestine can be as low as 10 mmHg (2% pO_2) of pO_2 (Albenberg, Esipova et al. 2014, Singhal and Shah 2020). This low-level environment is also named physiologic hypoxia and has vital effects on intestinal functions (Zheng, Kelly et al. 2015). The oxygen level drops gradually along the radial axis from the intestinal submucosa to the lumen (Zheng, Kelly et al. 2015) (Figure 1-3).

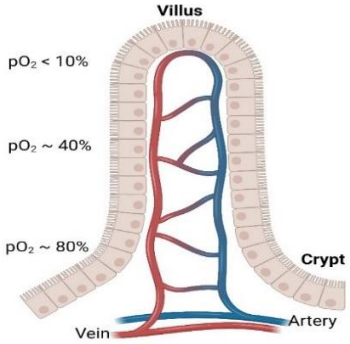

Figure 1-3. A model of blood flow dynamics in the healthy intestinal mucosa. Counter-current blood flow decreases local pO_2 along the crypt-villus axis and causes low pO_2 at the tip villus. Adapted from (Zheng, Kelly et al. 2015)

Hypoxic condition in epithelium leads to the activation of hypoxia-inducible factor (HIF). HIF signal regulates oxygen homeostasis by promoting oxygen delivery and adapting oxygen deprivation in cells, for example IECs (Semenza 2012). The HIF signaling pathway is strongly associated with tissue barrier function and metabolic pathway in human intestinal epithelial cells. Importantly, miRNA-320a was identified to play a role in regulating barrier

function in human IECs and this miRNA was HIF dependent, which links hypoxia with epithelial homeostasis (Muenchau, Deutsch et al. 2019).

1. 2 Interferons

1.2.1 Introduction to Interferons

Interferons (IFNs) were first discovered to inhibit virus infection in 1950s by Isaacs and Lindenmann (Isaacs and Lindenmann 1957). Since then, many studies have brought to light the classification, molecular details, and functions of IFNs. IFNs are a family of cytokines that include three types: I, II, and III. In humans, type I IFN comprises 13 IFN-α genes, single genes for IFN-β, ε, κ, and ω (Stanifer, Guo et al. 2020). All 17 types I IFNs share a heterodimeric receptor complex consisted of a single chain of IFNAR1 and IFNAR2. IFNAR1 and IFNAR2 are widely expressed in all nucleated cells (Gibbert, Schlaak et al. 2013). In contrast to the type I IFN family, the type II IFN family consists of a single member, IFN-γ, which is mainly secreted by immune cells (Schroder, Hertzog et al. 2004). IFN-γ receptors are composed of two subunits of IFNGR1 and IFNGR2, and, have broad tissue distribution. Thus, nearly all cell types can be responsive to IFN-γ (Schroder, Hertzog et al. 2004). Type III IFNs, also named interferon lambda (IFN-λ), include four members, IFN-λ1, IFN-λ2, IFN-λ3 and the newly discovered member IFN-λ4 (Kotenko, Gallagher et al. 2003, Prokunina-Olsson, Muchmore et al. 2013). IFN-λs signal through a heterodimeric receptor complex composed of a single chain of IFNLR1 and IL10R2. IL10R2 is also part of the IL-10 receptor family which consist of IL-10, IL-22, and IL-26 receptors. IL10R2 is widely expressed in all cell types, whereas IFNLR1 is strictly distributed to epithelial cells (Sommereyns, Paul et al. 2008). Therefore, many cell types respond poorly, or not at all, to type III IFNs. Once IFNs bind to their receptors on the cell surface, they initiate a complex signaling cascade, finally leading to the induction of interferon stimulated genes (ISGs).

1.2.2 IFN induction pathways

The host innate immune system provides the first line of fighting against microbial invasion. The host defence signal cascade is triggered by cellular sensors that recognize pathogen molecules and switch on the production of host defence genes, such as IFNs (Barber 2011). Vertebrates have two complementary systems to detect and counteract invading pathogens: the intrinsic and circulating immune systems. The intrinsic innate immune system employs

several germline-encoded receptors called pattern-recognition receptors (PRRs) to recognize pathogen-associated molecular patterns (PAMPs). PAMPs are conserved molecular structures present on pathogens such as viral genomes and intermediate products, which are recognized by the (retinoic acid-inducible gene I) RIG-like receptors (RLRs) and Toll-like receptors (TLRs) (Figure 1-4). Once PRRs are activated, they can recruit different adapter proteins, such as myeloid differentiation primary response 88 (MyD88), TIR-domain-containing adapter-inducing interferon-β (TRIF), and mitochondrial antiviral-signalling protein (MAVS) to transmit upstream signal to downstream molecules (Chow, Gale Jr et al. 2018).

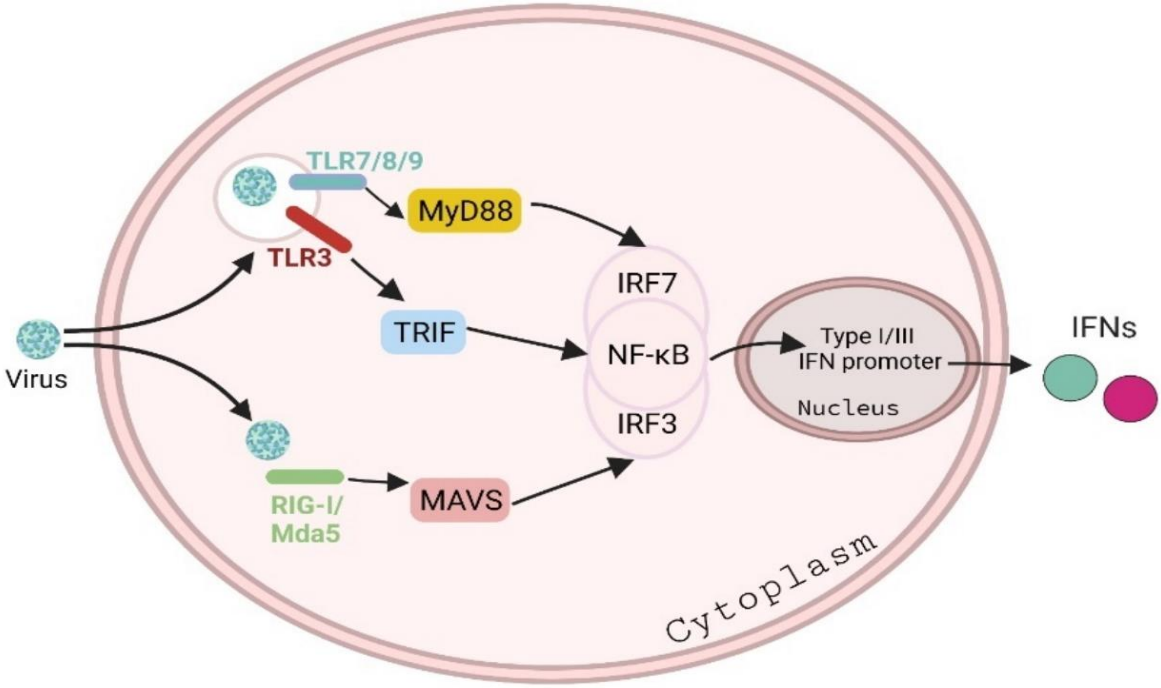

Figure 1-4. Induction of type I and III IFN upon viral infection. Viral products are recognised by intracellular pattern recognition receptors (PRRs), located in the cytoplasm such as RIG-I or MDA5 or on the endosomes like TLR3, 7, 8 and 9. Activated PRRs mediate the production of IFNs through different kinds of signalling pathways involving the IRFs and the NF-κB. Adapted from (García-Sastre and Biron 2006)

The RLRs contain three members, which are RIG-I, melanoma differentiation- associated gene 5 (MDA5) and laboratory of genetics and physiology 2 (LGP2). The RIG-I and MDA5 are mainly responsible for detecting the viral RNA from RNA viruses in the cytosol, and LGP2 is reported to regulated RIG-I and MDA5 signalling during the recognition of viral RNA. In normal condition, RLRs are ubiquitously expressed in most cell types at low levels. The expression of RLRs is rapidly induced by virus infection or interferon stimulation. Following RLR activation, MAVS assembles into prion-like aggregates to recruit E3 ubiquitin ligases and TNF-receptor associated factor 2 (TRAF2), TRAF3 and TRAF6 to form a "signalosome".

This complex mediates the phosphorylation and nuclear translocation of transcriptional factors IRF3 and IRF7 and the activation of NF-κB to induce the expression of type I and III IFNs, proinflammatory cytokines and chemokines, which cooperate to combat virus infections.

TLR family are conserved transmembrane proteins. Currently 10 human TLRs have been described, of which TLR3, TLR7, TLR8 and TLR9 are capable of sensing RNA during virus infection (O'neill, Golenbock et al. 2013) (Figure 1-4). Activated TLR3 signals through TIR-domain-containing adapter-inducing interferon-β (TRIF) to activate IRF3 and NF-κB to produce interferons, proinflammatory cytokines and chemokines. In contrast, activated TLR7 and TLR8 signal through myeloid differentiation primary response 88 (MyD88) adaptor which initiates signalling cascades resulting in activation of NF-κB for the induction of proinflammatory cytokines and IRF5 and/or IRF7 to produce interferons.

1.2.3 IFN Signaling Pathways

Type I and III IFNs bind to distinct receptors in an autocrine (secreting cells) or paracrine way (bystander cells) to tigger the IFN signalling pathways. IFNs first bind to one receptor chain with high affinity (IFNAR2 or IFNLR1), and subsequently recruit the low-affinity chain (IFNAR1 or IL-10Rβ) to form a signalling-competent ternary complex. Upon binding, upstream signal passes through the extracellular domain of the receptors to the intracellular domain, causing receptor dimerization and inducing conformational change of the receptors. The conformational change triggers receptor-associated Janus kinases (JAK), Tyk2 and JAK1, to mediate the phosphorylation of tyrosine residues on the intracellular part of IFN receptors (Figure 1-5). Activated IFN receptors recruit signal transducer and activator transcription (STAT) proteins, which subsequently are phosphorylated by JAKs. Tyrosine-phosphorylated STATs form heterodimers and assembly with IRF9, forming a trimolecular complex transcription factor called interferon-stimulated gene factor 3 (ISGF3). ISGF3 translocates to the nucleus and binds to its cognate DNA sequences, interferon-stimulated response elements (ISREs; consensus sequence TTTCNNTTTC), driving the transcription of interferon stimulated genes (ISGs) (Kotenko, Rivera et al. 2019). Distinct from the formation of heterodimers of STATs, IFNs can also induce the homodimerization of STATs (such as STAT1). STAT1 homodimers translocate to the nucleus and bind to the gamma activated sequence elements (GAS; consensus sequence TTC/ANNNG/TAA) promoter, inducing the production of pro- or anti-inflammatory genes (Morris, Kershaw et al. 2018).

ISG-encoded proteins can inhibit viral transcription, translation, and replication, and degrade viral nucleic acids, and alter cellular lipid metabolism to control the spread of invading pathogens (MacMicking 2012). As type I and III IFNs employ the same signalling pathway, it is reasonable to speculate they have overlapping functions. However, type III IFNs exhibit their unique functions in mucosal immunity, immunomodulatory effects of adaptive immunity, anti-tumor and autoimmunity.

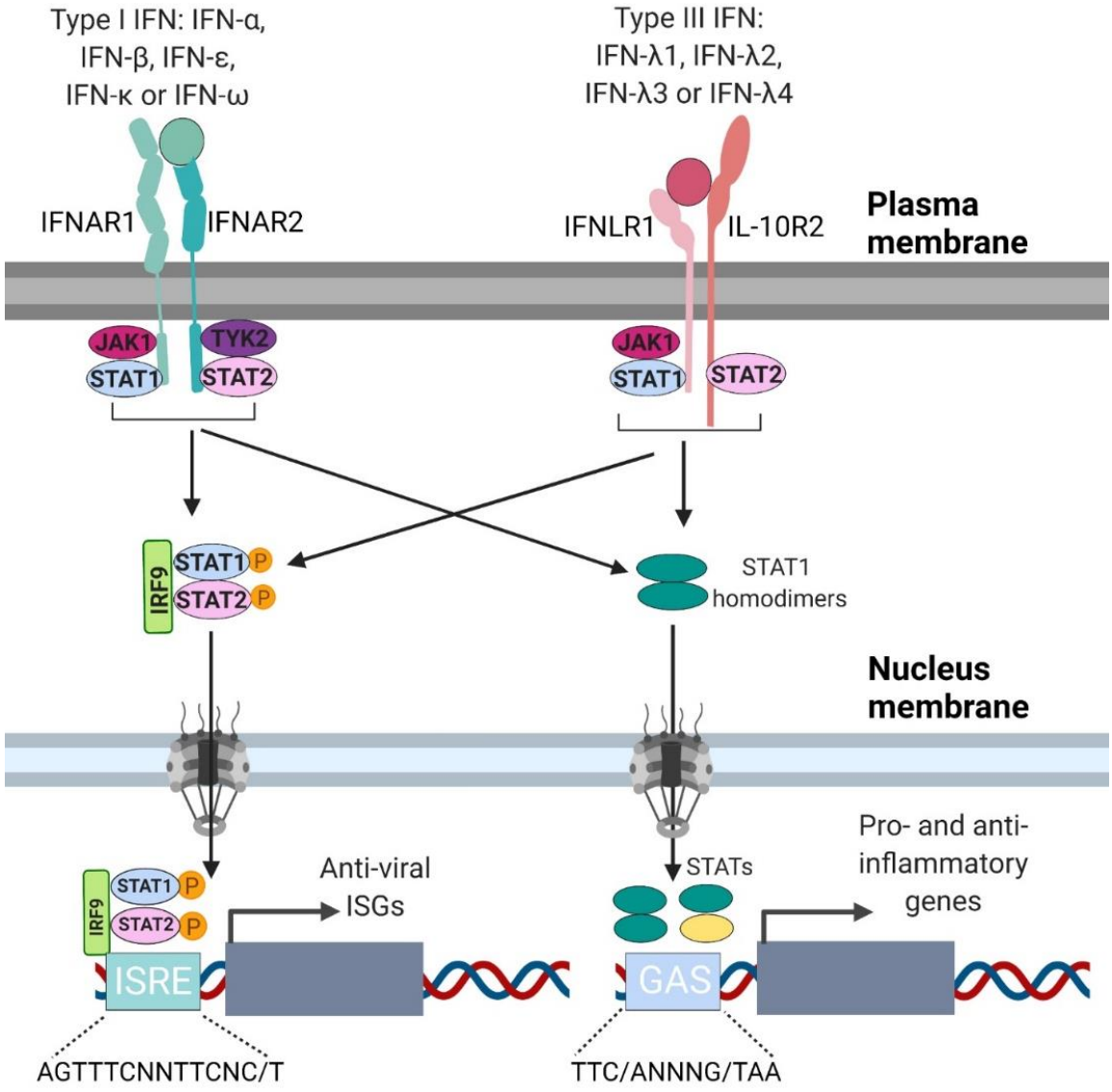

Figure 1-5. Classic type I and III IFN signaling pathway. Type I and III IFNs signal through different heterodimeric receptors, which result in the activation of the same JAK/STAT pathway. Following receptor activation, phosphorylated STAT1/STAT2 recruits IRF9 and form the ISGF3 complex. The complex translocates into nucleus and induces the production of hundreds of interferon-stimulated genes (ISGs). IFNs can also trigger the production of STAT1 homodimers. Activated STAT1 homodimers can translocate into nucleus and bind to the promoter GAS, inducing the production of pro- or anti-inflammatory genes. Adapted from (Morris, Kershaw et al. 2018)

1.2.4 IFN-III and mucosal immunity

IFN-λ favours the protection for mucosal surfaces against virus infections due to the preferential expression of IFNLR1 at mucosal tissues. Distinct functions of type I and III IFNs have been described in the gastrointestinal (GI) tract. Murine intestinal epithelial cells are shown to express higher levels of IFNLR1 and lower levels of IFNAR1 and IFNAR2 than immune cells in the lamina propria (Mahlakoiv, Hernandez et al. 2015). Loss of the IFNLR1 receptor leads to the increase in virus infection, while loss of the IFNLAR receptor shows little change in enteric virus infection, which leads to the model that IFNLR1 is critical to control the spread of several enteric viruses such as rotavirus, reovirus and norovirus infections in the gut (Pott, Mahlakõiv et al. 2011, Nice, Baldridge et al. 2015, Lin, Feng et al. 2016). It was identified that IECs are the dominant IFN-λ-responsive cells to control enteric virus in a knockout mice model. The expression of *Ifnlr1* is necessary for IECs to respond to IFN-λ in control of mouse norovirus (MNoV) and reovirus infection (Baldridge, Lee et al. 2017). By contrast, studies on the mouse intestine have demonstrated an age dependent on IFNs. Adult mice have epithelium cells that are responsive to type III IFN, but sulking mice are sensitive to both type I and III IFNs (Lin, Feng et al. 2016). It was reported that both adult and neonatal mice absent of IFN-λ receptors are vulnerable to oral rotavirus infection, whereas animals absent of receptors for type I IFN are like wild-type mice. Using Mx1 reporter for IFN responsiveness, subsequent work demonstrates that prime target cells of rotavirus, the epithelial cells are strongly responsive to IFN-λ but marginally responsive to type I IFN *in vivo* (Pott, Mahlakõiv et al. 2011).

Both IFNAR and IFNLR1 could control infections of enteric viruses (Pervolaraki, Rastgou Talemi et al. 2018, Pervolaraki, Guo et al. 2019). Recently, human intestinal enteroids (HIEs) have been shown to support the replication of human noroviruses (HuNoVs) and be excellent models to study HuNoV-host interactions. It was verified that type III IFNs instead of type I IFNs were elevated in HIEs after infection, suggesting the important role of IFN-λ in HuNoV-host interactions (Lin, Han et al. 2019). The latest studies show that human intestinal epithelial cells and human intestinal organoids support SARS-CoV2 replication and IFN-λ can control SARS-CoV-2 infection in human intestinal epithelial cells (Lamers, Beumer et al. 2020, Stanifer, Kee et al. 2020). Another group confirms that IFN-λ shows antiviral activity against SARS-CoV-2, while type I IFN inhibits SARS-CoV-1 replication (Felgenhauer, Schoen et al. 2020).

Compared to IFN-λ-specific responsiveness of intestinal epithelial cells, respiratory tract epithelial cells are responsive to both type I and III IFNs (Lazear, Schoggins et al. 2019). It was demonstrated that both *Ifnar1*$^{-/-}$ and *Ifnlr1*$^{-/-}$ mice are more susceptible respiratory viruses, suggesting that both type I and III IFNs can restrict respiratory replication in mice and respiratory epithelial cells (Wells and Coyne 2018). Studies in the lower respiratory tract infected by influenza A virus (IAV) demonstrate that both type I and III IFN exhibit protection against IAV (Jewell, Cline et al. 2010, Mahlakoiv, Ritz et al. 2012, Crotta, Davidson et al. 2013). Subsequent studies determine that type III IFNs mainly control virus infection in the upper respiratory tract, whereas type I and III IFNs have redundant functions in inhibiting respiratory virus in the lower respiratory tract (Klinkhammer, Schnepf et al. 2018).

1.2.5 IFN-III and adaptive immunity

The role of IFN-λ in adaptive immunity has been explored but the results are often controversial (Ye, Schnepf et al. 2019). It was reported that impaired CD8^{+} T cell and antibody responses were observed in IFNLR1.KO mice infected by a live-attenuated influenza virus. In this model, the virus induces the release of IFN-λ triggered M cells to produce thymic stromal lymphopoietin (TSLP) in the upper airways, which in turn, stimulates migratory dendritic cells and boosts antigen-dependent germinal centre reactions in draining lymph nodes. The IFN-λ-TSLP axis promotes the production of the immunoglobulins IgG1 and IgA.

In the inflamed intestine of a dextran sodium sulfate (DSS)-induced colitis mouse model, IFN-λ decreases the production of reactive oxygen species (ROS) and degranulation through specifically activating a translation-independent signalling pathway in neutrophils (Broggi, Tan et al. 2017). In another model of chronic intestinal inflammation, IFN-λs act directly on neutrophils to decrease the generation of ROS and their degranulation through a process mediated by JAK2 (Broggi, Tan et al. 2017). A latest study finds that IFN-λ contributes to systemic immune dysregulation in the skins and kidneys, which provides a unique role of IFN-λ in lupus immune-biology and tissue specific pathology (Goel, Wang et al. 2020). Some evidence also shows that IFN-λ promotes paneth cells death through STAT1 signalling in mice and is related to inflamed ileal tissue from patients with crohn's disease (Günther, Ruder et al. 2019). IFN-λ somehow also shows functions in antibacterial and antifungal immunity. Accordingly, IFNLR1$^{-/-}$ mice show higher fungal loads and emerged aggravated disease in the lungs and more severe fungal invasion in mice model of invasive aspergillosis with *Aspergillus fumigatus* (Espinosa, Dutta et al. 2017).

1.2.6 Different magnitude and pattern between IFN-I and IFN-III

Both type I and type III IFNs are produced at the transcriptional level but only type III IFNs are secreted in the supernatant when using viruses infect primary non-transformed human IECs (Pervolaraki, Stanifer et al. 2017). Human IECs can respond to both type I and III IFNs and produce ISGs that establish an antiviral state. However, the antiviral state established by type III IFNs strongly relies on the mitogen-activated protein kinase (MAPK) signaling pathway, suggesting that type III IFN employs a different pathway which is non-redundant compared to type I IFN (Pervolaraki, Stanifer et al. 2017). Type III IFN mediated signaling is demonstrated to be associated with a delayed and reduced pattern of ISGs induction compared to type I IFN in human intestinal epithelial cells and hepatocytes (Bolen, Ding et al. 2014, Pervolaraki 2018). Similar differences in the pattern of ISGs induction with type I and III IFN were also reported in murine intestinal and lung epithelial cells and immune cells as well as human primary keratinocytes, airway epithelial cells (Zhou, Hamming et al. 2007, Broggi, Tan et al. 2017, Galani, Triantafyllia et al. 2017). These kinetic differences are inherent to each signaling pathway and were shown to be independent of the corresponding IFN receptor levels in human IECs (Pervolaraki 2018).

1.2.7 Regulation of IFN signaling pathways

As IFN exhibits its host defence through a series of cellular and molecular events, the IFN signaling can be regulated at multiple levels, such as direct signaling molecules and epigenetic modification of gene expression program.

<u>Augmentation of IFN signaling</u>

The amplification of IFN signaling mainly attributes to several signaling molecules, such as STAT1 and IRF9, which are ISGs and induced by IFNs and other cytokines. Increased production of STAT1 results in its interaction with IFNAR, whereas increased IRF9 creates more ISGF3 which binds to target genes. Interestingly, low concentrations of IFNs induce increases in STAT1. Subsequently, STAT1 primes macrophages for enhanced responsiveness to IFNs at early infections. In addition, high levels of STATs and IRF9 expression can maintain the induction of a subset of ISGs for a prolonged period even though cytokines mediating this induction are absent (Ivashkiv and Donlin 2014). Additionally, secreted IFNs signals through JAK/STAT pathway to produce some transcriptional factors, such as cGAS, STING, RIG-I and IRF7. These factors act as a

positive feedback loop to enhance the induction of IFN-αs and IFN-λs, enabling a fast and strong host response.

Suppression of IFN signaling

To maintain tissue homeostasis, the host response is also controlled by negative regulators (Blumer, Coto-Llerena et al. 2017). Mechanisms suppressing IFN signaling usually are achieved by downregulating cell surface IFN receptor expression or inducing the production of negative regulators, such as ubiquitin carboxy-terminal hydrolase 18 (USP18) and suppressor of cytokine signaling (SOCS) proteins (Stanifer, Guo et al. 2020). p38 can also mediate priming phosphorylation of IFNAR, which helps the phosphorylation of the IFNAR mediated by casein kinase II (CK2), thus leading to the internalization, ubiquitylation and degradation of the receptor (Fuchs 2013). The suppression of IFN signaling by the negative regulators are introduced below:

USP18

USP18 (also called Ubp43) is one of IFN-induced genes and one member of ubiquitin-specific protease (USP) family. USP18 can reverse the ISG15-mediated conjugation process. USP18 has been reported to negatively regulate JAK/STAT signalling through competitively binding to IFNAR2 with JAK1 independent of de-conjugation of ISG15. In addition, USP18 was determined to bind to the IFNAR2 receptor subunit and block the interaction between JAK and the IFN receptor (Malakhova, Kim et al. 2006). Further studies demonstrate that USP18 mainly blocks IFN-α binding to the receptor complex (François-Newton, Magno de Freitas Almeida et al. 2011).

SOCSs

Type I IFN signalling is downregulated by suppressor of cytokine signalling 1 (SOCS1), SOCS3. It was reported that IFN-λ signalling is controlled by SOCS1 but not by SOCS3 (Blumer, Coto-Llerena et al. 2017). Precisely, SOCS1 inhibits JAKs activity by directly binding to the kinase inhibitory region (KIR) of JAKs. Notably, influenza virus inhibits the JAK/STAT signalling by producing SOCS1 and SOCS3, subverting host antiviral defence (Liu, Yan et al. 2019). In a study evaluating the potential of IFN-λ in chronic viral hepatitis, it was reported that overexpression of SOCS1 abolishes the mRNA expression of 2',5'-OAS and Mx1 induced by IFN-λ in hepatic cell lines (Brand, Zitzmann et al. 2005). On the contrary, IL-17A inhibits autocrine signalling loops by enhancing SOCS1 and SOCS3 expression, resulting in attenuating virus-induced IFN-λ in human airway epithelial cells (Niwa, Fujisawa et al. 2018). Notably, the negative regulators are also induced by other molecules that

activate JAK-STAT and MAPK pathways and by receptors sense fungal pathogens, such as dectin 1 (Goodridge and Underhill 2008). Therefore, pathogens that promote the induction of IFN negative regulators inhibit IFN signaling.

Epigenetic regulation of IFN signaling

The ISG induction by IFN requires chromatin remodeling, which furtherly mediates the recruitment of nucleosome-remodeling enzymes and histone acetyltransferases (HATs) through STAT1, STAT2 and IRF (Stark and Darnell Jr 2012). Therefore, events that affect these transcriptional factors furtherly regulate the epigenetic induction of IFN signaling through chromatin remodeling. It was demonstrated that genome enhancers can be activated by STAT1 during the differentiation or polarization of T cells and macrophages (Vahedi, Takahashi et al. 2012). Thus, STAT1 can change the epigenetic landscape, indicating the potential of IFNs in cell responses to subsequent stimuli. Another study shows that di-methylation of histone H3 at lysine 9 (H3K9me2) is identified as a negative regulator of IFNs and ISGs (Fang, Schaefer et al. 2012). It was shown that the abundance of H3K9me2 at IFN and ISG is inverse with the magnitude of IFN and ISG expression in fibroblasts and dendritic cells, thereby H3K9me2 controlling its abundance to regulate innate antiviral immunity (Fang, Schaefer et al. 2012). In addition, a transcriptional factor, p38, is a member of mitogen-activated protein kinase (MAPK) and is involved in IFN signaling. The inhibition of p38 results in diminished STAT1 Ser727 phosphorylation. P38 plays a key role in regulating STAT1 serine phosphorylation and transcriptional activity, further controlling the antiviral activity activated by IFNs (Goh, Haque et al. 1999).

1.3 IFN lambda 4

1.3.1 The discovery of IFN-λ4

The human IFN-λ family, IFN-λ1, IFN-λ2 and IFN-λ3 all exhibit more than 80% homology, but they only share about 30% homology with IFNλ4. The *IFNL4* gene was identified through sequencing of RNA samples extracted from primary human hepatocytes (PHH) which were treated with poly I:C (a synthetic double-stranded RNA) to imitate HCV infection (Prokunina-Olsson, Muchmore et al. 2013). IFN-λ4 is the newly discovered member of type III IFNs and was identified in 2013. The first report of IFN-λ4 was facilitated by genome-wide association studies (GWAS) in HCV infection and it is related to the control of HCV in some populations vs others. GWAS analysis identified three independent groups with single nucleotide

polymorphism (SNP) markers that were upstream of *IFNL3* in chromosome 19q13.13 (O'Brien, Prokunina-Olsson et al. 2014) (Figure 1-6). These SNPs share strong linkage disequilibrium (LD), suggesting that genotypes dependent on these SNPs are highly correlated. Subsequent studies find that these SNP markers are also related to the likelihood of spontaneous HCV elimination (Rauch, Kutalik et al. 2010).

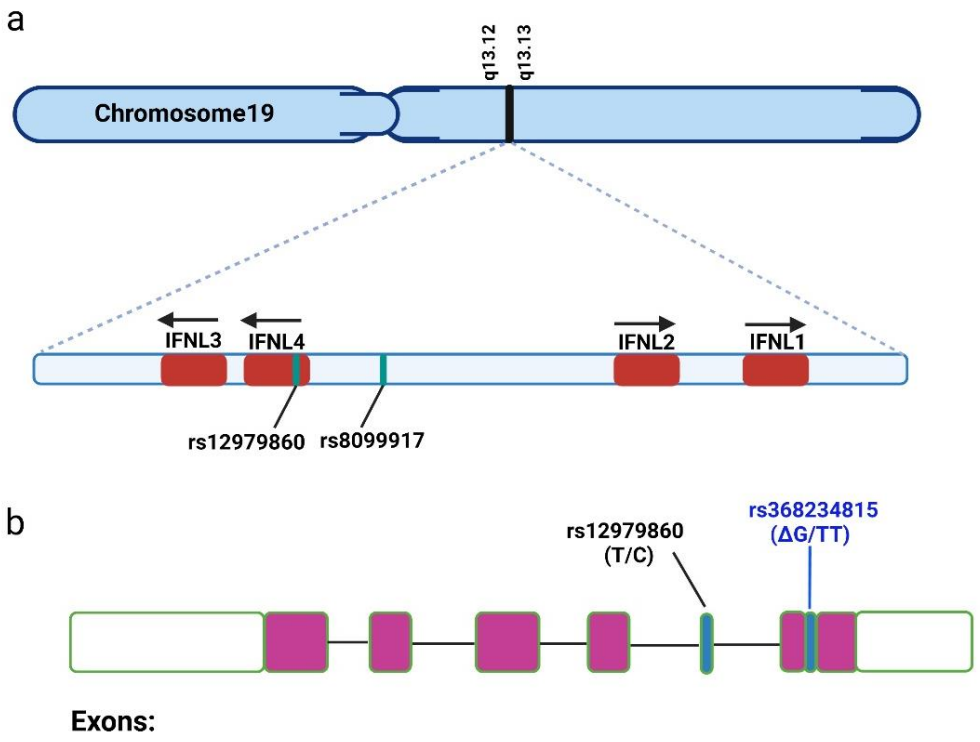

Figure 1-6. Schematic structure of IFNL4 gene and its variants. (a) Location of the IFN-λ gene family and genome-wide associated study markers rs12979860 and rs8099917 on chromosome 19; (b) exonic structure of *IFNL4* with the location the *IFNL4* rs12979860 and *IFNL4* rs368234815 (IFNL4-ΔG) polymorphisms. (O'Brien, Prokunina-Olsson et al. 2014)

Moreover, the rs12979860 SNP, as a host factor, was demonstrated to be strongly associated with feedback of pegylated IFN-α and ribavirin treated HCV-infected patients (Thompson, Muir et al. 2010). Individuals with two copies of rs12979860-C allele exhibit more responsiveness to treatment than those with the rs12979860-T allele (C/T and T/T genotypes). In addition, the rs12979860-T allele is more common in Africans than in Europeans or Asians (Thomas, Thio et al. 2009), consistent with previous observations that African Americans were less responsive to treatment for HCV infection.

IFNL4 gene is in the upstream of *IFNL3* gene on chromosome 19q13.13 and within several other transcripts. The production of *IFNL4* is regulated by a variant which is a single amino acid mutation converting the ΔG allele to a TT allele (rs368234815) (Prokunina-Olsson, Muchmore et al. 2013). The variant locates in exon1 of *IFNL4.* The *IFNL4*-TT yields a

frameshift resulting in the loss of active human IFN-λ4, whereas the *IFNL4*-ΔG allele produces a full length and active IFN-λ4 protein (Prokunina-Olsson, Muchmore et al. 2013). Therefore, *IFNL4*-ΔG regulates the generation of IFN-λ4 and is a functional variant.

The rs12979860 variant, *IFNL4* rs12979860, is located within intron of *IFNL4* (Figure 1-6). Asians (r^2=1.0) and Europeans (r^2>0.9) have high LD between *IFNL4*-ΔG and the *IFNL4* rs12979860-T allele, meaning that *IFNL4*-ΔG and *IFNL4* rs12979860-T allele are almost inherited together in these racial group. Nevertheless, Africans (r^2~0.7) have weaker LD between *IFNL4*-ΔG and *IFNL4* rs12979860-T than other groups (O'Brien, Prokunina-Olsson et al. 2014). In a Virahep study, *IFNL4*-ΔG and *IFNL4* rs12979860 genotypes yields similar HCV RNA decline after 28 days of treatment with pegylated IFN-α and ribavirin among patients of European ancestry because of strong LD. However, among African American patients, the HCV RNA decline is more strongly associated with a genotype for *IFNL4*-ΔG than *IFNL4* rs12979860 (Prokunina-Olsson, Muchmore et al. 2013). It was also reported that *IFNL4* rs12979860 is the strongest factor which is responsive to treatment with pegylated IFN-α and ribavirin (Thompson, Muir et al. 2010).

1.3.2 IFN-λ4 and antiviral activity

IFN-λ4 signals through IFNLR1 and IL10R2 receptor complex to activate JAK/STAT signaling pathways and induce the production of ISGs, establishing antiviral state. IFN-λ4 exhibits potent antiviral activity whereas it is harmful in the context of HCV infection (Hamming, Terczyńska-Dyla et al. 2013). IFN-λ4 can induce similar levels of ISGs and antiviral activity as IFN-λ3 on two different hepatic cell lines, Huh7 and HepG2 (Hamming, Terczyńska-Dyla et al. 2013). In addition, IFN-λ4 and IFN-λ3 show comparable antiviral potency against two different human coronaviruses, HCoV-229E and MERS-CoV in primary human bronchial epithelial cells (Hamming, Terczyńska-Dyla et al. 2013). mRNA expression was analyzed in the *IFNL4* region from liver biopsy specimens of patients with chronic hepatitis C, chronic hepatitis B, or nonviral liver diseases, and patients without liver disease. The results suggest *IFNL4* to be present in 50% patients with HCV infection but absent in the specimens from patients with other liver diseases or normal liver (Amanzada, Kopp et al. 2013). The results mean that *IFNL4* mRNA expression in the liver might be distinct from HCV infection. Konishi and others find that ISG levels are positively correlated with *IFNL4*-ΔG levels, and that the expression levels of two ISGs (*ISG15 and USP18*) in the liver tissue are higher in the *IFNL4*-ΔG carriers with transplant recipients with chronic HCV infection (Konishi, Motomura et al. 2014). Hepatic expression of ISGs is also found to be correlated

with *IFNL4* in patients with chronic HCV infection (Honda, Shirasaki et al. 2014). Recent study finds that IFNLR1 expression level are much higher in liver biopsies from HCV-infected patients than noninfected controls (Honda, Shirasaki et al. 2014). Among HCV-infected patients, IFNLR1 production is significantly upregulated in patients who carry the *IFNL4* rs12979860-T allele, which has a very strong LD with the *IFNL4*-ΔG allele (Honda, Shirasaki et al. 2014). These results indicate that IFN-λ4 may contribute to up-regulation of IFNLR1 to impair HCV clearance. Recently, Sheahan and others employ laser capture microdissection to dig the transcriptional profiles of HCV-infected cells and neighboring uninfected cells. They find that innate antiviral immune signature was the dominant transcriptional files, and it is greater and more diverse in infected cells than uninfected cells. Cells from people who hold *IFNL4*-ΔG are more infected, and the antiviral potency in infected cells from such patients is less effective than in the infected cells from people with *IFNL4*-TT/TT genotype (Sheahan, Imanaka et al. 2014). These results indicate that the antiviral program for effective HCV clearance may be impaired by IFN-λ4. In general, IFNs are secreted proteins, whereas IFN-λ4 is primarily intracellular (Prokunina-Olsson, Muchmore et al. 2013). The secretion of IFN-λ4 is impaired due to inefficient post-translational glycosylation (Hamming, Terczyńska-Dyla et al. 2013). Thus, intracellular accumulation of non-glycosylated IFN-λ4 could be toxic and lead to cell death.

Single amino acid substitution mutation of IFN-λ4 from a proline at position 70 to a serine (P70S) significantly alters its antiviral activity (Bamford, Aranday-Cortes et al. 2018). Lower ISG expression levels are shown in patients harboring the impaired IFN-λ4-P70S but these patients display better treatment response rates and spontaneous clearance rates than patients with the fully active IFN-λ4-P70 variant. Therefore, the production of IFN-λ4 drives high ISG expression but poor HCV clearance (Terczyńska-Dyla, Bibert et al. 2014). Studies identified another three active variants of IFNλ4: P70S, (leucine to phenylalanine at position 79) L79F and (lysine to glutamic acid at position 154) K154E, of which L79F and K154E are rare variants. The two variants increase the secretion and potency of IFN-λ4, enhancing IFN-λ4 antiviral activity dramatically. K154E is found in African Congo rainforest “Pygmy” hunter-gatherers and greatly promoted antiviral activity (HCV, Zika virus and influenza virus) and ISGs production *in vitro*. The most common form of IFN-λ4 in humans has attenuated antiviral activity due to a single amino acid mutation compared to the counterpart of other mammalian orthologues. Some populations still show a more active variant although the attenuating mutation appeared very early during human evolution due to a likely defect in secretion and potency of IFN-λ4 in human (Bamford, Aranday-Cortes et al. 2018). K154 is

widely distributed in the human population, but non-human primates and other mammals harbour the ancestral amino acid, E154, at position 154.

1.4 IL-22

1.4.1 Introduction to IL-22

Interleukin-22 (IL-22) is one of the best studied members in the IL-10 cytokine family. This family also includes IL-10, IL-19, IL-20, IL-24, and IL-26 as well as IFN-λs, IL-28A, IL-28B and IL-29 (Sabat, Ouyang et al. 2014). IL-22 has a profound effect on regeneration, host defense and pathology progress, which makes IL-22 an attractive target for clinical development.

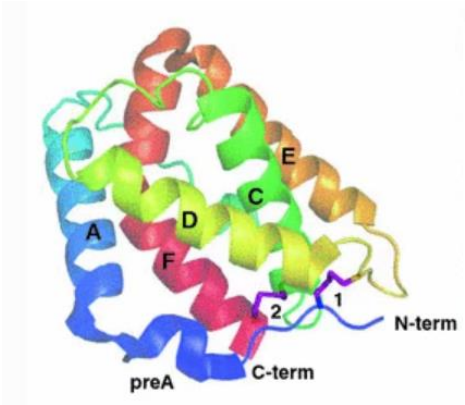

Figure 1-7. 3D crystal structure of IL-22. The independent monomers of IL-22. The IL-22 monomer consists of six helices named A-F and a small N-terminal helix termed helix preA. IL-22 helices are folded together forming a compact six-helix bundle. Adapted from (Trivella, Ferreira-Júnior et al. 2010)

The human *IL22* gene is located at chromosome 12q15, close to genes encoding IFN-λ and IL-26 (Dumoutier, Louahed et al. 2000). The open reading frame of the *IL22* gene contains 537bp, encoding 179 amino acids which is 79% similarity between mice and humans. The active form of this cytokine only contains 146 amino acids after a 33-amino-acid signal peptide is removed. IL-22 is expressed in many tissues like brain, gut, liver, lung (Sabat, Ouyang et al. 2014). The IL-22 receptor, a type 2 cytokine receptor, is a heterodimer which are composed of interleukin-22 receptor alpha (IL-22RA) and interleukin-10 receptor 2 (IL-10R2) (Dudakov, Hanash et al. 2015). The receptor contains three domains: extracellular domain, transmembrane domain, and cytoplasmic signal domain (Bleicher, de Moura et al. 2008). The 3D crystal structure of human IL-22 showed that the protein consists of six α-helix and a small N-terminal helix (Figure 1-7) (Trivella, Ferreira-Júnior et al. 2010).

Binding studies demonstrate that IL-22 has no affinity for IL-10R2 but a high affinity for IL-22R1; however, IL-10R2 has a strong affinity for IL-22-IL-22R1 complex (Jones, Logsdon et

al. 2008). Other cytokines from IL-10 family also have been reported to have the two-stage cytokine binding (Reineke, Schneider-Mergener et al. 1999). Recent studies also show that IL-22R1 is serine-phosphorylated by GSK3β at positions 410 and 414, which stabilizes IL-22R and prevents its ubiquitin proteasome-mediated degradation (Weathington, Snavely et al. 2014).

1.4.2 Production of IL-22

Primarily cells that produce IL-22 are derived from the lymphoid lineage. They include innate lymphoid cells (ILCs), αβ T cells and natural killer T (NKT) cells. However, some myeloid and nonhematopoietic cells, like macrophages, neutrophils, and fibroblasts, can also produce IL-22.

Intestinal ILC3

Group 3 ILCs (ILC3s) can express RoRγt and are potent producers of IL-22 (Spits et al., 2013). ILC3s exist in at least two subsets that differ developmentally, transcriptionally, and functionally: lymphoid tissue inducer cells (LTi)-like ILC3 (characterized by surface expression of CCR6) and natural cytotoxicity receptor (NCR)+ ILC3 that express NKp46 in mice (Vonarbourg, Mortha et al. 2010) and NKp44 in humans (Hughes, Becknell et al. 2009). Intestinal human and mouse ILC3 are vital to generate organized lymphoid tissue in the intestinal wall during development (LTi-like cells) and they regulate microbiota content and integrity of the intestinal barrier (Kiss, Vonarbourg et al. 2011, Kim, Hashimoto-Hill et al. 2016). ILC3 proliferation is stimulated by cytokines, such as IL18 in human tonsils (Victor, Nalin et al. 2017), or combination of TNF-like cytokine 1A, IL-1β, IL-23 and IL-2 in both human and mouse intestinal tissue (Zhou, Chu et al. 2019).

αβ T cells

Three different kinds of T cells are identified to produce IL-22 with the stimulation of IL-6 and tumor growth factor (TGF). They are Th1, Th17 and Th22 cells. Approximately 50% of IL-22-producing $CD4^+$ T cells are Th22 cells (only producing IL-22), 33% are Th1 cells (also producing IFN-γ), and 15% are Th17 cells (co-expressing IL-17) (Duhen, Geiger et al. 2009). In mouse T cells, Th17 cells are the main producers of IL-22 dependent on TGF and IL-6 (Wilson, Boniface et al. 2007). Several other cytokines, such as IL-23 and IL-1β, can regulate the production of IL-22 in T cells. TGF-β is required for the formation of Th17 cells and regulatory T cells (Tregs) (Mangan, Harrington et al. 2006). Given that Th17 also requires RORγt for its formation, and IL-23 signalling is crucial for Th17 cells to produce IL-

22 and, IL-6 promotes the expression of RORγt and IL-23R, driving T cell polarization towards Th17 cells. TGF-β concentration controls the balance of between Tregs and Th17 cells; low concentration of TGF-β upregulates RORγt and IL-23R, inducing the formation of Th17 cells, whereas higher concentration of TGF-β decreases IL-23R, inhibiting the production of IL-22 (Rutz, Noubade et al. 2011).

NKT cells

Natural killer T (NKT) cells can produce IL-22 with the stimulation of IL-23 (Rachitskaya, Hansen et al. 2008). Notably, TCR-CD1d interaction is required to produce IL-22 for NKT cells (Doisne, Soulard et al. 2011). A recent study shows that IL-7 is required for the maintenance and survival of NKT cells (Webster, Kim et al. 2014).

1.4.3 IL-22-STAT3 signaling pathway

IL-22 signals through the heterodimeric receptor complex, IL-22R1 and IL-10R2, activating JAK/STAT pathway (Figure 1-8). IL-10R2 is ubiquitously expressed, whereas IL-22RA is

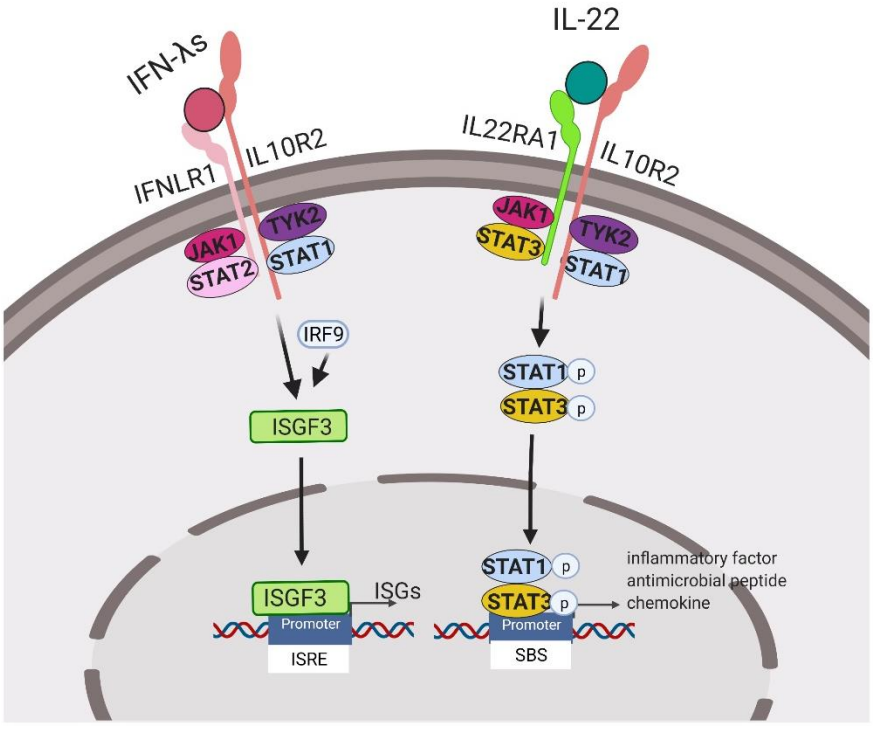

Figure 1-8. Comparison of IFN-λ-STAT1-STAT2 and IL-22-STAT1-STAT3 signaling pathways. IFN-λs bind to IFNLR1-IL10R2 receptor and activate JAK-STAT1-STAT2 signaling pathway, inducing the expression of interferon-stimulated genes (ISGs); IL-22 bind to IL22RA1-IL10R2 receptor and activate JAK-STAT1-STAT3 signaling pathway, inducing the expression of inflammatory factors, antimicrobial peptides and chemokines. Adapted from (Foxall 2016)

strictly expressed on epithelial cells, indicating the target cell specificity of IL-22 (Wolk, Kunz et al. 2004). IL-22 initially binds to IL22RA subunit, that subsequently leads to a

conformational change, allowing the binding of IL-10R2. The dimerization recruits the intracellular receptor-associated kinases JAK1 and TYK2, which phosphorylate the tyrosine residues of IL22RA on the intracellular domain (ICD). IL-22-activated receptor-associated kinases recruit transcriptional factors, STAT1 and STAT3, activating downstream pathways. Subsequently, STAT1-STAT3 transcriptional factors translocate into nucleus to bind to the promoter, inducing the production of antimicrobial peptides and inflammatory factors.

1.4.4 Regulation of IL-22 production

As IL-22 is produced by several kinds of cells, several cytokines, such as IL-23, IL-7 and IL-1β, that regulate IL-22-producing cells can regulate the production of IL-22 (Table 1). Also, some other molecules, such as notch and aryl hydrocarbon receptor (AhR), can also regulate the differentiation of the IL-22-producing cells. Notably, IL-22BP can bock the process of IL-22 binding to its receptors, thus strongly inhibiting IL-22 production.

IL-23

IL-23, also signalling through STAT3, is one of the main inducers of IL-22 production (Muñoz, Heimesaat et al. 2009). Cell types, Th17 cells, ILC3s and γδ T cells, all express IL-23 receptor, and produce IL-22 following stimulation by IL-23 (Hunter 2005). IL-23 promotes the development of Th17 cells, which subsequently produce IL-22. Afterwards, IL-22 activates STAT3 to mediate IL-23-induced acanthosis and dermal inflammation (Zheng, Danilenko et al. 2007). In addition, IL-23 can also to produce IL-22, mediating mucosal immunity (Cella, Fuchs et al. 2009). It was reported that IL-23 was a critical player in initiating inflammatory responses dependent on γδ T cells in the intestinal mucosa infected by serotype Typhimurium (Godinez, Raffatellu et al. 2009).

IL-7

IL-7 can regulate most types of lymphoid cells, including cells capable of producing IL-22 (Vonarbourg and Diefenbach 2012). The cytokine plays a key role in the generation and development of IL-22-producing cells, like αβ T cells and γδ T cells. IL-7 appears to maintain RORγt expression, which is critical for the differentiation of IL-22-producing cells and optimizing *Il22* gene expression (Vonarbourg and Diefenbach 2012). IL-7 upregulates IL-22 expression through maintaining, developing, and proliferating αβ and γδ T cells. The roles of IL-7 in IL-22-producing cells contribute to lymphoid organogenesis, tissue homeostasis and repair at mucosal surfaces (Vonarbourg and Diefenbach 2012).

Table 1. Regulation of IL-22 production

Molecule	Up/down regulation	Mode of action	Refs
IL-23	Upregulation	Mediated via STAT3	(Muñoz, Heimesaat et al. 2009); (Hunter 2005); (Cella, Fuchs et al. 2009).
IL-1β	Upregulation	Directly induces Th17, NKT and ILC3 to produce IL-22	(Shaw, Kamada et al. 2012); (Hughes, Becknell et al. 2010).
IL-7	Upregulation	Differentiation and exp	(Vonarbourg and Diefenbach 2012); (Hughes, Becknell et al. 2010); (Sutton, Lalor et al. 2009).
AhR	Upregulation	Promotes maturation of ILCs and Th17	(Veldhoen, Hirota et al. 2008); (Godinez, Raffatellu et al. 2009).
Notch	Upregulation	Differentiation of ILC3 and induces IL-22 production via mediating AhR	(Alam, Maekawa et al. 2010).
IL-22BP	Downregulation	Has higher affinity for IL-22 than IL-22RA	(Kotenko, Izotova et al. 2001); (Wu, Li et al. 2008); (Yang, Gao et al. 2014).

IL-1β

Multiple cell types can produce IL-1β, like macrophages, neutrophils, B and T cells, endothelial, and epithelial cells (Shaw, Kamada et al. 2012). IL-1β controls NKT, γδ T cells to produce IL-22. It was reported that NKT cells released IL-22 in the induction of IAV-infected DCs dependent on IL-1β and IL-23, thereby protecting lung epithelial cells against death (Hughes, Becknell et al. 2010). However, differently from IL-23, IL-1β signalling is necessary for maintaining IL-22 production (Hughes, Becknell et al. 2010). In addition, IL-1β can induce γδ T cells to produce IL-22 independently of IL-23, amplifying Th17 response and autoimmunity (Sutton, Lalor et al. 2009).

Aryl Hydrocarbon Receptor (AhR)

IL-22 is regulated by AhR in two manners, which either regulates the expression and maturation of ILC3 and Th17 cells or directly adjust the production of IL-22 and other cytokines (Veldhoen, Hirota et al. 2008). Firstly, AhR is critical for ILC3 maintenance and function during *C. rodentium* infection, which regulates host immunity through the production of IL-22 (Qiu, Heller et al. 2012). In addition, AhR promotes Th17 cells to produce IL-22 in response to environmental toxins, which is linked to development of autoimmune disease (Veldhoen, Hirota et al. 2008).

Notch

Notch signalling is necessary for normal lymphopoiesis (Maillard, Fang et al. 2005) and required for differentiation of IL-22-producing cells. Also, Notch induces the stimulation of $CD4^+$ T cells to upregulate IL-22 production in the intestine, which is significant for epithelial cell proliferation and differentiation. In addition, Notch signalling stimulates the aryl hydrocarbon receptor to drive CD4+ T cells to secrete IL-22, thereby fine-tuning inflammatory responses (Alam, Maekawa et al. 2010). Notch signalling directly regulates RORγt expression and other IL-22 regulatory elements, like AhR and STAT3 to control the production of IL-22, contributing to both protective and pathological inflammatory responses (Alam, Maekawa et al. 2010).

IL-22BP

IL-22 also has a soluble-secreted receptor which is called IL-22 binding protein (IL-22BP) (Kotenko, Izotova et al. 2001). IL-22BP is firstly identified to inhibit IL-22 activity in hamster cells (Kotenko, Izotova et al. 2001). Subsequently, it is also identified in several other tissues, for example the major source of IL-22BP is $CD11b^+$ conventional dendritic cell (cDC) in the gastrointestinal tract (Martin, Bériou et al. 2014). IL-22BP is a strong negative regulator of IL-22 production. It is a soluble form of the IL-22R1 subunit, which has 1000 times higher binding affinity for IL-22 than IL-22 receptor complex. Therefore, IL-22BP can significantly inhibit IL-22 binding to the membrane-bound receptor, directly affecting the function of IL-22 (Wu, Li et al. 2008). Interestingly, IL-22 production increases with the decrease in IL-22BP in models of mouse colitis or lipopolysaccharide (LPS) administration (Wolk, Witte et al. 2007). In addition, a report shows that IL-22BP is upregulated in renal tissue of people with active renal disease (Yang, Gao et al. 2014).

1.4.5 IL-22 and inflammation

IL-22 promotes cell proliferation and regulates host defenses at barrier surface and contributes to inflammatory tissue pathology and tissue regeneration (Dudakov, Hanash et al. 2015).

IL-22 in inflammatory response

IL-22 has anti-inflammatory functions and prevents the advent of inflammatory pathology. Studies have shown that IL-22 is critical for limiting hepatocyte damage during acute liver inflammation. Mice deficient in IL-22 are extremely vulnerable to live damage during concanavalin A-induced hepatitis (Zenewicz, Yancopoulos et al. 2007). Moreover, IL-22 shows protective role during inflammatory bowel disease (IBD). IBD, a chronic inflammatory disease of the gastrointestinal tract, is caused by dysregulation in innate and/or adaptive immunity (Podolsky 2002). Previous work has shown IL-22 is highly upregulated in patients with either ulcerative colitis or Crohn's disease (Andoh, Zhang et al. 2005). IL-22 can induce the secretion of IL-6 and IL-8 and activate NF-κB and activator protein-1 (AP-1), causing proinflammatory effects on colon epithelial cells (Andoh, Zhang et al. 2005). In innate and T cell cell-driven colitis mice models, studies demonstrate that both CD4+ T cell and NK cells secret IL-22 to exhibit protective role during IBD (Zenewicz, Yancopoulos et al. 2008). Studies in primary epithelial cells revealed that IL-22 is mainly involved in innate inflammatory response, would-healing activities, and tissue protection (Wolk, Kunz et al. 2004, Ouyang, Kolls et al. 2008). Interestingly, IL-22 is not capable of inducing an anti-inflammatory response from leukocytes due to absence of IL-22R expression (El Kasmi, Holst et al. 2006). Above all, IL-22 mediated anti-inflammatory response is independent of its direct tissue protective activity. Additionally, studies demonstrated that IL-22 promotes the production of antimicrobial agents, such as regenerating islet-derived proteins (Reg) Reg3β and Reg3γ, β-defensins, and S100 proteins. These antimicrobial factors prevent the development of chronic inflammatory disorders and promote the clearance of harmful pathogens (Zheng, Valdez et al. 2008).

IL-22 in tissue regeneration

IL-22 is also identified as a critical factor in regulating intestinal immunity and tissue repair in murine models (Sonnenberg, Monticelli et al. 2011). Although IL-22 is critical for tissue protection, uncontrolled IL-22 response can cause tissue damage as well. Psoriasis is a chronic inflammatory disease of the skin featured by abnormal keratinocyte differentiation and proliferation, upregulated dilation and growth of blood vessels, and leukocyte infiltration

of the dermis and epidermis (Lowes, Bowcock et al. 2007). IL-22 has been identified as a key factor involved in psoriasis. Production of IL-22 has been found in psoriatic skin and not in healthy skin (Otkjaer, Kragballe et al. 2005). In psoriatic patients, the main sources of IL-22 in skin lesions are T cell, and T cells from the skin lesions, produces much more IL-22 than do T cells in circulation (Boniface, Guignouard et al. 2007). Moreover, T cells clones originated from psoriatic tissue are mostly $CCR6^{+}IL\text{-}22^{+}$ (Pène, Chevalier et al. 2008). Given that the IL-22 receptors are highly expressed on keratinocytes, IL-22 induces the production of various antimicrobial peptides, such as S100 family genes, by activating STAT3 in keratinocytes (Zheng, Valdez et al. 2008). The hallmark feature of psoriatic skin is the induction of S100A7 (also called psoriasis). In summary, IL-22 is critical for the key pathological features during the process of psoriasis.

1.4.6 IL-22 and host defense

IL-22 protects host against various infections to mediate host defenses in two main manners. Firstly, IL-22 directly induces innate immunity response from epithelial cells against invading pathogens, like bacteria and yeast. Secondly, IL-22 repairs tissue damage caused by infections and inflammation. Studies show that IL-22 and IL-23 are upregulated in the colon infected by *Citrobacter rodentium*, which is a gram-negative bacterium and induces acute infectious colitis (Zheng, Valdez et al. 2008). IL-22 is necessary for host defence during the early infection of *C. rodentium* (Zheng, Valdez et al. 2008). Mice deficient in IL-22 show systemic bacterial dissemination as well as more severe epithelial damage. IL-22 also plays a key role in inducing antimicrobial peptides, the Reg family, which is essential for the prevent of systemic bacterial dissemination in colon epithelial cells (Zheng, Valdez et al. 2008). It was reported that IL-22 is critical for host defence in the lung infected by *Klebsiella pneumoniae* (*K. pneumoniae*) (Aujla, Chan et al. 2008). Inhibition of IL-22 causes the early death of the infected animals. Together with IL-17, IL-22 promotes lung repair and induces the production of proinflammatory chemokines and cytokines, and Lipocalin-2, which play a role in killing *K. pneumoniae* in the lung. Another gram-negative bacterium, *Salmonella enterica*, can result in systemic infection or gastroenteritis in humans. Studies demonstrated the protective role of IL-22 in hepatocyte of $IL12p35^{-/-}$ mice model (Schulz, Köhler et al. 2008). It was also reported that IL-22 blocks *Mycobacterium tuberculosis* in human macrophages (Dhiman, Indramohan et al. 2009). However, compared to its protective function against bacterial infections, IL-22 can damage the intestine infected by parasite *Toxoplasma gondii* (*T. gondii*) (Muñoz, Heimesaat et al. 2009). $IL\text{-}22^{-/-}$ mice can resist the immunopathology induced by *T. gondii*. Absence of IL-22 slows the death rate and

decreases the intestine damage and inflammation after the infection (Muñoz, Heimesaat et al. 2009). Innate lymphoid cells are valuably infected by commensal bacteria in an IL-22 dependent manner. Mice with blockade of IL-22 signaling or ILC depletion fail to resist bacterial infection and valuably withstand systemic inflammation (Sonnenberg, Monticelli et al. 2012). Commensal bacteria are dispensable to maintain normal intestinal physiology through colonizing the gastrointestinal tract. Commensal bacteria are anatomically distributed to either lumen and surface of the intestine or within the underlying gut-associated lymphoid tissues (GALTs) (Hill and Artis 2009). IL-22 is necessary for the induction of antimicrobial peptides, such as RegIIIγ and RegIIIβ, by colonic epithelial cells during *C. rodentium* infection. Exogenous RegIIIγ improves the survival rate of IL-22-deficient mice, indicating the importance of IL-22 in protecting infected mice (Nagao-Kitamoto, Leslie et al. 2020).

IL-22 and antiviral activity

IL-22 signaling promotes barrier integrity maintenance and epithelial repair during influenza infection. IL-22$^{-/-}$ mice are more vulnerable to influenza infection compared to WT mice, suggesting that endogenous IL-22 exhibits a protective role in controlling pneumococcal burden (Hasegawa, Yada et al. 2014). IL-22 is also reported to show a protective role in inhibiting enteric viruses in the intestine, either through the inhibition of viral replication or the induction of epithelial cell proliferation and regeneration following tissue damage (Hasegawa, Yada et al. 2014, Seo, Giles et al. 2020). Whether IL-22 and IFN-λ work in concert really depends on the model system and the relative distribution of their receptors (Ahn and Prince 2020). It was demonstrated that ILC-derived IL-22 can protect host during influenza infection. Following influenza infection, lung NK cells are quickly triggered to produce both IL-22 and IFN-γ and have more cytotoxic potential. The IL-22 gene expression is sustained after infection, but the IL-22 protein in the lung tissue decreases shortly, gradually recovering to the baseline after virus clearance (Guo and Topham 2010). IL-22 increases expression of IFN-λ to curb enteric coronavirus replication. It was reported that prokaryotic IL-22 can control PoRV, PEDV and TGEV, which are the most common porcine diarrhea viruses, dependent on the activation of STAT3 signalling *in vitro* (Xue, Zhao et al. 2017).

1.4.7 Other functions of IL-22

IL-22 can stimulate epithelial cell turnover to maintain barrier integrity. Commensal bacteria translocate and predispose to destructive inflammation when internal or external stimulation

disrupts the intestinal barrier. Crypt-residing stem cells keep proliferate and replenish damaged epithelial cells to ensure intact barrier composition. ILCs produce IL-22 to preserve tissue-specific stem cells and limit tissue damage. Studies in IEC-specific STAT3-deficient mice demonstrate that intestinal epithelial STAT3 activation promotes IL-22-mediated mucosal would healing, regulating immune homeostasis in the gut (Pickert, Neufert et al. 2009). Rapid tissue repair following injury is critical for survival of living organisms. After tissue damage, innate immune cells initiate inflammatory and tissue repair processes when sensing DAMPs released by damaged cells. To repair injured tissues, three major steps of inflammation are employed to facilitate this process: the first step is to recruit key inflammatory cells induced by local chemotactic factors; the second phase is to switch important inflammatory cells, like macrophages, to an activated phenotype; the final step is to eliminate key inflammatory cells, like neutrophils, via apoptosis (Eming, Wynn et al. 2017).

IL-22 and Acute graft-versus-host diseases (aGVHD)

Graft versus host disease (GVHD) is a disease that might occur after allogeneic transplant. In GVHD, stem cells from donated bone marrow or peripheral blood attack the recipient body because they consider the recipient's body as foreign invaders. The gastrointestinal tract is a prominent target of GVHD, and the severity of damage in the intestine determines the outcome of GVHD. It was reported that recipient-derived IL-22 decreases mortality and tissue pathology in the gut and liver. In contrast, donor-derived IL-22 increases mortality and target tissue inflammation (Hanash, Dudakov et al. 2012). Nevertheless, protection from recipient-derived IL-22 is restricted during GVHD due to the removal of recipient-derived IL-22^+ ILCs by alloreactive T cells (Hanash, Dudakov et al. 2012). In addition, it was demonstrated that colon biopsy samples from IBD patients are deficient in IL-22^+ ILCs, T cells in the primate cell model (Xu, Zheng et al. 2014). In summary, tissue damage causing by deficiency in IL-22-producing cells appears not only in GVHD pathogenesis and the transplant setting but also in IBD and other tissue damage models.

Regulation of adaptive immunity

IL-22 is critical for endogenously regenerating thymic tissue and restoring T cell development during thymic injury (Dudakov, Hanash et al. 2012). It was also reported to have a remarkable capacity of tissue repair in deficiency of T cells caused by cancer cytoreductive therapies and BMT (Boehm and Swann 2013). Researches find that IL-22 levels in the thymus can be upregulated in response to radiation damage and it contributes to thymic repair (Dudakov, Hanash et al. 2012). Endogenous thymic regeneration is critical for renewal of immune competence in response to stress, infection, or immune depletion.

Studies show that levels of IL-22 in the thymus are upregulated after thymic insult, and thymic recovery is inhibited in IL-22$^{-/-}$ mice (Dudakov, Hanash et al. 2012).

2 Materials and methods

2.1 Materials

2.1.1 General chemicals, media, enzyme, and reagents

Chemicals and reagents not listed below are described at the methods part (2.2) together with the methods for which they were used.

Table 2. List of chemicals, media, enzyme, and reagents

Name	Manufacturer
30% Acrylamide/Bis-acrylamide solution (37.5:1)	Carl Roth
Agarose Standard	Carl Roth
Albumin Standard	Thermo Fisher Scientific
Ammonium Persulfate (APS)	Carl Roth
Ampicillin (100 mg/mL)	Carl Roth
Antibiotic-Antimycotic (Anti-Anti)	Gibco™/Invitrogen
Avidin-HRP 1000x	BioLegend
A-83-01	Tocris
β-Mercaptoethanol	Sigma-Aldrich
Bovine Serum Albumin	New England Biolabs™
BsmbI-HF	New England Biolabs™
Bromophenol Blue	AppliChem
B-27	Invitrogen
Cell Recovery Solution	Corning
Chemiluminescence (ECL) film (Amersham Hyperfilm ECL)	GE Healthcare
Collagen (from rat tail)	Sigma-Aldrich
Complete protease inhibitor cocktail EDTA-free	Roche
DAPI	Sigma
DC Protein Assay Kit I	Bio-Rad
dNTP set (100 mM)	Thermo Fisher Scientific

Dulbecco's Modified Eagle Medium (DMEM)	Gibco™/Invitrogen
Dulbecco's Modified Eagle Medium: Nutrient Mixture F-12 (DMEM/F-12) (1:1) (1X)	Gibco™/Invitrogen
DMSO (Dimethyl Sulfoxide), anhydrous	Life Technologies
DRAQ5	Thermo Fisher Scientific
Enhanced chemiluminescence (ECL) Western Blotting reagents	GE Healthcare
Ethylenediaminetetraacetic acid (EDTA)	Sigma-Aldrich
Ethanol	Thermo Fisher Scientific
Ethidium bromide solution (10 mg/mL)	Carl Roth
Fetal Bovine Serum (FBS) Superior	Biochrom AG
Gateway BP-Clonase Enzyme Mix II	Thermo Fisher Scientific
Gateway LR-Clonase Enzyme Mix II	Thermo Fisher Scientific
Gel Loading Dye, purple, 6x	New England Biolabs™
GlutaMax	Gibco™/Invitrogen
HEPES	Invitrogen
Human IL-6 ELISA MAX™ Standard Sets	BioLegend
Human recombinant R-spondin	Produced in HEK-293T cells
Human recombinant IFN-beta1a (IFN-β)	Biomol
Human recombinant IFN-λ1 (IL-29)	Peprotech
Human recombinant IFN-λ2 (IL-28A)	Peprotech
Human recombinant IFN-λ3 (IL-28B)	Cell signaling
Iscove's Modified Dulbecco's Medium (IMDM)	Gibco™/Invitrogen
Isopropanol	Carl Roth
Kanamycin (50 mg/mL)	Carl Roth

LB agar and medium powder	Carl Roth
[Leu15]-Gastrin I	Sigma-Aldrich
Matrigel	BD-bioscience
Methanol	Sigma-Aldrich
Mouse recombinant Epidermal Growth Factor (EGF)	Invitrogen
Mouse recombinant Noggin	Peprotech
NEBuffer 3.1	New England Biolabs™
Nicotinamide	Sigma-Aldrich
Nitrocellulose membrane (Amersham Hybond ECL)	GE Healthcare
Essential Amino Acids (NEAA)	Gibco
Non-fat dried milk powder	AppliChem
N-acetyl-cysteine	Sigma-Aldrich
N-2	Invitrogen
Pen-Strep (Penicillin Streptomycin)	Gibco™/Invitrogen
Phosphate buffered saline (PBS)	Sigma-Aldrich
PhosphoSTOP phospatase inhibitor cocktail	Roche
Phusion HF buffer (5x)	Thermo Fisher Scientific
Phusion hot start II DNA polymerase	Thermo Fisher Scientific
Proteinase K	Thermo Fisher Scientific
Precision Plus Protein Dual Colour	Bio-rad
ProLong Gold Antifade Mountain with DAPI	Molecular Probes
2-Propanol	Sigma
Puromycin (10 mg/ml)	Sigma
Pyridone-6 (pJAKi)	Calbiochem
Quick-Load 1 kb DNA ladder	New England Biolabs™
SB202190 (p38i)	Tocris
SOC Outgrowth medium	New England Biolabs™
Sodium chloride	Carl Roth
Sodium dodecyl sulfate (SDS)	Carl Roth

SP600125 (JNKi)	Tocris
SsoAdvanced Universal SYBR Green	Bio-Rad
TEMED	Carl Roth
TMB High Sensitivity Substrate Solution	BioLegend
Trypsin–EDTA 0,25% and 0,05%	Gibco/Life Technologies
T4 DNA Ligase Reaction Buffer, 10x	New England Biolabs™
Tris base	Sigma-Aldrich
TritonX-100	Sigma-Aldrich
Tween 20	MP Biomedical
U0126 (ERKi)	Cell Signaling
Western Bright Chemiluminescent Substrate Sirius	Biozym
Wnt3A	Produced in L929 cells
Y27632	Sigma-Aldrich

2.1.2 Media and buffers

Table 3.List of media and buffers

Name	Composition
Advanced Dulbecco's Modified Eagle Medium: Nutrient Mixture F-12 (DMEM/F-12) (1:1) for organoid media	Advanced DMEM/Ham's F-12 10 mM HEPES 1 x GlutaMAX 1% (v/v) Pen-Strep
Blocking solution (western blot) I	Non-fat dried milk powder 5% (w/v) 1 x TBS-T
Blocking solution (western blot) II	BSA 5% (w/v) 1 x TBS-T
Culture medium for HEK-293T human embryonic kidney cells	IMDM, 1°% (v/v) FBS 1% (v/v) 100 U/mL Pen-Strep

Culture medium for T84 colon carcinoma cells	DMEM/F-12 10% (v/v) FBS 1% (v/v) Pen-Strep
Basal Culture medium for human intestinal organoids	Advanced DMEM/F-12 50% (v/v) Wnt3a conditioned media 20% (v/v) R-Spondin conditioned media 1 x B-27 1 x N-2 500 nM A-83-1 50 ng/mL EGF 10 nM Gastrin 2 mM GlutaMAX 10 mM HEPES 1 mM N-acetyl-cystein 10 mM Nicotinamide 100 ng/mL Noggin 1 x Pen-Strep 10 µM Sb202190
Fixation Buffer for smRNAFish	5 mL 37% Formaldehyde solution 5 mL 10 x Phosphate Buffered Saline (PBS), RNase-free 40 mL Nuclease-free water
Hybridization buffer	(For 1 mL) 900 µl Stellaris RNA FISH Hybridization Buffer (Biosearch Technologies Cat# SMF-HB1-10) 100 µl Deionized Formamide
Laemmli buffer (4x)	200 mM Tris base (pH 6.8) 8% (w/v) SDS 40% (v/v) glycerol 4% (v/v) β-Mercaptoethanol 0.08% (v/v) bromophenol blue
LB agar (pH 7.0)	10 g LB agar powder 150 mL H_2O
LB medium (pH 7.0)	12,5 g LB medium powder 500 mL H_2O

Phosphate buffered saline (PBS) 10x	137 mM NaCl 2,7 mM KCl 10 mM Na_2HPO4 2 mM KH_2PO4 in H_2O
RIPA	150 mM sodium chloride 1% (v/v) Triton X-100 0.5% (w/v) sodium deoxycholate 0.1% (w/v) SDS 50 mM Tris base (pH 8.0) Complete protease inhibitor PhosphoSTOP phosphatase inhibitor
SDS-Tris-Glycine buffer (1x)	25 mM Tris base 200 mM Glycine 0.1% (w/v) SDS
SDS-PAGE separation gel buffer (4x)	1.5 M Tris base (pH 8.8) 0.4% (w/v) SDS
SDS-PAGE separation gel (12%)	3.6 mL 30% Acrylamide/Bis-acrylamide solution 3.15 mL millipore H_2O 2.25 mL running gel buffer 75 ul APS (10% w/v) 15 ul TEMED
SDS-PAGE stacking gel buffer (4x)	0.5 M tris base (pH 8.8) 0.4% (w/v) SDS
SDS-PAGE stacking gel (5%)	0.5 mL 30% Acrylamide/Bis-acrylamide solution 1.75 mL millipore H_2O 0.75 mL separation gel buffer 25 ul APS (10% w/v) 5 ul TEMED
SOC medium	2.66% (w/v) SOB-medium powder 20 mM D-(+)-Glucose
TBE buffer (0.5%)	50 mM Tris-base

	50 mM Boric-acid 1 mM EDTA-Na_2
TBS	50 mM Tri-HCL, pH 7.5 150 mM NaCL
TBS-T	50 mM Tri-HCL, pH 7.5 150 mM NaCL 0.1% Tween
Transfer buffer	20 mM Tris-base 160 mM Glycine 20% methanol
Tris-borate EDTA (TBE) running buffer 5x (agarose gel electrophoresis)	60,5 g Tris base 31 g H_3BO_3 3,7 g EDTA in H_2O
Wash buffer A	(For 150 mL) 30 mL Stellaris RNA FISH Wash Buffer A (Biosearch Technologies Cat# SMF-WA1-60) Add 105 mL Nuclease-free water Add 15 mL Deionized Formamide
Wash buffer B	Add 88 mL of Nuclease-free water to bottle (Biosearch Technologies Cat# SMF-WB1-20)
William's media	FCS (10%), human insulin (4 µg/mL), hydrocortisone hemisuccinate (50 µM), and Pen-Strep (1%)

2.1.3 Antibodies

Table 4. List of primary antibodies

Antibody	Source	Species	Application
Anti-β actin	Sigma (#A5441)	monoclonal mouse	WB: 1:5,000
Anti-E-cadherin	BD (#610181)	monoclonal mouse	IF: 1:100

Anti-EF2	Santa Cruz Biotechnology (# sc-13004)	polyclonal goat	WB: 1:3,000
Anti-ERK	Cell Signaling Technology (#4695)	polyclonal rabbit	WB: 1:1,000
Anti-IFIT1	Abnova (#H00003434-DO1)	polyclonal rabbit	WB: 1:1,000
Anti-IRF1	Cell Signaling Technology (#8478)	polyclonal rabbit	WB: 1:1,000
Anti-Mucin-2	Santa Cruz Biotechnology (#sc-5334)	polyclonal rabbit	IF: 1:100
Anti-MxA	Georg Kochs-Freiburg, Germany	monoclonal mouse	WB: 1:1,000
Anti-phospho-STAT1	BD (#612233)	monoclonal mouse	WB: 1:1,000
Anti-SAPK/JNK	Cell Signaling Technology (#9258)	polyclonal rabbit	WB: 1:1,000
Anti-STAT1	BD (#610115)	monoclonal mouse	WB: 1:1,000
Anti-ZO1	Invitrogen (#339100)	monoclonal mouse	IF: 1:100
Anti-µNS	GenScript, USA	monoclonal mouse	WB, IF: 1:1,000
Anti-phospho-STAT3 (Y705)	Cell Signaling Technology (#9145)	monoclonal rabbit	WB, IF: 1:1,000
Anti-SOCS1	Santa Cruz Biotechnology (sc-518028)	monoclonal mouse	WB, IF: 1:1,000

Anti-USP18	Cell Signaling Technology (#4813)	monoclonal rabbit	WB, IF: 1:1,000

Table 5. List of secondary antibodies

Antibody	Source	Species	Application
anti-mouse IgG Alexa Fluor 568	Invitrogen (A-11004)	polyclonal goat	IF: 1:1,000
anti-mouse IgG Alexa Fluor 647	Invitrogen (A-21235)	polyclonal goat	IF: 1:1,000
anti-rabbit IgG Alexa Fluor 568	Invitrogen (A-11011)	polyclonal goat	IF: 1:1,000
anti-rabbit IgG Alexa Fluor 647	Invitrogen (A-21244)	polyclonal goat	IF: 1:1,000
ECL anti-goat IgG HRP	Jackson ImmunoResearch (#705-035-147)	polyclonal donkey	WB: 1:5,000
ECL anti-mouse IgG HRP	GE-Healthcare (NA931)	polyclonal sheep	WB: 1:5,000
ECL anti-rabbit IgG HRP	GE-Healthcare (NA934)	polyclonal donkey	WB: 1:5,000

2.1.4 Primer and probe

Table 6. List of primer sequence used for qRT-PCR analysis

	Gene Symbol	Forward primer (5'-3')	Reverse primer (5'-3')
#1	CXCL10	TGAAATTATTCCTGCAAGCCAA	GACATCTCTTCTCACCCTTCTTT
#2	CYP3A4	GATGGCTCTCATCCCAGACTT	AGTCCATGTGAATGGGTTCC
#3	ETV7	AAGAACCGGGTGAACATGAC	TTGTCCTGGACCATCTTTCC
#4	GBP1	CTATGAGGAACCGAG	CACGTTCCACTTCAATCTCC

#5	HPRT1	CCTGGCGTCGTGATTAGTGAT	AGACGTTCAGTCCTGTCCATAA
#6	IFIT1	AAAAGCCCACATTTGAGGTG	GAAATTCCTGAAACCGACCA
#7	IFITM3	GATGTGGATCACGGTGGAC	AGATGCTCAAGGAGGAGCAC
#8	IFNAR1	CACTGACTGTATATTGTGTGAAAGCCAGAG	CATCTATACTGGAAGAAGGTTTAAGTGATG
#9	IFNAR2	ATTTCCGGTCCATCTTATCAT	ACTGAACAACGTTGTGTTCC
#10	IFN-β	GCCGCATTGACCATCTAT	GTCTCATTCCAGCCAGTG
#11	IFN-λ2/3	GCCACATAGCCCAGTTCAAG	TGGGAGAGGATATGGTGCAG
#12	IL10RB	TTGCTGTGGTGCGTTTACAAG	CTTTCAGGTGCTGTGGAAGAGA
#13	IFNLR1	ACCTATTTTGTGGCCTATCAGAGC	CGGCTCCACTTCAAAAAGGTAAT
#14	IRF1	CCAAGAGGAAGTCATGTG	TAGCCTGGAACTGTGTAG
#15	ISG15	CCTCTGAGCATCCTGGT	AGGCCGTACTCCCCCAG
#16	Lysozyme	ACAAGCTACAGCATCAGCGA	GTAATGATGGCAAAACCCCA
#17	MX1	GAGCTGTTCTCCTGCACCTC	CTCCCACTCCCTGAAATCTG
#18	Mucin-2	TGTAGGCATCGCTCTTCTCA	GACACCATCTACCTCACCCG
#19	OLFM4	ACCTTTCCCGTGGACAGAGT	TGGACATATTCCCTCACTTTGGA
#20	SOCS3	GCGAGGATCCTGGTGACA	CCAGGATGGTTCCCTTCAG
#21	Sucrase isomaltose	AATCCTTTTGGCATCCAGATT	GCAGCCAAGAATCCCAAAT
#22	TBP	TGCACAGGAGCCAAGAGTGAA	CACATCACAGCTCCCCACCA
#23	USP18	TATGTGAGCCAGGCACGAT	TCCCGACGTGGAACTCAG
#24	VIPERIN	GAGAGCCATTTCTTCAAGACC	CTATAATCCCTACACCACCTCC
#25	Mouse CA9	CCATTTGGAAGAAATCTCGG	CTCAGTTTCACTGTCTCATTG
#26	Mouse CK2α	GCATGTTAGCGAGCATGATATTCC	GTTCATCTGTCCCCAGAACCTT
#27	Mouse VEGF1	AAAATCAGTTCGAGGAAAGG	TACGTTCGTTTAACTCAAGC

2.2 Methods

2.2.1 Cell culture, viruses, and viral infection

2.2.1.1 Culture of human cell lines

T84 human colon adenocarcinoma cells (ATCC CCL-248) were maintained in a 1:1 nutrient mixture of Dulbecco's modified Eagle's medium (DMEM) and F-12 supplemented with 10% fetal bovine serum (FBS) and 1% (100 U/ml) penicillin and 1% (100 µg/mL) streptomycin. Caco2 human colon adenocarcinoma cells (ATCC HTB 37) were maintained in DMEM with 10% FBS and 1% penicillin/streptomycin. HepaRG cells were cultured in complete William's media with 10% FBS, insulin, hydrocortisone and pen-strep. T84 cells were cultured in collagen coated T25 flasks and split in 1:2 ratio every 3-4 days by treatment with 0.25% Trypsin/EDTA. HEK-293T human embryonic kidney cells (ATCC) were cultured in T75 cell culture flasks using Iscove's Modified Dulbecco's medium (IMDM) supplemented with 10% FBS and 1% penicillin/streptomycin. All mammalian cells were cultured at 37 ^{o}C and 5% CO_2.

2.2.1.2 Culture of human intestinal mini-gut organoids

Human colon and intestinal tissue were received from colon resections from the University Hospital Heidelberg, Germany and human ileum and jejunum were purchased from Baylor University, USA. The resected tissue was washed several times with ice-cold PBS containing 1 x Antibiotic-Antimycotic (Anti-Anti) and stem cells containing crypts were isolated following 2 mM EDTA dissociation of tissue sample for 1 h at 4 °C, with rocking. Crypts were spun and washed in ice-cold PBS. Fractions enriched in crypts were resuspended in Matrigel and maintained in Advanced DMEM/F-12, supplemented with penicillin/streptomycin, HEPES, Wnt3A, B-27, N-2, GlutaMax, EGF, R-Spondin, Noggin, N-acetylcysteine, nicotinamide and A-83-01 (basal organoid medium). At 24 h post-isolation, the open crypts were resealed, and round organoid structures were apparent. Medium was changed every 2-3 days and for the first two days post isolation, the Rho–associated coiled-coil containing protein kinase (ROCK) inhibitor Y-27632 (10 µM) was added to the basal organoid culture medium. Organoids were split every 7-10 days by passaging the Matrigel containing organoids through a $27^{1/2}$ gauge needle several times. Differentiation media is the same as above except without Wnt3A, nicotinamide and 50% reduced levels of R-Spondin and Noggin.

2.2.1.3 Ethics Statement

Human gut tissue was received from colon and small intestine resection from the University Hospital Heidelberg, Germany. All subjects gave written informed consent in accordance with the Declaration of Helsinki. All samples were received and maintained in an anonymized manner. The protocol was approved by the "Ethic commission of University Hospital Heidelberg" under the approved study protocol S-443/2017. Human ileum was purchased from Baylor University, USA and transferred by signed MTA.

2.2.1.4 Viruses and viral infection

VSV-luc was a kind gift from Sean Whelan (Washington University in St. Louis) and was produced as described (Cureton, Massol et al. 2009). A multiplicity of infection (MOI) of 1 was used to infect T84 cells, and an MOI of 0.2 was used to infect HepaRG cells. Titters were determined as described (Stanifer, Cureton et al. 2011). The infectious rate by Vesicular stomatitis virus luciferase (VSV-luc) was assessed through VSV luciferase assay. Encephalomyocarditis virus (EMCV) was produced in Vero cells following low MOI infection (MOI = 0.0001) and harvested between 1 and 2 days when extensive cytopathic effect was observed. EMCV infectivity was quantified by TCID50 and typically grew to titers of 10^8/mL. The infectious rate by EMCV was assessed through DRAQ5 fluorescent probe to measure loss of cells.

2.2.2 Cloning and generation of stable cell lines

2.2.2.1 Cloning and generation of KO cell lines

Knockouts of SOCS1, SOCS3 and USP18 in T84 cells were achieved by using the Clustered Regularly Interspaced Short Palindromic Repeats/Caspase 9 (CRISPR/Cas9) system. Three different single-guide RNAs (sgRNAs) per gene were used to target the coding region of SOCS1, SOCS3 and USP18 and inserted into the lentiviral vector lenti-CRISPR v2 (Addgene #52961) also encoding the Cas9 nuclease. The following sgRNAs were used: SOCS1(#1) 5′ CGCTGCCGGTCAAATCTGGA 3′, (#2) 5′ GCCGGTAATCGGCGTGCGAA 3′ (#3) 5′ TAGGATGGTAGCACACAACC 3′; SOCS3 (#1) 5′ AAACTTGCTGTGGGTGACCA 3′, (#2) 5′ CACAGCAAGTTTCCCGCCGC 3′, (#3) 5′ CTTAAAGCGGGGCATCGTAC 3′; USP18 (#1) 5′ GCAAATCTGTCAGTCCATCC 3′, (#2) 5′ AGGGCACGTTGCACTTCTGC 3′, (#3) 5′ ATGACCATGAGGGTAGTCCC 3′. Lentiviruses were produced and T84 cells were transduced twice using 1:2 diluted stocks of lentiviral particles encoding sgRNA #1, 2 or 3. At 36 h post-transduction, transduced cells were selected using puromycin for 2-3 weeks

and then used for experiments. To establish KO cells, clonal selection was performed via single-cell dilution in a 96-well plate. KO cells were confirmed by sequencing and functional tests.

2.2.2.2 Production and use of lentiviral vectors

HEK-293T cells with a low passage number were cultured in 10 cm dishes until 80-90% confluence. After reaching the appropriate confluence, medium was changed and the cells were transfected with a transfection mixture of 4 µg pMDG.2, 4 µg psPAX2 and 8 µg of the expression vector containing the construct of interest using poly-ethylenimine (PEI). The Transfection mixture was added dropwise to cells and culture medium was exchanged the next day. After 3 days, virus containing supernatant was harvested, centrifuged at 4,000 x g for 10 mins and filtered (Millex-HA, 0.45 µm, Millipore, SLHA033SS). Purified virus was concentrated by ultracentrifugation at 27,000 rcf in an SW40 Ti rotor (Beckman-Counter) at 4 °C for 2 h and stored at -80 °C.

For transduction of T84 cells with lentivirus, 300,000 cells per well were seeded in a 6-well plate and 20-40 µl of the concentrated lentivirus stock was added in 3 mL of cell culture medium together with 10 µg/ml polybrene. After two days, cells were transduced for second time with the same mixture of lentivirus stock and polybrene and two days later, the medium was replacing with selection medium containing the appropriate antibiotic (10 µg/mL puromycin or blasticidin). Cells were cultured in selection medium for 2-3 weeks, before being used for experiments.

2.2.3 Cell biology techniques and protein biochemistry

2.2.3.1 Protein extraction and quantification

At the time of harvesting, media was removed, cells were rinsed one time with 1 x cold PBS and lysed with 1 x RIPA buffer. Cells were incubated at 4 °C for 20 mins. Afterwards, lysates were collected and centrifuged at 12,000 rpm for 20 mins at 4 °C. Supernatant was transferred to a new tube and protein concentration was determined using the DC Protein Assay Kit I (Bio-Rad), according to the manufacturer's instructions. Absorption was measured at a wavelength of 750 nm using the Bio-Rad iMark microplate reader and protein concentration was calculated by using the BSA standard curve.

2.2.3.2 Western blot (WB)

Lysates of equal protein amounts (6-12 µg, depending on the experiment) were supplemented with laemmli buffer, boiled at 95 °C for 10 mins, spun down at 12,000 rpm for 1 min and separated by sodium dodecyl sulfate polyacrylamide gel electrophoresis (SDS-PAGE). Proteins were separated according to their electrophoretic mobility in 8-12% SDS-PAGE gels at 120 V. For immunoblotting, proteins were transferred to a nitrocellulose blotting membrane with 0.45 µm pore size (GE Healthcare) by wet blotting at 100 V for 1.5 h in pre-cooled transfer buffer by using the Bio-Rad Tank blot system. After blotting, membranes were blocked for 1-2 h shaking at RT in TBS containing 0.1% Tween 20 (TBS-T) with 5% milk or 5% BSA. Primary antibodies were diluted in blocking buffer and incubated overnight at 4 °C. Membranes were washed in TBS-T for 4 x 10 mins at RT. Secondary antibodies were diluted in blocking buffer and incubated at RT for 1 h with rocking. Membranes were washed in TBS-T for 4 x 10 mins at RT. For protein visualization, HRP detection reagent (ECL Western Blotting Detection Reagents or Western Bright Chemiluminescent Substrate Sirius) was mixed 1:1 and incubated at RT for 3-5 mins. Membranes were exposed to high performance chemiluminescence films (GE healthcare) and developed. Quantitative immunoblot analysis was performed using Fiji software.

2.2.3.3 Indirect Immunofluorescence (IFA)

T84 cells were seeded in a 24-well plate and fixed in 2% paraformaldehyde for 20 mins at RT and washed with PBS and permeabilized using 0.5% Triton X-100 for 15 mins. After blocking with 3% BSA in PBS for 1 h at RT, cells were incubated with primary antibodies in 3% BSA for 1 h at RT. After washing with PBS, cells were stained with secondary antibodies in 3% BSA for 45 mins at RT. To stain human mini-guts, organoids were embedded in optimal cutting temperature (OCT) compound (Tissue-Tek) and cryo-sectioned using the Leica CM1950 (Leica) cryostat. Afterwards, 10 µm cryosections were fixed in 80% ethanol for 10 mins at RT, followed by a 2-min incubation in ice-cold acetone. After blocking in 5% goat serum in PBS containing 1% triton for 1 h at RT, sections were incubated with primary antibodies in blocking solution for 2 h at RT or overnight at 4 °C. After washing in PBS, sections were stained with secondary antibodies in 1% BSA in PBS containing 0.5% Triton for 2 h at RT. Nuclear DNA was stained with ProLong Gold DAPI. Slides were imaged by epifluorescence using a Nikon Eclipse Ti-S (Nikon) microscope or by confocal tile scans on a Zeiss LSM 780 (Zeiss) microscope. Image processing was performed using Fiji software. For infection experiments, the percentage of infected cells was determined by counting at least 600-1,000 cells detected in 10 fields of view for each condition.

2.2.3.4 VSV luciferase assay

Luciferase activity was measured as read out for VSV-Luc replication. T84 cells were seeded in a white F-bottom 96-well plate (Greiner bio-one) 1-day prior to experiment. Cells or organoids were pre-treated prior to infection or treated post-infection as indicated with increasing concentrations of type I or type III IFNs. VSV-Luc was added to the wells and the infection was allowed to proceed for 8 h. At the end of the infection, media was removed, cells were washed 1 x with PBS and lysed with luciferase cell Lysis Buffer (Promega) at RT for 20 mins. A 1:1 dilution of Steady Glo (Promega) and Lysis Buffer were added to the cells and organoids and incubated at RT for 15 mins. Luminescence was measured using a Tecan Infinite M200 Pro.

2.2.3.5 STATs multiplex Luminex assay

At time of harvest, media was removed, cells were rinsed one time with 1 x PBS and lysed with 1 x MILLIPLEX MAP Lysis buffer (EMD Millipore catalog# 43-040) supplemented with protease inhibitors (Sigma-Aldrich) for 20 mins at 4 °C. Lysates were collected, filtered (EMD Millipore catalog# UFC30DV00) and equal protein amounts were used to detect the phospho STATs presence using the phospho STATs (STAT1 (Tyr701), STAT2 (Tyr690), STAT3 (Tyr705), STAT5A/B (Tyr694/699) and STAT6 (Tyr641)) Magnetic Bead Mapmate kit (EMD Millipore catalog# 48-610MAG) according to manufacturer's instructions.

2.2.3.6 DRAQ5 fluorescent probe assay

HepaRG cells were seeded in a clear bottom 96-well plate. Cells were pre-treated prior to infection as indicated time points and concentrations of IFN-λ3, IFN-λ4 and its variants K154E, P70S. EMCV was added to the wells and the infection was allowed to proceed for 24 h. Cells were fixed with 2% PFA for 20 mins at RT. Cells were permeabilized in Triton-X (0.5% in PBS, v/v) for 15 mins at RT. Cells were washed with PBS 3 times after permeabilization. Cells were treated with DRAQ5 fluorescent probe (0.01%, in BSA-PBS (1%, w/v), v/v) for 30 mins at RT. HepaRG cells were light-protected during DRAQ5 treatment. Cells were washed with PBS for 3 times prior to measurement by Li-COR Odyssey@ CLx imaging system.

2.2.4 RNA analysis

2.2.4.1 RNA purification and cDNA-synthesis

Purification of total RNA from cells or mini-gut organoids were performed using the

NucleoSpin RNA extraction kit (Macherey-Nagel) according to manufacturer's instructions. In summary, cell lysates were passed through a DNA elimination column and the flow through was mixed with 70% ethanol, added to a RNeasy spin column, allowing RNA binding to the membrane. Columns were washed with two buffers of decreasing salt concentration and RNA samples were eluted in 40-60 µl nuclease free water and stored at -80 °C for further analysis. RNA concentration was determined by measuring the absorbance at 260 nm with the NanoDrop Lite spectrophotometer (Thermo Fisher Scientific). For cDNA generation, 50-200 ng of total RNA was reverse transcribed using the iScript™ cDNA Synthesis kit (Bio-Rad) according to the manufacturer's instructions using the following reaction:

Table 7. Components of cDNA synthesis reaction

Component	Volume (µl)
iScript reaction buffer	**4**
Reverse transcriptase	**1**
RNA template (50-200 ng)	**15**

Components were mixed, and reverse transcription was performed according to the following program using the thermal cycler (Bio-Rad):

Table 8. Thermal cycler program for cDNA synthesis

Step	Temperature (°C)	Time (min)
Priming	25	5
Reverse transcription	42	30
Reverse transcription termination	85	5

2.2.4.2 Quantitative real time polymerase chain reaction (qRT-PCR)

Following cDNA-synthesis, the resulting cDNA was diluted 1:1 with nuclease-free water before proceeding to the quantitative real time polymerase chain reaction (qRT-PCR). qRT-PCR was performed in 96-well format using SSO Advanced Universal SYBR Green Supermix (Bio-Rad) with the following reaction per well:

Table 9. Components of the qRT-PCR reaction

Component	Volume (µl)
SSO Advanced Universal SYBR Green Supermix	7,5

Primer reverse (2 µM)	1,9
Primer forward (2 µM)	1,9
Millipore H_2O	1,7
cDNA (1:2 diluted)	2

The reaction was performed using the Bio-Rad CFX96 Real-Time PCR Detection System with the following settings:

Table 10. Program for qRT-PCR

Step	Temperature (°C)	Time	Number of cycles
Activation	95	30”	
Melting	95	5”	40
Primer annealing and Elongation	60	30”	40
Plate read			
Melting curve generation	65	5”	
		+0,5 °C/cycle to 95 °C	

The obtained data were then analyzed with the Bio-Rad CFX Manager 3.0 using HPRT1 and/or TBP as housekeeping genes to normalize mRNA expression. The data obtained by qRT-PCT were calculated as relative expression levels (ΔΔCq) normalized to input mock sample of initial time point.

2.2.4.3 mRNA sequencing

Raw RNA sequencing reads (fastq) were aligned to the ensembl human GRCh38 genome reference using Rsubread (Liao, Smyth et al. 2014) with default settings. Read summarization was done using feature counts (Liao, Smyth et al. 2014). Various quality metrics of the raw reads and alignment statistics were analyzed using Multi-QC (Ewels, Magnusson et al. 2016). Differential gene expression analysis was performed using DSeq2, rlog transformed data was used for multi-dimensional scaling and clustering analyses. Signaling programs were quantified using *PROGENy* (Schubert, Klinger et al. 2018).

Transcription factor activities were computed using *DoRothEA* (Garcia-Alonso, Holland et al. 2019) and VIPER (Alvarez, Shen et al. 2016). Enrichment analysis on the most differentially expressed genes (-1< logFC >+1 and adjusted p value < 0.05) was performed using enrichR (Kuleshov, Jones et al. 2016).

2.2.5 Organoid techniques

2.2.5.1 Single molecule RNA fluorescence in situ hybridization on human intestinal organoid

Hybridization buffer containing probe was prepared and 2 µl of probe stock was mixed with 200 µl of hybridization buffer for one sample. The final working probe solution is 125 nM. Organoids were washed in Wash Buffer A for 2-5 mins and subsequently Wash Buffer A was removed. Afterwards, organoids were incubated with Hybridization Buffer containing probe in the dark at 37 °C for at least 4 h (up to 16 h). Then, hybridization Buffer containing probe was removed and organoids were washed by Wash Buffer A in the dark at 37 °C for 30 mins. Subsequently, Wash Buffer A was removed, and organoids were stained with DAPI in the dark at 37 °C for 30 mins. Then, DAPI was removed, and organoids were washed with Wash Buffer B for 2-5 mins. Afterwards, wash buffer B was removed. Then, 20-50 µl of prolong gold mounting media was used to mix organoids and transferred into an 8-well chamber slide for imaging (Femino, Fay et al. 1998, Tesch, Lan et al. 2006, Raj, Van Den Bogaard et al. 2008).

2.2.5.2 Immunofluorescence staining of human intestinal organoid

Medium was removed and discarded from wells containing organoids. Pipette tips were coated with FBS before using to prevent organoids sticking to the inner wall of tips. Then 1 mL of cold cell recovery solution was added to the well using the coated tips. Organoids stayed in the cell recovery solution for 3-5 mins and were transferred to the coated microcentrifuge tube. Subsequently, organoids were incubated on ice for 20-30 mins and tubes with organoids were inverted regularly to prevent clumping and heterogeneous Matrigel dissociation. Incubation on ice should be stopped when Matrigel is sufficiently dissolved, which can be checked under a microscope. After that, organoids were spined for 5 mins at 400 rpm/min and 4 °C. Supernatant was removed and 1 mL of 4% formaldehyde was applied to fix organoids for 2 h at RT with constant rolling of the tube to ensure homogeneous fixation. After fixation, organoids were permeabilized using 1 mL permeabilization buffer for 1-2 h at RT with constant rolling. Afterwards, organoids were incubated in 1 mL blocking buffer for 1 h at RT with constant rolling. Then, 200-500 µl of

primary antibodies diluted in blocking buffer was used to incubate organoids over night at 4 °C with constant rolling. Subsequently, organoids were washed in 3 times of PBS for 10 mins at RT with constant rolling. After washing, 200-500 µl of secondary antibodies and DAPI diluted in blocking buffer was used to incubate organoids for 1-2 hours in the dark at 4 °C with constant rolling. Organoids were washed 3 times with PBS and once with Milli-Q-purified water to prevent crystal formation. Then, 20-50 µl of prolong gold mounting media was used to mix organoids and transferred into an 8-well chamber slide for imaging.

2.2.5.3 EdU (5-ethynal-2'-deoxyuridine) incorporation cell proliferation assay

Stock solutions of EdU and buffer additive were prepared and put at -20 °C for further steps. Prior to incubation of EdU and organoids, a 2-x working solution of EdU was prepared in fresh medium and pre-warmed for next step. Half of the organoid medium was replaced with the 2-x EdU. Organoids were incubated with 1 x EdU for 6 h. Afterwards, organoids were collected, fixed and permeabilized according to the method in the section *4.2.5.2*. After that, a reaction cocktail is prepared for next step (Table 11). The prepared reaction cocktail should be used in 15 mins.

Table 11. The reaction cocktail in the same order as described in the following table

Material	Component colour code	1 assay	2 assays	5 assays	10 assays
Deionized water	Not provide	379 µl	758 µl	1895 µl	3790 µl
Reaction buffer (10x)	orange	50 µl	100 µl	250 µl	500 µl
Catalyst solution	green	20 µl	40 µl	100 µl	200 µl
Dye Azide (10 mM)	red	1 µl	2 µl	5 µl	10 µl
Buffer additive (10x)	blue	50 µl	100 µl	250 µl	500 µl
Total volume		500 µl	1 mL	2.5 mL	5 mL

Then, organoids were incubated in 500 µl of reaction cocktail for 1 h at RT without light. Afterwards, the reaction buffer was removed, and organoids were washed for 3 times with PBS. To prevent crystal formation, organoids were washed again with Milli-Q-water. Finally, 20-50 µl of prolong gold mounting media was used to mix organoids and transferred into an 8-well chamber slide for imaging.

3 Results

3.1 Interaction of type I and III Interferon pathways

The text and figures of this part have been adapted from (Pervolaraki, Guo et al. 2019).
Given that type I and type III IFNs activate the same JAK/STAT pathway and induce almost identical pools of ISGs, it has been suggested that both IFNs have redundant functions. Nevertheless, recent studies reported that type I IFN and type III IFN lead to the distinct magnitude and kinetics of induction of ISGs in epithelial cell lines and intestinal organoid models (Pervolaraki, Rastgou Talemi et al. 2018). It is increasingly documented that signal transduction pathways induced by type I and type III IFNs are different in regulating the production and patterns of ISGs. Nonetheless, it is still not explored whether there is an interaction occurring between the type I and type III IFN signalling pathways. To directly investigate whether the absence of a functional type III IFN mediated signalling cascade can impact type I IFN signalling and vice versa, intestinal epithelial cells where either the type I or type III IFN receptors knockout were constructed. Using this method, I explored that the deficiency in type I or type III IFN receptors influenced the production of ISGs and antiviral activity of the reciprocal IFN.

3.1.1 Type I and type III IFN receptor specific knock-outs alter interferon stimulated gene expression

As the downstream signaling of the type I and type III IFNs is similar, it is important to know whether both receptors could regulate each other's signal transduction and antiviral activity through an inter-receptor molecular crosstalk. To check a functional interaction between type I and type III signal cascades, the transcriptional activity of IFNs in T84 cells deficient for either the IFNAR1 (IFNAR1$^{-/-}$) or the IFNLR1 (INFLR1$^{-/-}$) (Pervolaraki *et al.*, 2017) was explored. IFNAR1$^{-/-}$ T84 cells exhibited a higher base line expression of ISGs (IFIT1 and Viperin) compared to WT cells, whereas IFNAR1$^{-/-}$ T84 cells displayed a greatly reduced base line expression of ISGs (IFIT1 and Viperin) (Figure 3-1A-B). Wild type (WT) and receptor knock-out cells were treated with type I or type III IFNs and the expression levels of two representative ISGs (IFIT1 and Viperin) were detected at different time points post-IFN treatment. IFNAR$^{-/-}$ cells displayed a decrease in the levels of IFIT1 and Viperin expression especially at later time points following type III IFNs treatment (Figure 3-1C-D). On the contrary, IFNLR1$^{-/-}$ cells showed increased expression levels of ISG induction upon

type I IFN treatment compared to WT cells (Figure 3-1E-F). There is no change in kinetic pattern of ISG induction in receptor deficient cells compared to WT cells. Notably, in all cell lines type III IFN treatment induces lower magnitude of ISG expression with delayed ISG expression compared to type I IFN treatment, consistent with previous reports (Marcello, Grakoui et al. 2006, Bolen, Ding et al. 2014, Jilg, Lin et al. 2014, Bhushal, Wolfsmüller et al. 2017, Pervolaraki, Stanifer et al. 2017, Pervolaraki, Rastgou Talemi et al. 2018).

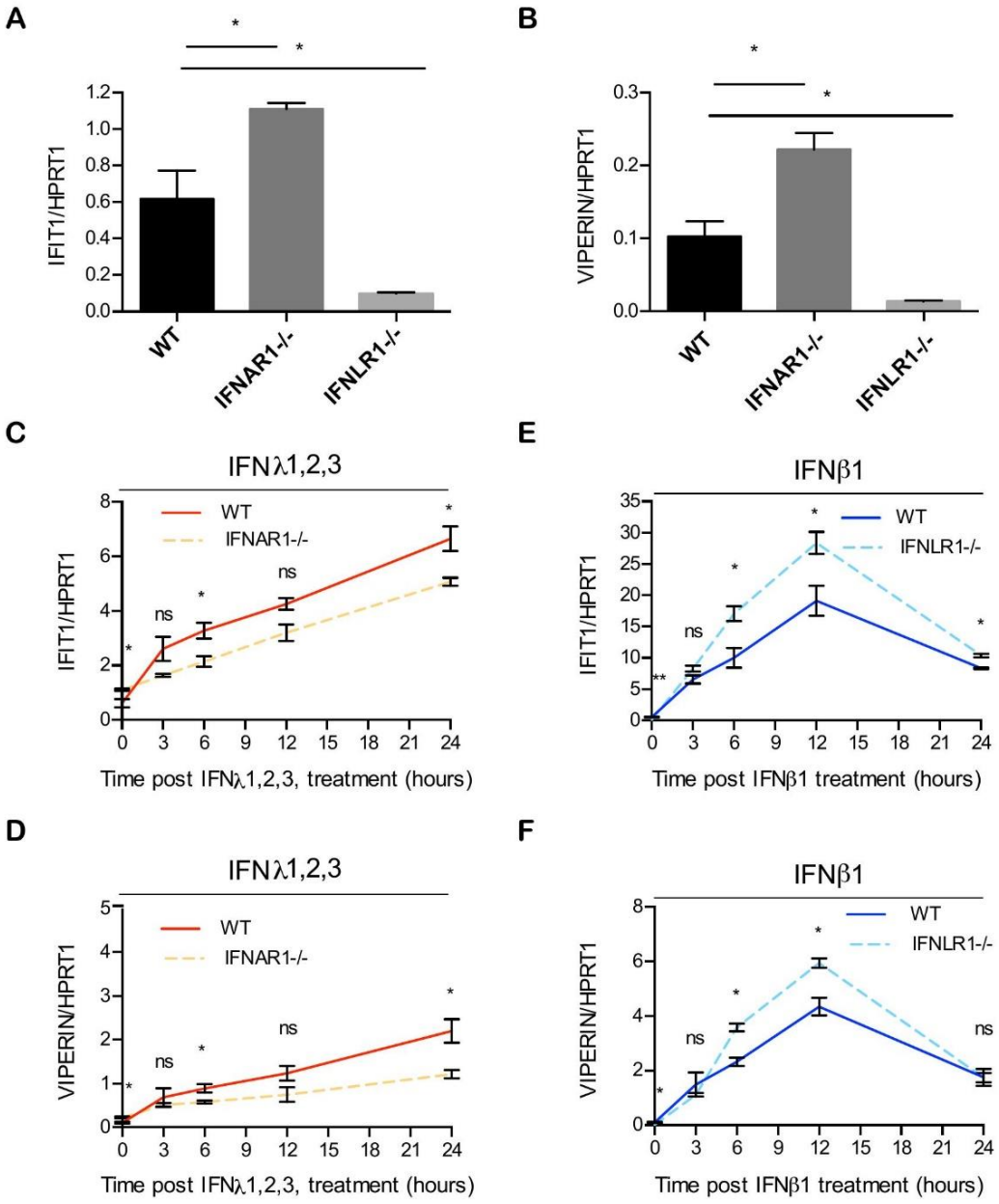

Figure 3-1. IFN receptor knockouts show differential levels of ISG expression. (A-B) The basal transcript levels of (A) IFIT1 and (B) Viperin were quantified in WT, IFNAR1$^{-/-}$ and IFNLR1$^{-/-}$ T84 cells by qRT-PCR. (C-D) WT and IFNAR1$^{-/-}$ T84 cells were treated with 300 ng/mL of type III IFNs (100 ng/mL of each IFN-λ1, 2, 3). Cells were harvested at indicated time points and the transcript levels of the ISGs were evaluated by qRT-PCR. (E-F) WT and IFNLR1$^{-/-}$ T84 cells were treated with 2000 IU/mL of type I IFN (β). Cells were harvested at indicated time points and the transcript levels of the ISGs were evaluated by qRT-PCR. Experiments were performed in triplicate; error bars indicate standard deviation. *$P < 0.05$, ns means not significant (unpaired *t*-test).

To directly monitor if the difference in ISG expression is the result of the knock-out of the individual IFN receptors, rescue experiments were performed through transducing CRISPR/Cas9 guide RNA resistant IFNAR1 or IFNLR1 constructs into the corresponding IFN receptor knock-out cells. As previously reported in my group, the ISG expression can be rescued in the overexpression of the IFN receptors in the corresponding knock-out cell lines (Pervolaraki, Rastgou Talemi et al. 2018). Importantly, rescue of IFNAR1 in the IFNAR1$^{-/-}$ cells increased ISG production upon type III IFN treatment (Figure 3-2A-B). However, rescue of IFNLR1 in IFNLR1$^{-/-}$ cells decreased ISG expression upon type I IFN treatment (Fig 3-2C-D). Altogether, these results strongly indicated that a functional crosstalk occurred between the signaling pathways downstream of both type I and III IFN receptors, where the type III IFN receptor negatively regulates type I IFN signaling while type I IFN receptor positively regulates the type III IFN signalling.

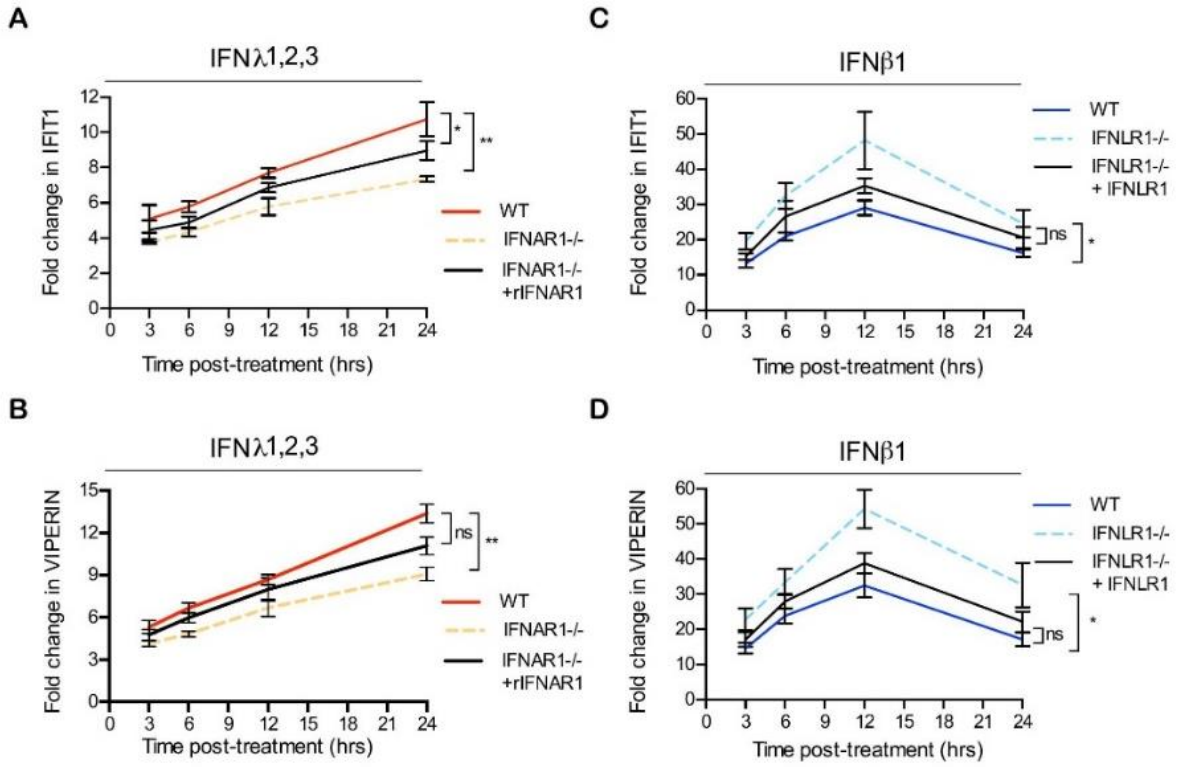

Figure 3-2. Trans-complementation of IFN receptor in IFN receptor knock-out cells rescue ISG expression. (A-B) IFNAR1$^{-/-}$ cells were transduced with lenti-viruses expressing CRISPR/Cas9 cleavage resistant IFNAR1 (rIFNAR1) to rescue the knock-out phenotype. WT, IFNAR1$^{-/-}$ and IFNAR1$^{-/-}$ over expression IFNAR1 (IFNAR1$^{-/-}$ + rIFNAR1) T84 cells were treated with 300 ng/mL of type III IFNs (100 ng/mL of each IFN-λ1, 2, 3). Cells were harvested at indicated time points and the expression of the ISGs was evaluated by qRT-PCR. (C-D) IFNLR1$^{-/-}$ cells were transduced with lentiviruses expressing CRISPR/Cas9 cleavage resistant IFNLR1 (rIFNLR1) to rescue the knock-out phenotype. WT, IFNLR1$^{-/-}$ and IFNLR1$^{-/-}$ over expression IFNLR1 (IFNLR1$^{-/-}$ + rIFNLR1) T84 cells were treated with 2000 IU/mL of type I IFN (β). Cells were harvested at indicated time points and the upregulation of the ISGs was evaluated by qRT-PCR. Experiments were performed in triplicate; error bars indicate standard deviation. *P < 0.05, **P < 0.01, ns means not significant (unpaired t-test), each point was evaluated and the whole data set showed the same statistics which is displayed at the end for clarity.

3.1.2 IFN receptor specific neutralizing antibodies reveal a functional crosstalk between type I and III IFNs

To determine whether the differential induction of ISGs seen in the IFN receptor knock-out cell lines could be blocked through acute inhibition of IFN signaling, neutralizing antibodies were applied against each IFN receptor. T84 cells were treated with either IFNAR2 or IFNLR1 antibody prior to treatment with type I or type III IFN, respectively (Figure 3A). Pre-treatment of cells with the IFNAR neutralizing antibody resulted in decreased ISG production upon type I IFN treatment (Figure 3-3A) or while IFNLR resulted in deceased ISG production upon type III IFN treatment (Figure 3-3C). Interestingly IFNAR neutralization led to a decrease in ISG expression following type III IFN treatment (Figure 3-3A) while IFNLR neutralization led to an increase in type I IFN signaling (Figure 3-3C) consistent with the results in knock-out cells. To address whether the decrease in ISG production correlated with reduction in antiviral potency, T84 cells were mock treated or treated with the IFNAR2 or IFNLR1 neutralizing antibody prior to stimulation of cells with type I IFN or type III IFN, respectively. Subsequently, T84 cells were infected by VSV expressing a luciferase reporter (VSV-luc) (Figure 3-3B). As expected, the decrease in ISG levels led to an increase in VSV-luc replication (Figure 3-3B-D). Notably, inhibition of the type III IFN signaling caused an increase in the level of ISG expression and antiviral potent upon type I IFN treatment (Figure 3-3D). Conversely, inhibition of the type I IFN receptor led to a significant reduction in type III IFN-mediated ISG induction and antiviral activity (Figure 3-3B). This demonstrates that the type I IFN receptor upregulates type III IFN-mediated ISG induction and antiviral activity whereas type III IFN receptor downregulates type III IFN-mediated induction of ISGs and antiviral function.

All together these results confirm the observations from the knock-out cells showing the positive influence of the type I IFN receptor on type III IFN-mediated signaling and function as well as the negative crosstalk that the type III IFN receptor plays on type I IFN-mediated signaling.

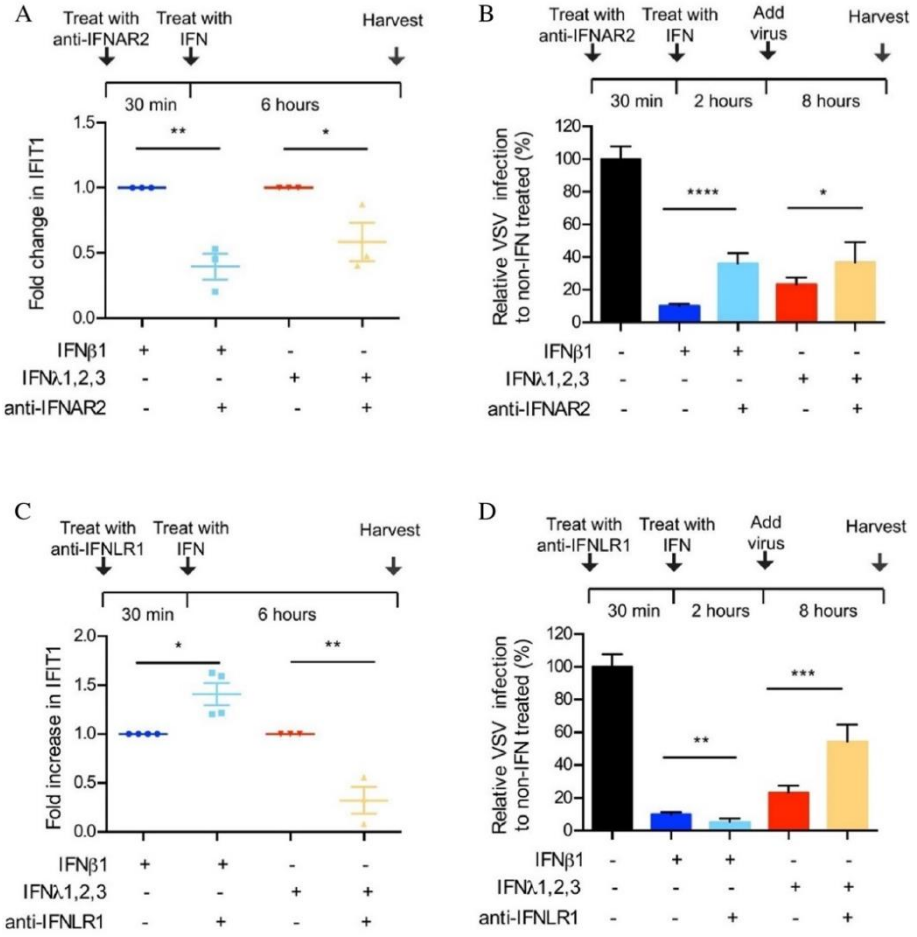

Figure 3-3. Neutralizing antibody treatment of human IECs confirms the crosstalk between the type I and III IFN receptors. (A) Schematic depiction of neutralizing antibody experiment to test for effect of receptor inhibition on ISG induction. T84 cells were treated with an IgG antibody (5 ng/mL) and a neutralizing antibody against IFNAR2 (5 ng/mL) or a neutralizing antibody against IFNLR1 (5 ng/mL) 30 mins prior to 100 IU/mL of type I IFN (β) treatment. Antibody was maintained during IFN treatment and the upregulation of the ISG IFIT1 was evaluated by qRT-PCR 6 h post-IFN treatment. (C) Same as A except cells were treated with 1 ng/mL type III IFN. (B) Schematic depiction of neutralizing antibody experiment to test for effects of receptor inhibition on antiviral function. T84 cells were treated with an IgG antibody (5 ng/mL), a neutralizing antibody against IFNAR2 (5 ng/mL) or a neutralizing antibody against IFNLR1 (5 ng/mL) 30 mins prior to 100 IU/ml of type I IFN (β) treatment. IFN and the neutralizing antibody were maintained 2 hours prior to infection of cells by vesicular stomatitis virus expressing luciferase (VSV-luc). Infection was performed in the presence of both the neutralizing antibody and IFN. Virus infection was evaluated 8 h post-infection by bioluminescence measurements. (D) Same as B except cells were treated with 1 ng/mL of type III IFN. Experiments were performed in triplicate; error bars indicate standard deviation. **P* < 0.05, ***P* < 0.01, ****P* < 0.001, *****P* < 0.0001, ns means not significant.

3.1.3 Differential activity of type I and III IFN signaling pathway is not due to different expression levels of receptors

The observed increased activity of type I IFN-mediated signaling in the absence of type III IFN receptor could attribute to an increase in the type I IFN receptor levels. Similarity, the reduced type III IFN activity in the absence of type I IFN receptor could be explained by a decrease in the IFNLR1 expression levels. To determine these possibilities, the levels of

both receptors were evaluated in WT, IFNLR1$^{-/-}$ and IFNAR1$^{-/-}$ cells. Data showed that the basal level of IFNLR1 were unchanged in in IFNAR1$^{-/-}$ cells (Figure 3-4B), while the levels of IFNLR1 were slightly reduced in IFNLR1$^{-/-}$ cells compared to WT cells (Figure 3-4A). Notably, the decrease was only minimum and inadequate to explain the upregulation in type I IFN signaling upon genetic ablation of IFNLR1 (Figure 3-3C) or upon treatment of cells with an anti-IFNLR1 neutralizing antibody (Figure 3-3A and 3-3C). In addition, the levels of IFNAR2 and IFNLR1 were controlled by qRT-PCR. WT cells treated with either type I or III IFN show similar IFNAR1 or IFNLR1 expression levels compared to mock treated WT cells (Figure 3-4A-B). Afterwards, IFNAR1$^{-/-}$ cells were treated with type III IFN and the levels of IFNLR1 were measured by qRT-PCR. As with WT cells, there was no change in receptor level in knock-out cells in the presence or absence of type III IFN treatment (Figure 3-4B). Similarly, IFNLR$^{-/-}$ cells did not display a change in IFNAR1 levels in knock-out cells upon type III IFN treatment or in mock treated conditions (Figure 3-4A). Together, these results demonstrated that the distinct ISG expression and antiviral potency observed upon IFN receptor knock-out or inactivation were not due to changes in the reciprocal IFN receptor levels.

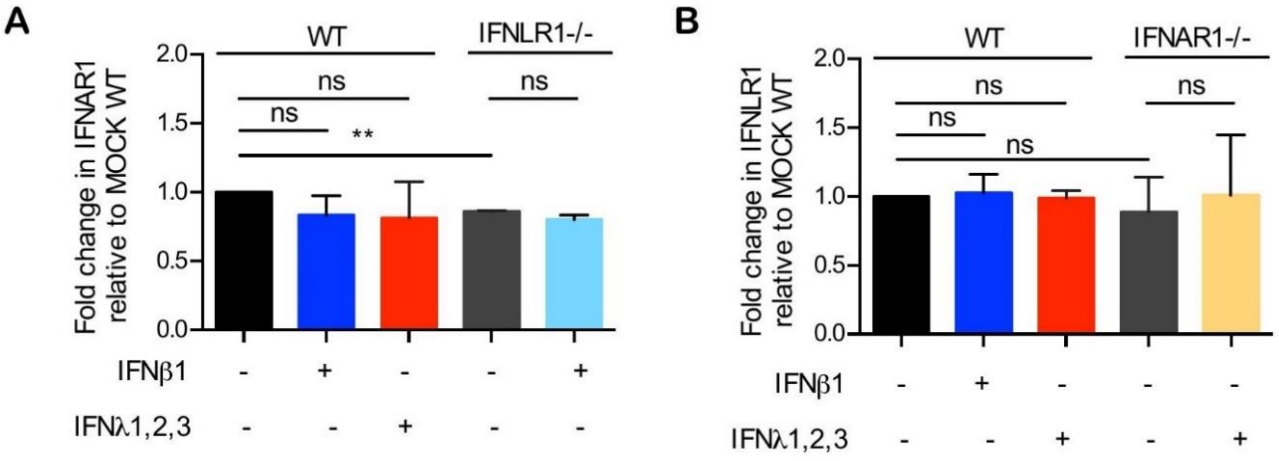

Figure 3-4.IFN receptor levels are not altered in reciprocal IFN receptor knock-out cells. (A) WT and IFNLR1$^{-/-}$ cells were treated with 2000 IU/mL of type I IFN (β) or 300 ng/mL of type III IFNs (100 ng/mL of each IFN-λ1, 2, 3) and the levels of IFNAR1 were evaluated 12 h post-treatment by qRT-PCR. (B) WT and IFNAR1$^{-/-}$ cells were treated with 2000 IU/mL type I IFN (β) or 300 ng/mL of type III IFNs (100 ng/mL of each IFN-λ1, 2, 3) and the levels of IFNLR1 were evaluated 12 h post-treatment by qRT-PCR. Experiments were performed in triplicate, error bars indicated standard deviation, ns means not significant (unpaired *t*-test).

3.1.4 Modulation of STAT1 expression levels and STAT1 activation drives the differential IFN-mediated signaling observed upon IFN receptor knock-out

As JAK/STAT signaling molecules are the critical proteins in the signaling downstream of type I and III IFN receptors, I investigated whether the observed crosstalk arises from differential induction of STAT1. Luminex assay was employed to compare the phosphorylation kinetics of STAT1 in IFNAR1$^{-/-}$ and WT cells treated with type III IFN. Consistent with the ISG induction (Figure 3.1), reduced amount of STAT1 phosphorylation (p-STAT1) was detected in IFNAR1$^{-/-}$ cells compared to WT cells upon type III IFN treatment (Figure 3-5A). Additionally, western blot analysis was applied to verify the activation pattern of p-STAT1 and explore the total level of STAT1 in IFNAR1$^{-/-}$ cells (Figure 3-5B and C). As with the Luminex data, the western blot displayed a reduction in p-STAT1 levels in IFNAR1$^{-/-}$ cells treated with type III IFN compared to WT cells (Figure 3-5B-C). Analysis of the total STAT1 levels showed that there was no significant distinction between WT and IFNAR1$^{-/-}$ cells in both mock and type III IFN treated cells (Figure 3-6A).

The kinetics of STAT1 activation in IFNLR1$^{-/-}$ and WT cells upon treatment with type I IFN were furtherly investigated through Luminex assay. The phosphorylation of STAT1 was upregulated in IFNLR1$^{-/-}$ cells upon type I IFN treatment (Figure 3-5E) which is consistent with the increase in ISG levels detected after IFN treatment (Figure 3-1). Subsequent western blot analysis confirmed the increased activation of p-STAT1 in IFNLR1$^{-/-}$ cells upon type I IFN treatment compared to WT cells (Figure 3-5F-H). Quantification of total STAT1 levels showed no major difference between IFNLR1$^{-/-}$ and WT cells (Figure 3-6B). Altogether, these results reveal a functional crosstalk between type I and III IFN receptors where the type I IFN receptor upregulates type III IFN signaling by fostering STAT1 phosphorylation and conversely where type III IFN downregulates type I IFN signaling through reducing STAT1 phosphorylation.

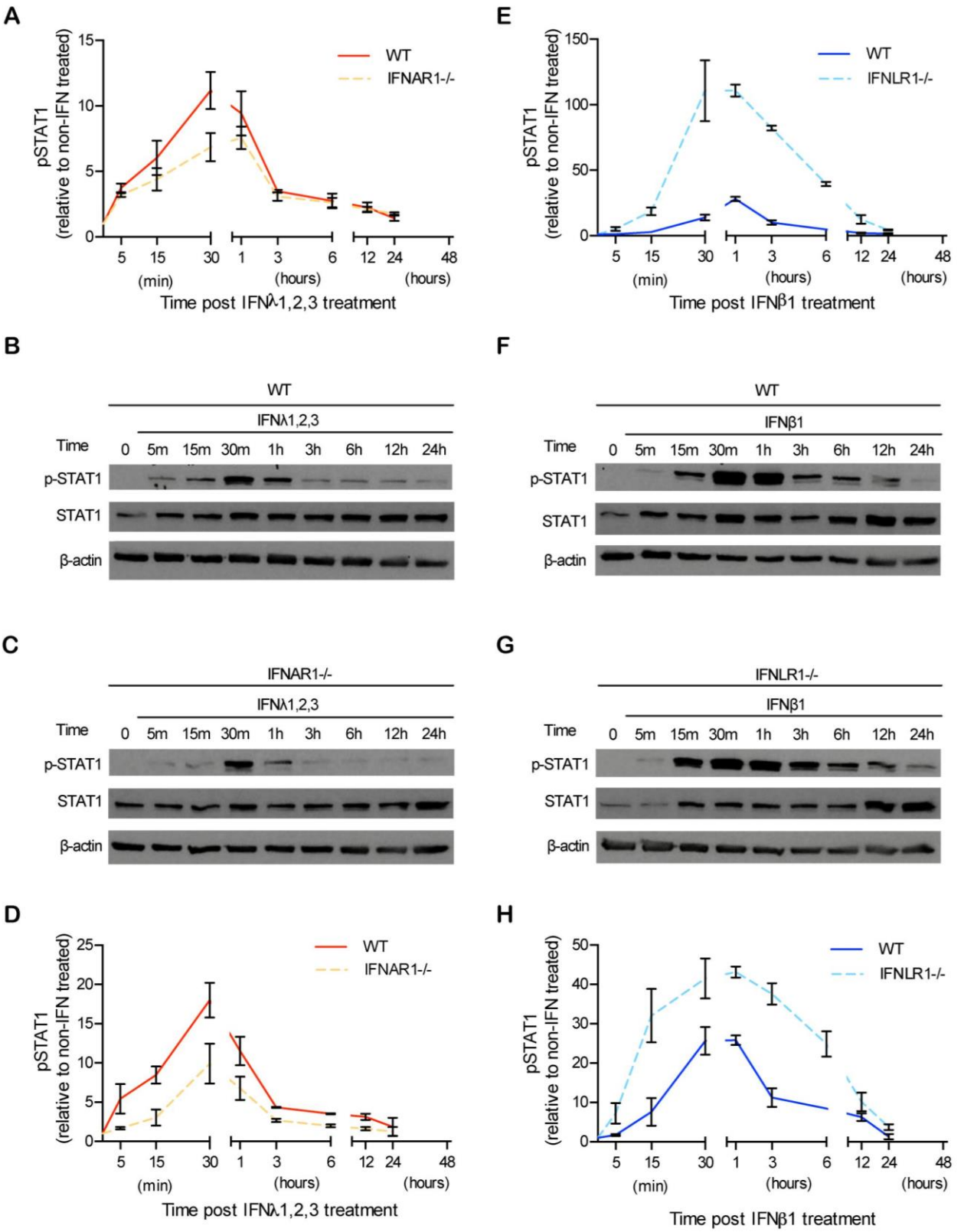

Figure 3-5. IFN receptor knock-out influence the activation of STAT1. (A) WT and IFNAR1$^{-/-}$ cells were treated with 300 ng/mL of type III IFN (100 ng/mL of each IFN-λ 1,2,3). At indicated time points cells were harvested and the levels of STAT1 phosphorylation was assessed by Luminex assay. (B-C) Same as A except that activation was followed by monitoring the level of p-STAT1 using western blot. (D). Quantification of p-STAT1 shown in B and C using non-treated cells as the normalizing control. (E-H) Same as A-D except that IFNLR1$^{-/-}$ cells were treated with 2000 IU/mL of type I IFN (β). Experiments were performed in triplicate; error bars show standard deviation.

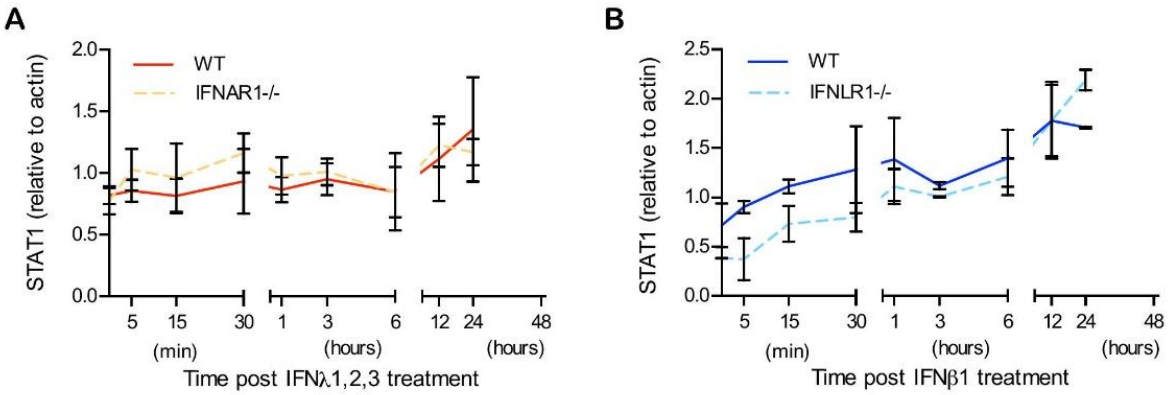

Figure 3-6. Quantification of total STAT1 levels in IFN receptor knock-out cells. WT, IFNAR1$^{-/-}$ and IFNLR1$^{-/-}$ cells were treated with either 300 ng/mL of type III IFN (100 ng/mL of each IFN-λ1,2,3) or 2000 IU/mL of type I IFN (β) respectively. At indicated time points cells were harvested and the levels of STAT1 was assessed by western blot. (A)Total level of STAT1 was quantified from figure 3-5 B-C and (B) from figure 3-5 F-G and β-actin was used as loading control to normalize the quantification. Experiment was performed in triplicate; error bars indicate standard deviation.

3.2 Conserved induction of distinct antiviral kinetics by primate IFN lambda 4

The text and figures of this part have been adapted from (Guo, Reuss et al. 2021).
IFNs were discovered to inhibit virus infection in 1950s (Isaacs and Lindenmann 1957). They include three types: I, II and III. For type III IFNs, there are four members, IFN-λ1, 2, 3 and 4. IFN-λ4 was newly discovered member of type III IFNs in 2013 and was found to be associated with HCV clearance (Prokunina-Olsson, Muchmore et al. 2013). *IFNL4* gene is in the upstream of *IFNL3* and is very diversity due to variants within the *IFNL4* gene (Prokunina-Olsson, Muchmore et al. 2013).

Two variants were identified through the functional diversity analysis of IFN-λ4. One variant is an additional hypoactive variant L79F (leucine to phenylalanine at position 79), and another is K154E (lysine to glutamic acid at position 154), which greatly improve IFN-λ4 antiviral potent by enhancing its secretion and potency (Bamford, Aranday-Cortes et al. 2018). Interestingly, K154 is widely distributed in the human population whereas E154 is the conserved amino acid at this position in non-human primates and other mammals. Thereby, chimpanzee and rhesus macaque IFN-λ4 have stronger antiviral potent compared to human IFN-λ4, which can be reversed by an E154 mutation. However, it remains poorly understood that what unique biological features IFN-λ4 exhibits. Accordingly, I compared the kinetics of signaling and antiviral potency of a series of IFN-λ4 variants with IFN-λ3 in hepatocytes and intestinal epithelial cells.

3.2.1 IFNs display unique STAT1 phosphorylation kinetics

IFN-λs bind to their receptor complex and activate downstream signaling cascades, ultimately establishing an antiviral state (Kotenko, Gallagher et al. 2003). The JAK/STAT pathways are activated following by IFN-λ binding. An emerging point is that the critical determinant of the antiviral activity of IFN-λs is the kinetics of such downstream response of JAK/STAT (Obajemu, Rao et al. 2017, Pervolaraki, Rastgou Talemi et al. 2018). To determine the temporal basis of IFN-λ signaling, the phosphorylation of STAT1 at Y701 was measured over time. Human hepatocyte, HepaRG cells were stimulated with equivalent amounts of IFN-λs (IFN-λ3, IFN-λ4 WT, P70S, L79F, and K154E) for 15, 30, 60, 120, 240 mins and 24 h. After the stimulation, protein lysates were collected and STAT1 phosphorylation was determined by immunoblot (Figure 3-7A). Conditioned media generated post-transfection of an EGFP plasmid served as a negative control. Results

revealed that all IFN-λs could induce the production of p-STAT1 (Figure 3-7A, quantified in Figure 3-8A). L79F induced significantly low levels of p-STAT1 which related to its limited activity as previously described (Bamford, Aranday-Cortes et al. 2018). Notably, IFN-λ3 and IFN-λ4 variants activated different kinetics of p-STAT1 phosphorylation (Figure 3-7A and Figure 3-8A). Interestingly, IFN-λ4 WT and P70S showed a peak at 30 mins to 1 h, while IFN-λ3 and K154E peaked at 30 mins and displayed a persistent activation of p-STAT1. Importantly, levels of p-STAT1 activation were consistent with previous determined antiviral activity with K154E > WT> P70S (Bamford, Aranday-Cortes et al. 2018). Given that IFN-λs could activate other tissues besides human liver, T84 cells were assayed to determine their response to IFN-λ4 and its variants. Intestinal T84 cells were stimulated with IFN-λs and the activation of STAT1 was detected over time by immunoblot (Figure 3-7B and Figure 3-8B). T84 cells also displayed similar p-STAT1 activation as HepaRG cells, K154E > WT > P70S; however, the kinetics and lengths of STAT1 activation were distinct from that in HepaRG cells. Altogether, the data demonstrated that both intestinal and hepatic cells were responsive to IFN-λ3 and IFN-λ4 and showed that the JAK/STAT pathway could be induced with distinct kinetics.

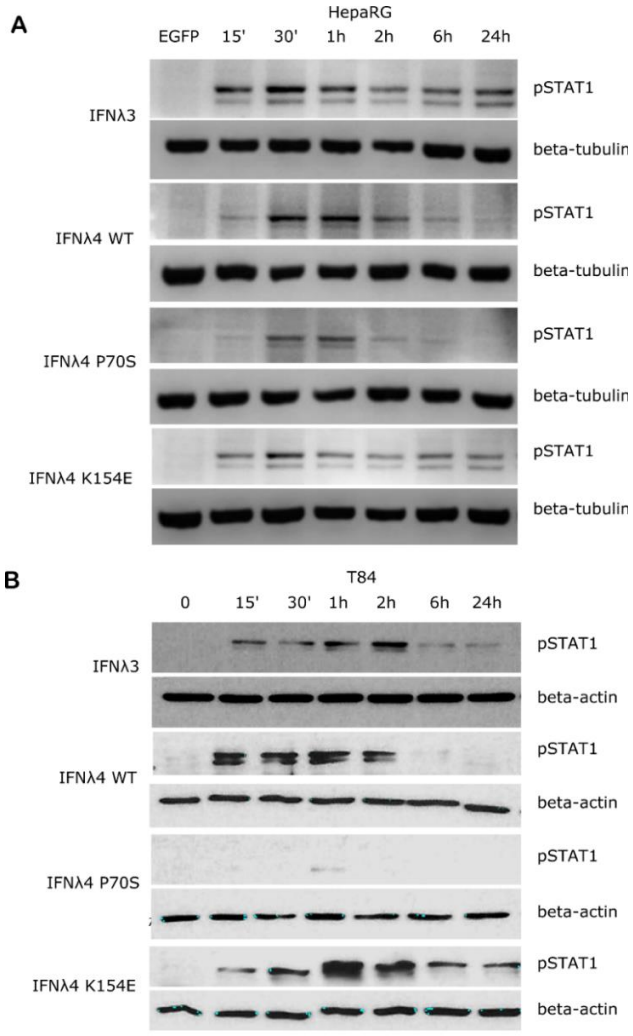

Figure 3-7. IFN-λs each have a distinct kinetic of STAT1 phosphorylation. HepaRG (A) and T84 (B) cells were incubated with IFN-λs (IFN-λ3-HiBiT, IFN-λ4-HiBiT: WT, P70S, and K154E for the indicated times and the levels of p-STAT1 was assayed by immunoblot. Beta-tubulin (HepaRG) or beta-actin (T84) served as loading controls. EGFP (A) or timepoint 0 (B) serves as a conditioned media control. Representative images of 2-3 replicates are shown.

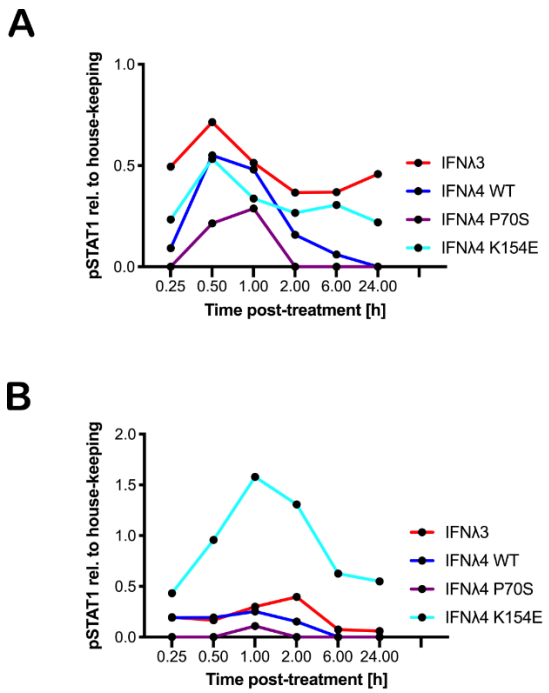

Figure 3-8. pSTAT1 quantification over time for IFN-λs on liver and gut cells. Quantification of p-STAT1 and STAT1 from images in figure 3.7 by densitometry analysis for HepaRG (A) and T84 (B) cells (IFN-λ3-HiBiT [red], IFN-λ4-HiBiT: WT [blue], P70S [purple], and K154E [cyan]. A house keeping gene (β-tubulin (HepaRG) or β-actin (T84) was used as control.

3.2.2 ISG expression over time following IFN-λ stimulation

STAT1 phosphorylation activated by IFN-λs leads to the dimerization of STAT1/2 and translocation to the nucleus to drive ISG transcription, ultimately establishing antiviral state (Kotenko, Gallagher et al. 2003). Previous work showed that ISG expression was regulated by IFN variants at 24 h post-treatment (Bamford, Aranday-Cortes et al. 2018). To figure out whether the ISG induction differed at earlier times after treatment in agreement with p-STAT1, a panel of ISGs (*IFIT1*, *MX1*, *ISG15*, and *RSAD2/VIPERIN*) was measured in comparison with EGFP-treated conditioned media in HepaRG (Figure 3-9A-D) and T84 cells (Figure 3-9E-H). Results showed that all IFN-λs could induce detectable induction of ISG mRNA with different magnitude in HepaRG cells. T84 cells could also induce measurable induction of ISGs in the supernatants, while L79F barely induced the expression of ISGs (Figure 3-9E-H). In addition, HepaRG cells were more sensitive to IFN-λs and displayed higher induction of all ISGs compared to T84 cells (Figure 3-9). The amounts of ISG induction of both cell lines were similar to the p-STAT1 induction that was observed previously (K154E > WT > P70S > L79F) (Figure 3-7). IFN-λ4 K154E induced ISG production with a similar pattern as IFN-λ3 in both cell lines. Notably, cell lines displayed the different kinetics of ISG induction. In T84 cells, most IFN-λs showed a consistent rise in ISG expression, while all IFN-λs displayed an early peak of ISG induction and subsequently

declined over time in HepaRG cells (Figure 3-9). In T84 cells, WT IFN-λ4 and P70S barely induced or induced low levels of ISG mRNA. In HepaRG cells, IFN-λ4 K154E appeared to induce slightly faster ISG expression and peaked at 2 h where all other IFN-λs peaked at 6 h. Altogether, the data revealed that K154E resulted in the highest magnitude of ISGs while P70S induced the lowest ISG production in a tissue dependent manner.

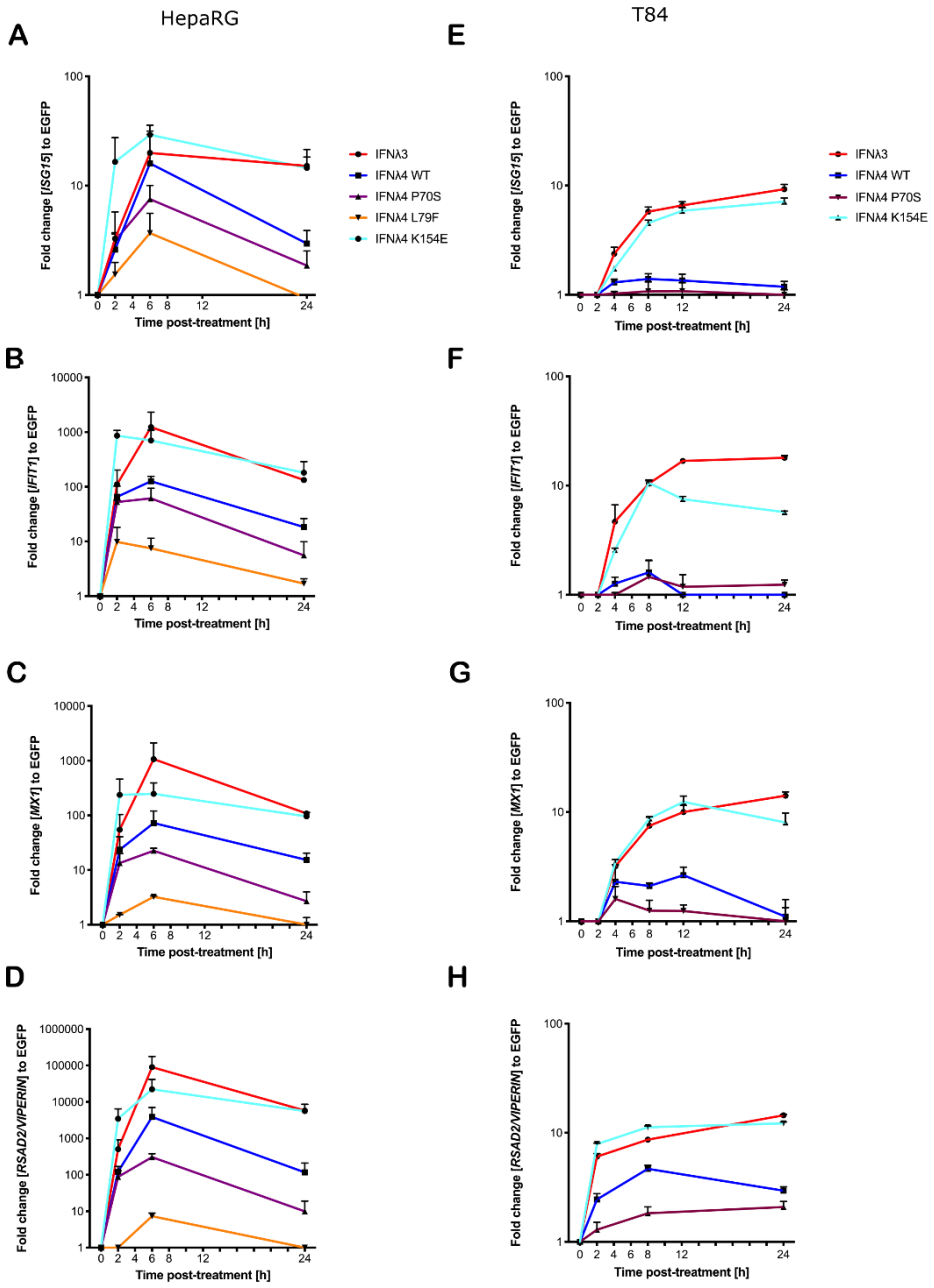

Figure 3-9. IFN-λ4 variants induce unique magnitudes of ISG mRNA. HepaRG (A-D) and T84 (E-H) cells were incubated with IFN-λs (IFNλ3-HiBiT [red], IFNλ4-HiBiT [blue]: WT, P70S [purple], L79F [yellow] and K154E [cyan]) for indicated times. At the respective time, total RNA was isolated, and qRT-PCR was performed for ISGs: IFIT1 (A and E), ISG15 (B and F), MX1 (C and G) and RSAD2/VIPERIN (D and H). EGFP-treated cells were used as a mock control and all values were normalized against this value at each time. GAPDH (HepaRG) or HPRT1 (T84 cells) were used as housekeeping genes. L79F did not induce any detectable ISG induction in T84 cells. Error bars represent the mean ± SEM from 2-3 biological replicates.

3.2.3 IFN-λ4 variants have distinct antiviral activity

Establishment of an antiviral state is the main downstream result of IFN signaling. To investigate the correlation of STAT1 phosphorylation and ISG expression with antiviral potency, hepatic and intestinal cells were infected with two kinds of viruses, EMCV and VSV. The reason for choosing EMCV and VSV to assess kinetics of antiviral activity is that they replicate fast and are highly cytopathic. Cytopathic effects were assayed to determine EMCV infectivity and replication while luciferase assay was used to measure VSV infectivity through using a VSV encoding luciferase (VSV-luc). As the antiviral potency of IFN-λ4 has been previously tested in hepatocyte cell lines (Bamford, Aranday-Cortes et al. 2018), the antiviral protection from IFN-λ4 was assessed in T84 cells against VSV. HepaRG and T84 cells were incubated with increasing doses of EGFP or IFNs 24 h prior to virus infection. After IFN pre-treatment, cells were infected with EMCV (MOI of 0.3) or VSV (MOI of 1) in the presence of the IFNs and infectivity was measured at 24 post-infections for EMCV (Figure 3-10A) and 8 h post-infection for VSV (Figure 3-10B and C). Results revealed that VSV infection was blocked by all IFNs in both cell lines (Figure 3-10B-C). WT IFN-λ4 and K154E exhibited similar antiviral activity but required a much higher concentration than IFN-λ3 to have full antiviral potency. In contrast, P70S could only slightly decrease virus replication even at the highest concentrations. HepaRG cells also revealed the similar results against EMCV (Figure 3-10A). As T84 cells were highly resistant to the cytopathic effects of EMCV and were lowly infected with EMCV, the antiviral potency was not measured in this cell line.

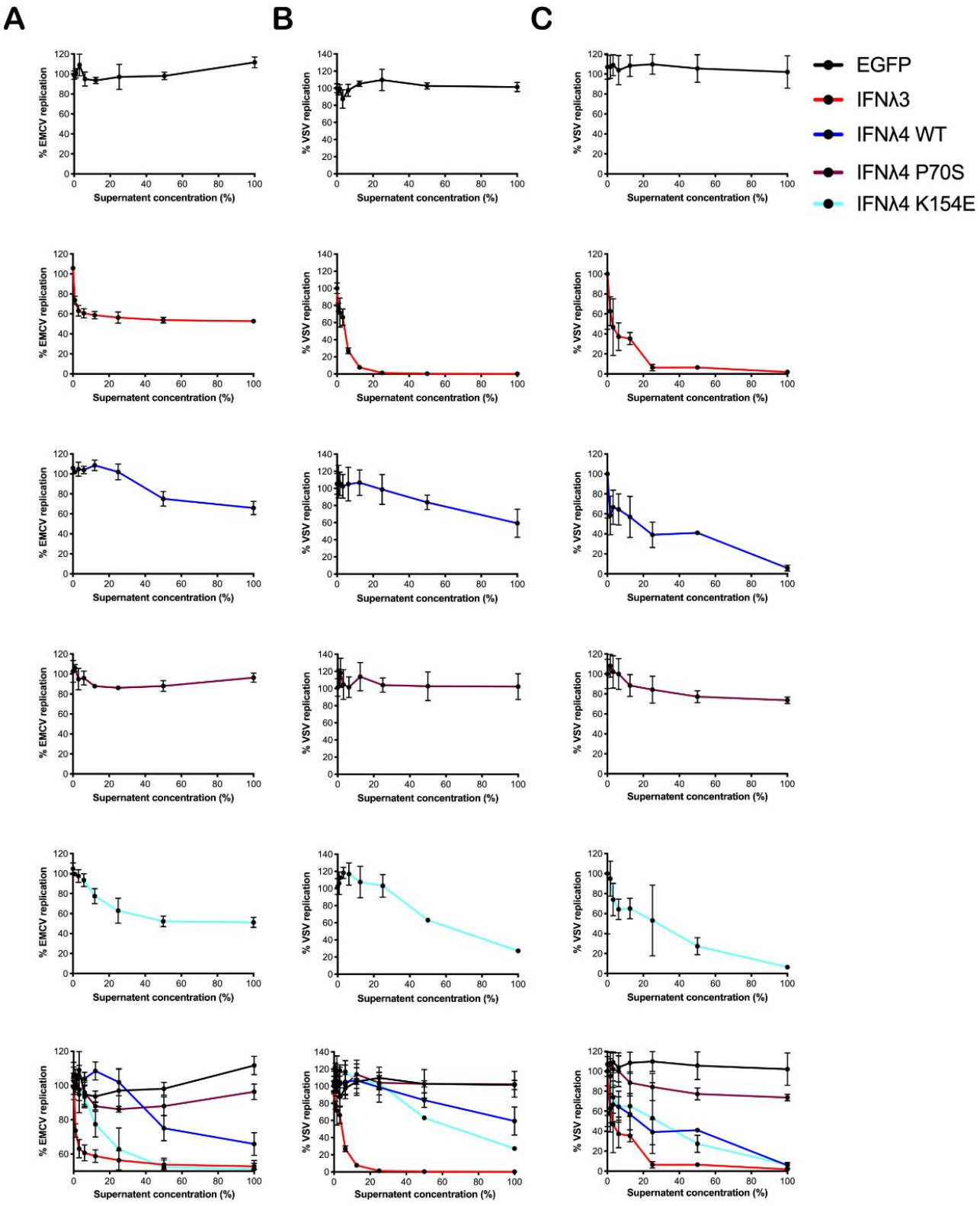

Figure 3-10. Antiviral activity against EMCV or VSV of IFN-λs on HepaRG and T84 cells. HepaRG (A and B) or T84 (C) cells were stimulated with different concentrations of supernatant containing the panel of IFN-λs (IFN-λ3-HiBiT [red], IFN-λ4-HiBiT [blue]: WT, P70S [purple], and K154E [cyan]) before being challenged with EMCV (A) or VSV (B and C) and antiviral activity calculated, shown here as percentage of viral replication at each dilution compared to mock treated controls. Experiments were performed in triplicate and errors bars represent the standard deviation.

3.2.4 IFN-λ4 variants have distinct kinetics of antiviral activity

To verify whether IFN-λs activity was time dependent and their antiviral potency was maintained in the presence of IFN-λs, kinetics analysis of antiviral potency with washing was performed. To achieve this aim, HepaRG (against EMCV) or T84 (against VSV) cells were pre-incubated with IFN-λs for different time points prior to virus infection. IFN-λs were either maintained for the time course or removed for subsequent assay (Figure 3-11A). In line with previous results, all IFN-λs exhibited antiviral potency in both cell lines. Under washed condition, all IFN-λs slightly lost their antiviral activity, suggesting that they had weak association with the receptor and their presence was necessary for attaining full antiviral potency (Figure 3-11B-I). Notably, for IFN-λ3, early washing affected more on antiviral potency than IFN-λ4 and its variants (Figure 3-11B-I). The effect of washing was detected in both HepaRG and T84 cells. Interestingly, antiviral activity of all IFN-λ4 stayed longer after their removal than IFN-λ3, indicating that either their signaling was sustained longer than IFN-λ3 or they had higher binding affinity for the receptor.

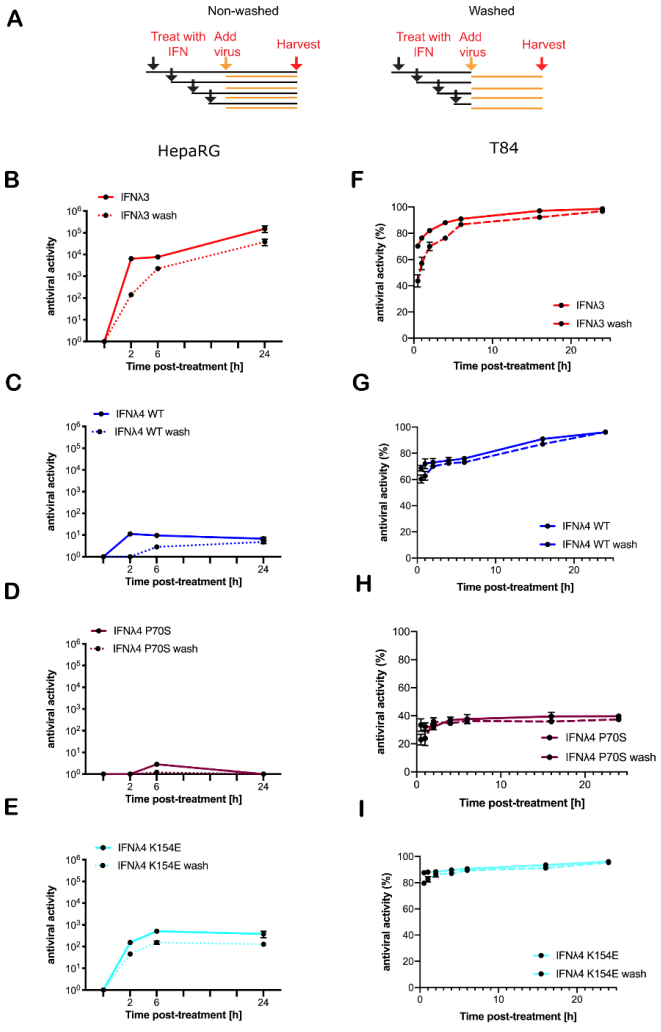

Figure 3-11. Antiviral activity does not require continued presence of IFN-λs. (A) Schematic description of the experiment to show how IFN-λ was added and maintained or removed by washing. HepaRG (B-E) and T84 (F-I) were stimulated with IFN-λs: IFN-λ3-HiBiT (B and F), IFN-λ4-HiBiT WT (C and G), P70S (D and H), and K154E (E and I) at indicated time prior to infection with EMCV (HepaRG) or VSV (T84). EMCV infection (B-E) was assayed by cytopathic effect 24 h post-infection of a series of two-fold serial dilutions of supernatant. VSV-luc (F-I) was assayed 8 h post-infection by luminescence after incubation with supernatants were used at 100% concentration (T84). For washing experiments (dashed lines), IFN-λ was removed and rinsed with PBS before being replaced with media containing virus. Error bars indicate the standard deviation. Error bars represent the mean ± SEM from 2-3 biological replicates.

3.2.5 Kinetics is independent of human IFN-λ system

Previous results suggested that human IFN-λ4 and its variants exhibited distinct antiviral activity compared to human IFN-λ3. It was also reported that IFN-λ4 from different primate species showed different antiviral activity. Therefore, the species-specific difference in signaling kinetics was also explored. Firstly, the homology among IFN-λ3, IFN-λ4, IFNLR1 and IL10R2 was analysed in humans, chimpanzees, and rhesus macaque (Figure 3-12A). Protein sequence analysis revealed that these IFN-λ4 share high (92-97%) homology and even single amino acid difference in IFN-λ4 could signal differently. Considering the genetic differences, the antiviral kinetics of non-human IFN-λs was determined. HepaRG cells were incubated with human and non-human IFN-λs, and washed and/or infected at 2, 6 or 24 h after stimulation (Figure 3-12B). Interestingly, chimpanzee IFN-λ4 showed greater activity than human and macaque IFN-λ4 although all IFN-λs were antiviral (Figure 3-12B-C), which was consistent with previous results. In addition, human IFN-λ3 exhibited higher antiviral potency than macaque IFN-λ3 (Figure 3-12C). Washing experiments revealed that human IFN-λ4, non-human primate IFN-λ4 was more antiviral at early time than human or macaque IFN-λ3 (Figure 3-12B-C). To investigate whether this different kinetics also happened in non-human cells, IFN-λs were also tested in rhesus macaque respiratory epithelial cell line LLCMK2 (Figure 3-12D-E). The data demonstrated that all IFN-λ4s had similar patterns of antiviral potency but different levels of potencies in HepaRG cells. Results from washing following immediate infection showed the similar results as the initial washing experiments (Figure 3-12F-G).

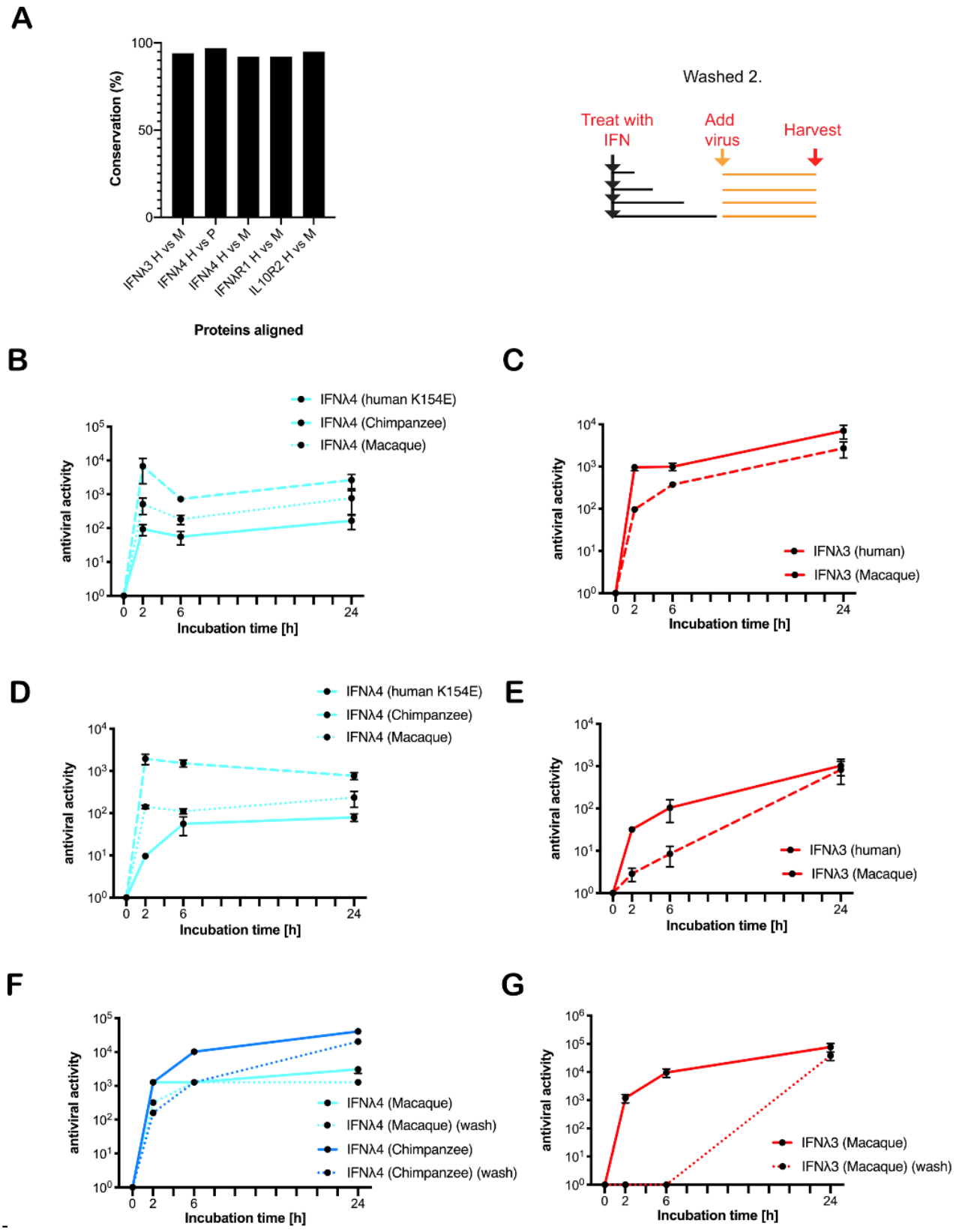

Figure 3-12. Kinetics of antiviral activity of non-human primate IFN-λs. The percentage identity of IFN-λ pathway proteins (IFN-λ3, IFN-λ4, IFNλR1 and IL10R2) between humans, chimpanzees and/or macaques was measured using BLAST (A). A washing/incubation protocol was used (B) and HepaRG (B and C, and F and G) or Rhesus macaque LL-CMK2 (C and E) cells were pre-treated with IFN-λ4 (B, D and F) or IFN-λ3 (C, E and G) for the indicated times prior to infection with EMCV. 24 (HepaRG) or 72 (LL-CMK2) h post-infection antiviral activity was measured by CPE assay. Antiviral activity of IFN-λs on HepaRG cells was measured using the alternative washing protocol (F and G). Results are shown as mean ± SD n=4 biological replicates.).

3.2.6 IFN-λ1 with receptor-interacting face mutations retain parental kinetics

The interactions between cytokine ligand and their cognate receptors are complex and dynamic, leading to different signaling output (Schreiber 2017). IFN-λ4 is greatly divergent compared with IFN-λ1-3, suggesting that molecular determinants were contained in IFN-λ4 compared to the other human IFN-λs (Hamming, Terczyńska-Dyla et al. 2013). To identify those determinants, chimeric IFN-λs between IFN-λ4 and human IFN-λ1 were constructed to evaluate the impact of key domains. The reason to choose IFN-λ1 is that it has similar kinetics as IFN-λ4 but unlike IFN-λ3, is glycosylated (Marcello, Grakoui et al. 2006), which is thought to be processed more like IFN-λ4 than IFN-λ3. Initially, conserved amino acids of IFN-λ4 were compared to that of IFN-λ1-3 (human and macaque) in receptor-interacting interfaces, identifying a divergent receptor binding interface (Figure 3-13A). Three surface-exposed residues in relevant helices, A, D and F were identified. Two chimeric IFN-λs were generated based on IFN-λ1 and contain IFN-λ4 residues from IFNLR1-binding helix F (named F), and IL10R2-binding helices A and D (named AD). An additional chimera was designed, termed ADF that contains all domain changes. Firstly, a split-luciferase assay confirmed that IFN-λ1 and chimeras were abundantly expressed and secreted into the supernatant although chimeras with helices A and D has reduced expression (Figure 3-13B). To determine the antiviral potency, HepaRG cells were pre-incubated with IFNs and the indicated chimeras for 2, 6 or 24 h prior to EMCV infection. My data revealed that IFN-λ1 exhibited stronger antiviral activity than IFN-λ4 (Figure 3-13C). In addition, IFN-λ1 containing each of all IFN-λ4 substitutions lost antiviral potency (IFN-λ1 > F > AD > ADF) (Figure 3-13C). To investigate whether the chimeras influenced IFN binding, HepaRG cells were pre-incubated with WT IFNs and each of the chimeras for 2, 6 and 24 h prior to EMCV infection. The IFNs were either maintained for the duration of the infection or eliminated at the time of infection. Results showed that washing significantly decreased the antiviral activity of all IFNs (Figure 3-13D). Precisely, the chimera F showed lower antiviral activity than IFN-λ1 whereas the reduced potency of AD was likely attributing to reduced protein (Figure 3-13D). Nevertheless, the kinetics stayed conserved like IFN-λ1, and alteration of the receptor interaction surfaces was not sufficient to change the antiviral kinetics. Together, our results demonstrated the distinct yet conserved antiviral kinetics of human and non-human primate IFN-λ4 compared with other IFN-λs.

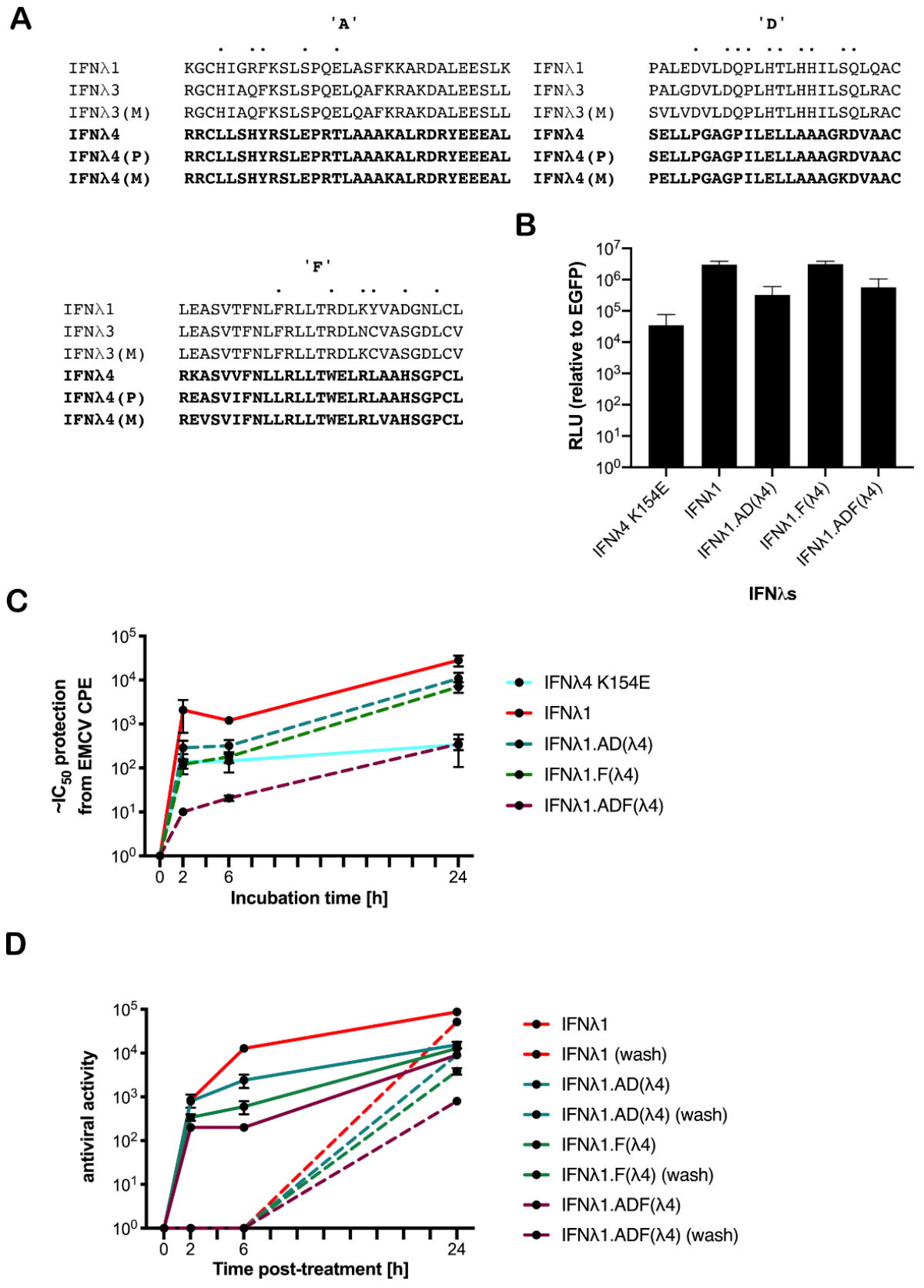

Figure 3-13. IFN-λ1 receptor-interacting interface mutants retain their kinetics. IFN-λ1/4 chimeras were generated based on critical differences in helices A, D and F identified by alignment and comparative approaches (A). Relative secretion of IFN-λs by HiBiT assay following transfection of expression plasmids into HEK-293T cells measured at 48 h after transfection (B). Effect of incubation time [2, 6 or 24 h] (C) and washing [2, 6 or 24 h, washed as hashed lines] (D) of antiviral activity in HepaRG cells was calculated as outlined previously.

3.3 Transient synergetic effect of IL-22 and IFN-λ in human intestinal cells and human intestinal organoids

The text and figures of part 3.3 will be submitted as part of a manuscript (Guo et al., 2022). This corresponds to a first author manuscript resulting directly from my PhD research project.

Upon viral infection of the gastrointestinal tract, intestinal epithelium cells (IECs) and tissue resident immune cells release a plethora of cytokines which induce signaling pathways that control and clear the viral infection (Wu and Chen 2014). One key cytokine, acting on IECs, is IFN-λ which is sufficient to clear enteric virus infection by inducing hundreds of ISGs (Iwasaki 2012). Like IFN-λ, IL-22 is also a member of the IL-10 family, and it was shown that cooperation of IFN-λ and IL-22 can optimize the induction of ISGs and control of rotavirus infection (Hernández, Mahlakoiv et al. 2015). However, the mechanism underlying this synergetic effect of both cytokines remains unclear.

3.3.1 IL-22 promotes IFN-λ-mediated p-STAT1 expression in human intestinal epithelial cells

To investigate if IL-22 can promote IFN-λ-mediated activation of STAT1, T84 cells were seeded into collagen coated 24-well plates. At 24 h post-seeding, T84 cells were treated with increasing concentrations of IFN-λ (0.01, 0.1 and 1 ng/mL) and 100 ng/mL of IL-22 (Figure 3-14A). At 0.25-, 0.5-, 1-, 2- and 4-h post-treatment, protein was harvested and p-STAT1 was detected through western blot (Figure 3-14B-E) and quantified (Figure 3-14F-I). Results showed that co-treatment of IFN-λ and IL-22 induced significantly more p-STAT1 than IFN-λ treatment alone in all different concentrations of IFN-λ (Figure 14B-I). Moreover, IFN-λ could induce the production of p-STAT1 at a very early time point (15 mins) and peaked at 30 mins post IFN-λ treatment (Figure 14B-D). IL-22 alone could induce very high level of p-STAT1 at a very early time point where p-STAT1 levels were sharply decreased within 1 h or IL-22 treatment (Figure 14E).

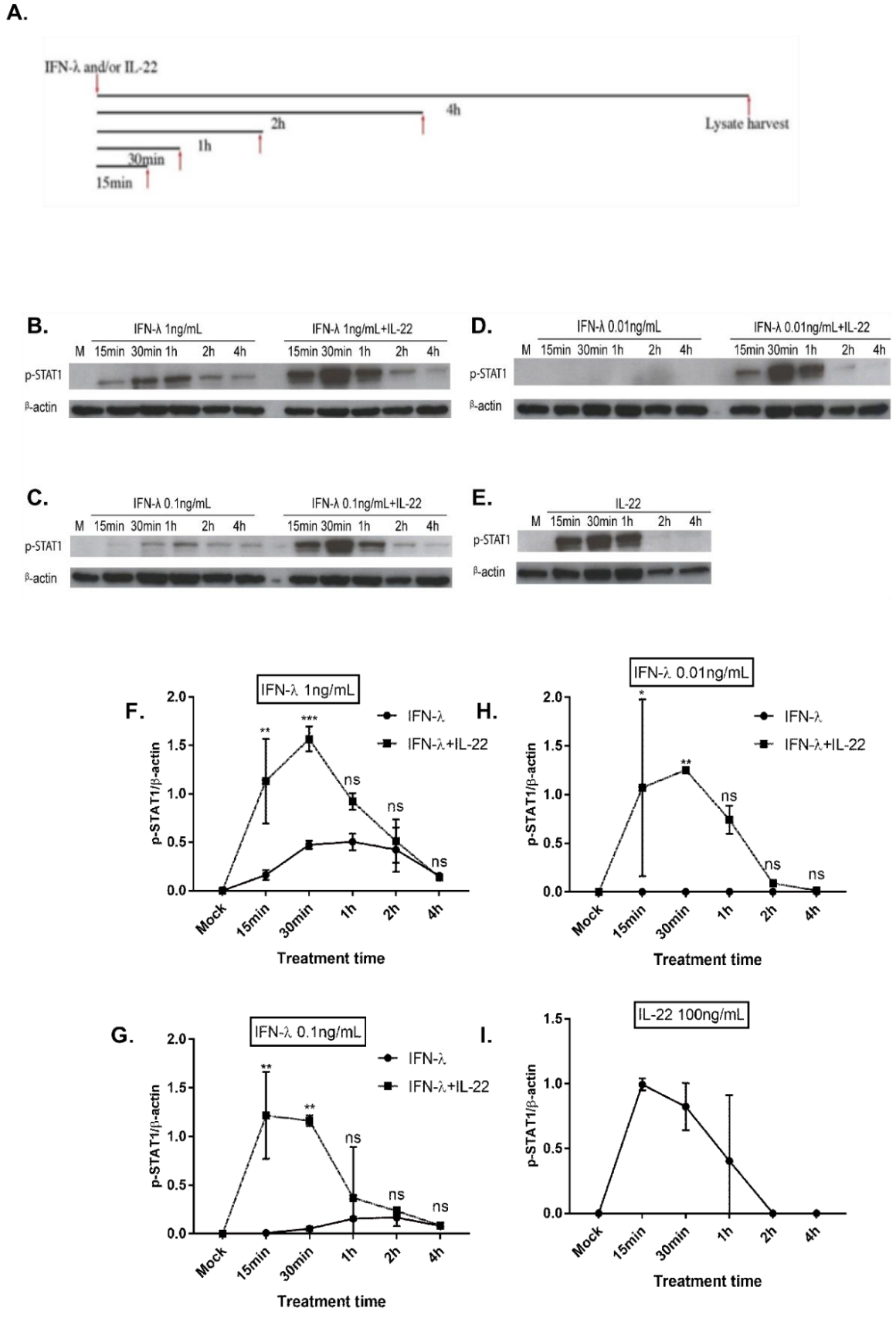

Figure 3-14. Activation of STAT1 by IFN-λ and IL-22 in human intestinal epithelial cells. (A-E) Human colon carcinoma cells were treated with indicated concentrations of IFN-λ and IL-22. At different time points, protein samples were collected for WB. (B-E) Cells were treated with 1, 0.1 and 0.01 ng/mL of IFN-λ and/or 100 ng/mL of IL-22. (F-I) WB Quantification was done by Fiji software. Data represent the mean values of two independent experiments. Error bars indicate the SD. ns means no significant, **P* < 0.1 ***P* < 0.01, ****P* < 0.001 (two-way ANOVA).

3.3.2 IL-22 fails to enhance IFN-λ-induced interferon-stimulated genes in human intestinal epithelial cells

As my results showed that co-treatment of IL-22 and IFN-λ could induce more p-STAT1 than IFN-λ treatment, it is reasonable to speculate that IL-22 may help IFN-λ induce more ISGs. To confirm my hypothesis, T84 cells were treated with 300 ng/mL of IFN-λ1, 2, 3 and/or 100 ng/mL of IL-22 for 3, 6, 12 and 24 h. Following treatment, RNA samples were harvested and the expression of ISGs was determined by qRT-PCR for representative ISGs, ETV7, GBP1, CXCL10, IFIT1 and ISG15. Results showed that IL-22 did not alearly increase IFN-λ-induced ISGs, such as ETV7 (Figure 3-15A), GBP1(Figure 3-15B), CXCL10 (Figure 3-15C), IFIT1 (Figure 3-15D), and ISG15 (Figure 3-15E), expression at different indicated time points, which was inconsistent with the findings in the murine model (Hernández, Mahlakoiv et al. 2015). These results suggested that IL-22 was acting differently in human and mouse cells.

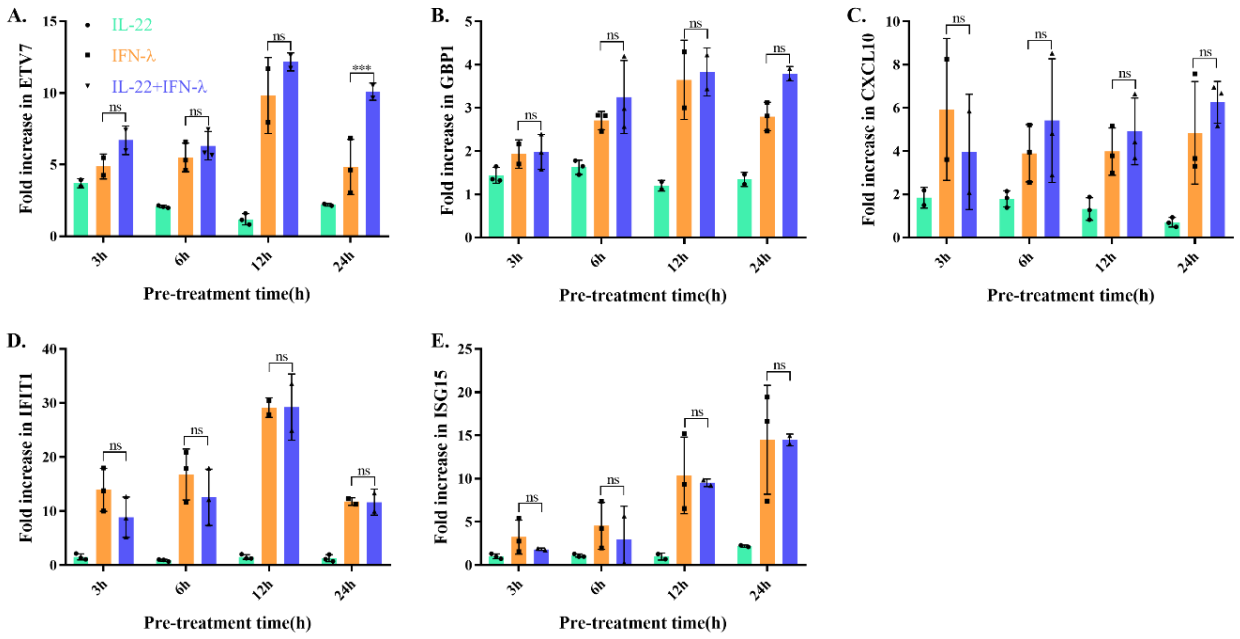

Figure 3-15. RNA expression of ISGs induced by IFN-λ and IL-22 in human intestinal epithelial cells. (A-E) Human colon carcinoma cells were treated with indicated concentrations of IFN-λ and IL-22 for 3, 6, 12, 24 h. RNA samples were collected for q-PCR. ISGs, ETV7, GBP1, CXCL10, IFIT1 and ISG15 were detected. Data represent the mean values of three independent experiments. Error bars indicate the SD. ns means no significant, ***$P < 0.001$ (two-way ANOVA).

3.3.3 IL-22 fails to help IFN-λ more antiviral

Since IFN-λ establishes antiviral activity by inducing ISGs, it is reasonable to speculate IL-22 may not help IFN-λ more antiviral. To verify this hypothesis, the antiviral capacity of IFN-λ and IL-22 combination was determined. To determine the amount of IFN-λ or IL22 required to inhibit VSV-luc replication, T84 cells were treated with increasing concentrations of each cytokine. At 24 h post-treatment, T84 cells were infected with VSV, and luciferase was measured by luminescence assay at 6 h post-infection (Figure 3-16A). Results revealed that IFN-λ and IL-22 exhibited dose-dependent antiviral response in T84 cells (Figure 3-16B). However, IFN-λ showed a greater antiviral activity than IL-22 (Figure 3-16B). To determine if combined treatment of IFN-λ and IL-22 would impact VSV-luc replication, T84 cells were treated with 1, 0.1 and 0.01 ng/mL of IFN-λ, which respectively represents 90%, 60% and 20% inhibition of VSV-luc replication.

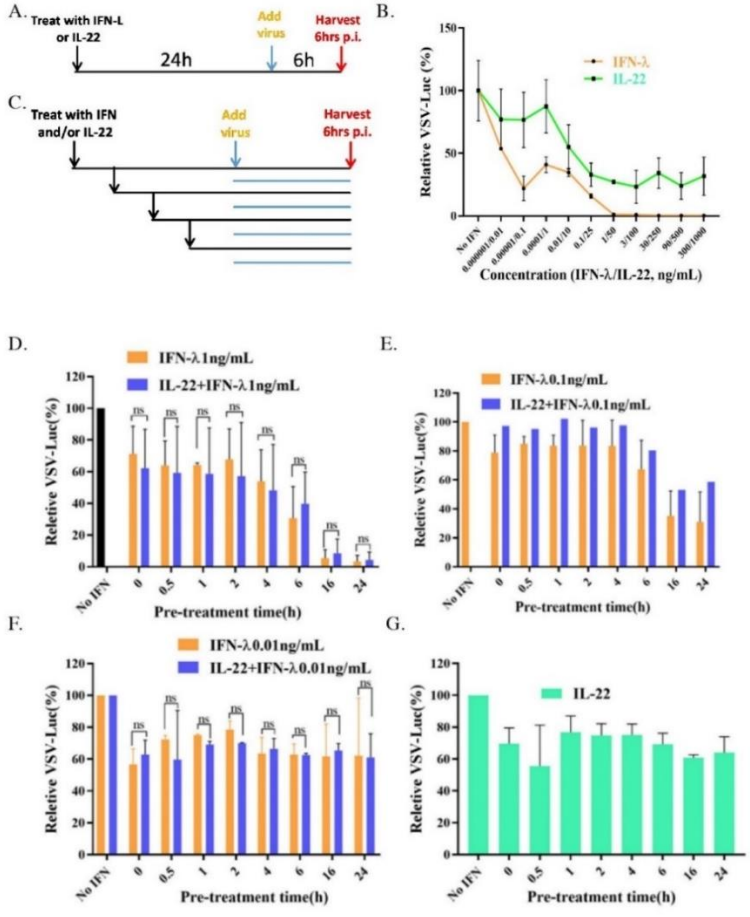

Figure 3-16. Antiviral activity mediated by IL-22 and IFN-λ in human intestinal epithelial cells. Human colon carcinoma cells were treated with the indicated concentrations of type III IFN (λ1−3) or IL-22 for 24 h prior to infection with vesicular stomatitis virus (VSV) expressing Firefly luciferase (VSV-Luc) (MOI = 1). Viral replication was assayed by measuring the luciferase activity. (C-F) Human colon carcinoma cells were treated with indicated concentrations of type III IFN (λ1−3) and IL-22 (100 ng/mL) for the indicated times prior to infection. (G) Same as F except that only IL-22 was added prior to VSV-luc infection. Data represent the mean values of two to three independent experiments. Error bars indicate the SD. ns means not significant (two-way ANOVA).

Subsequently, T84 cells were treated with IL-22 and/or IFN-λ for indicated time prior to VSV-luc infection (Figure 3-16C). Results showed that co-treatment of IL-22 and IFN-λ failed to induce stronger antiviral activity than IFN-λ treatment (Figure 3-16D-G). For the group with 0.01 ng/mL of IFN-λ, as only one repeat worked well, there was no error bar here. More repeat for this group is required. These results were inconsistent with the results from the murine model which showed that IL-22 promoted IFN-λ-mediated antiviral activity through inducing more ISGs and p-STAT1 in mice (Hernández, Mahlakoiv et al. 2015). Antiviral results furtherly supported my hypothesis that co-treatment of IL-22 and IFN-L activities was a species or cell type independent characteristic.

3.3.4 IL-22 and IFN-λ activate different STATs

To assess the different STATs activated by IFN-λ and IL-22, Luminex assay was applied to detect the phosphorylation of STAT1, STAT2, STAT3, STAT5 and STAT6 induced by IFN-λ and/or IL-22. T84 or IFNLR1.KO cells were treated with 1 ng/mL of IFN-λ and/or 100 ng/mL of IL-22 for 0.25, 0.5, 1, 2 and 4 h. Protein samples were collected and analysed by Luminex assay. Results showed that IFN-λ induced the phosphorylation of STAT1 and STAT2 (Figure 3-17A-C and 3-18A-C), while IL-22 activated the phosphorylation of STAT1 and STAT3 (Figure 3-17A-C, D-F). Co-treatment of IFN-λ and IL-22 induced significantly more p-STAT1 than IFN-λ treatment (Figure 3-17A-C). As co-treatment of IFN-λ and IL-22 failed to induce more ISGs and promote IFN-λ-mediated antiviral activity, I predicted that IFN-λ and IL-22 activated different pathways although they share the receptor IL-10R2 and both trigger the phosphorylation of STAT1. It is reasonable to speculate that IL-10R2 is responsible for the phosphorylation of STAT1, and IFNLR1 is responsible for the activation of STAT2, and IL-22RA is responsible for the activation of STAT3. In addition, p-STAT2, p-STAT5 and p-STAT6 were also determined in WT and IFNLR.KO cells treated with IFN-λ and/or IL-22 by Luminex assay. Luminex assay revealed that only IFN-λ could induce the phosphorylation of STAT2 (Figure 3-18A-C) and both IFN-λ and IL-22 barely activated STAT5 (Figure 3-18D-F) and STAT6 (Figure 3-18G-I).

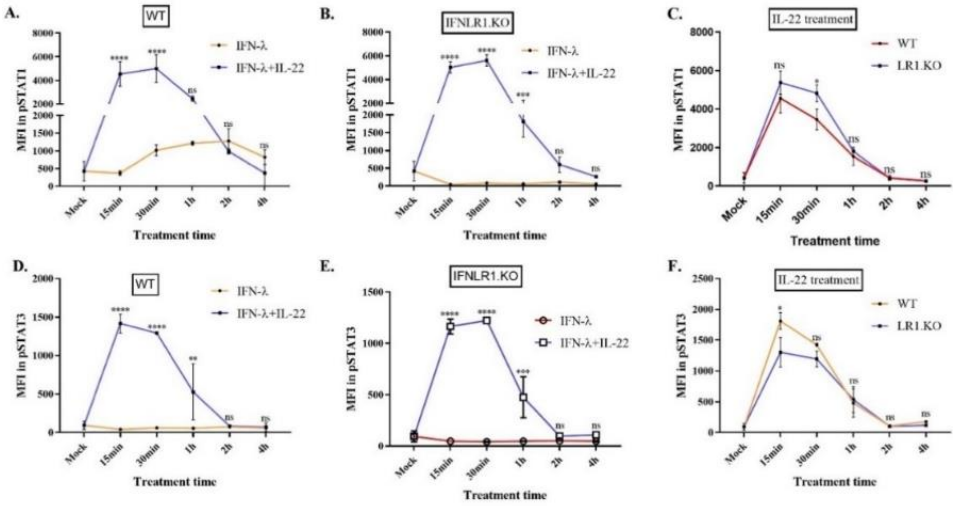

Figure 3-17. Activation of STATs (1 and 3) by IFN-λ and IL-22 in human intestinal epithelial cells. (A-F) T84 or IFNLR1.KO T84 cells were treated with indicated concentrations of IFN-λ and IL-22. At different time points, protein samples were collected for Luminex assay. (A) P-STAT1 levels in WT cells treated with 1 ng/mL of IFN-λ and 100 ng/mL of IL-22. (B) P-STAT1 levels in IFNLR1.KO T84 cells treated with 1 ng/mL of IFN-λ and 100 ng/mL of IL-22. (C) P-STAT1 levels in WT and IFNLR1.KO T84 cells treated with 100 ng/mL of IL-22. (D) P-STAT3 levels in WT cells treated with 1 ng/mL of IFN-λ and 100 ng/mL of IL-22. (E) P-STAT3 levels in IFNLR1.KO T84 cells treated with 1 ng/mL of IFN-λ and 100 ng/mL of IL-22. (F) Phospho-STAT3 levels in WT and IFNLR1.KO T84 cells treated with 100 ng/mL of IL-22. Data represent the mean values of two independent experiments. Error bars indicate the SD. ns means not significant, *P < 0.1 **P < 0.01, ***P < 0.001 (two-way ANOVA).

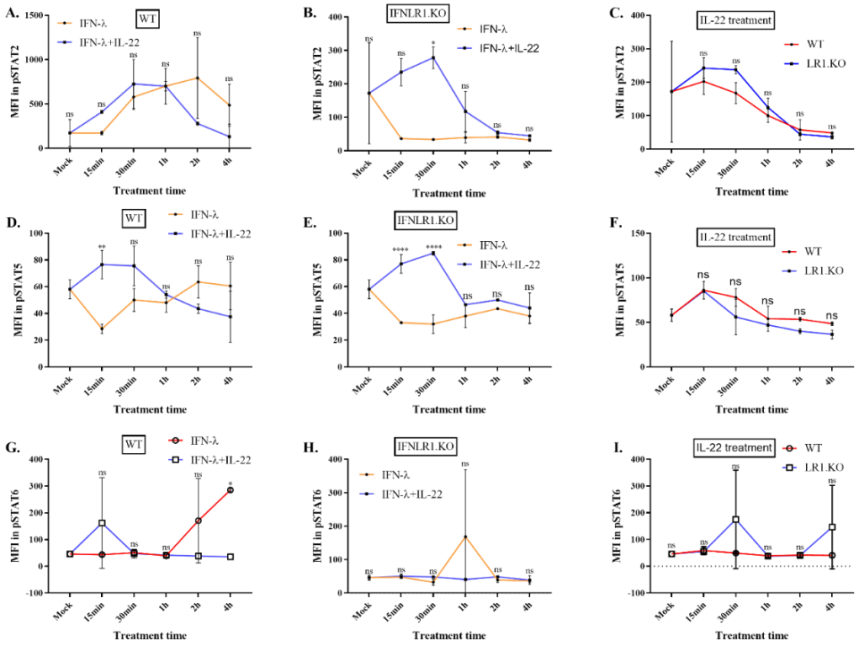

Figure 3-18. Activation of STATs (2, 5 and 6) by IFN-λ and IL-22 in human intestinal epithelial cells. (A-I) T84 or IFNLR1.KO T84 cells were treated with indicated concentrations of IFN-λ and IL-22. At different time points protein samples were collected for Luminex assay. (A) P-STAT2 levels in WT cells treated with 1 ng/mL of IFN-λ and 100 ng/mL of IL-22. (B) P-STAT2 levels in IFNLR1.KO T84 cells treated with 1 ng/mL of IFN-λ and 100 ng/mL of IL-22. (C) P-STAT2 levels in WT and IFNLR1.KO T84 cells treated with 100 ng/mL of IL-22. (D-F) P-STAT5 levels in WT cells and IFNLR1.KO T84 cells. (G-I) P-STAT6 levels in WT cells and IFNLR1.KO T84 cells. Data represent the mean values of two independent experiments. Error bars indicate the SD. ns means not significant, *P < 0.1 **P < 0.01, ***P < 0.001 (two-way ANOVA).

3.3.5 IL-22 and IFN-λ activate relatively independent signaling pathways

To capture the greater overview of the genes responsive to IFN-λ and IL22 co-treatment, whole transcript analysis was employed.

T84 cells were treated with 300 ng/mL of IFN-λ1, 2, 3 and/or 100 ng/mL of IL-22 for 3, 6, 12 and 24 h. RNA samples were qualified and sent for Bulk mRNA-seq. The hierarchical clustering of sample similarity showed that replicates were consistent between samples (Figure 3-19A). In addition, the multidimensional scaling (MDS) analysis showed that relations between samples were more time dependent than treatment dependent (Figure 3-19B). The heatmap for expression levels of main proteins involved in JAK/STAT pathway demonstrated that IFN-λ and/or IL-22 treatment did not change the expression levels theIL-22 and IFN-λ receptors or their downstream signaling molecules JAK1 and TYK2. Interestingly, results confirmed that only IFN-λ can upregulate p-STAT2 expression while IL-22 upregulates the expression of p-STAT3, whereas activated STAT1 (Figure 3-19C-D). Subsequently, signalling pathways activated by treatment were analysed through *PROGENy*. The analysis demonstrated that IL-22 and IFN-λ trigger relatively independent pathways, for example IL-22 activated MAPK, EGFR, and NF-kB signalling whereas IFN-λ activated JAK/STAT and Wnt signalling (Figure 3-19E). Furthermore, top 20 genes were chosen from each group to plot a heatmap of the chosen genes (76 in total). The heatmap clearly revealed that top genes induced by IFN-λ and IL-22 were relatively independent and had no crosstalk (Figure 3-19F). Differential gene expression analysis of ISGs showed that most ISGs were upregulated by IFN-λ, and only very few genes were upregulated by both (Figure 3-19G). Finally, transcriptional factor activity was also determined by *DoRothEA*, showing that IL-22 and IFN-λ activated independent transcriptional factors, IL-22 could activate STAT3, BCL3 and RELA, while IFN-λ activated STAT1/2 and IRF1/2 (Figure 3-19H). Together these results are consistent with my previous observations, showing that IFN-λ-mediated ISG induction was not enhanced by IL-22. Although both activated p-STAT1, the resulting signaling cascades were independent and unique to each cytokine with little to no overlapping pathways being activated.

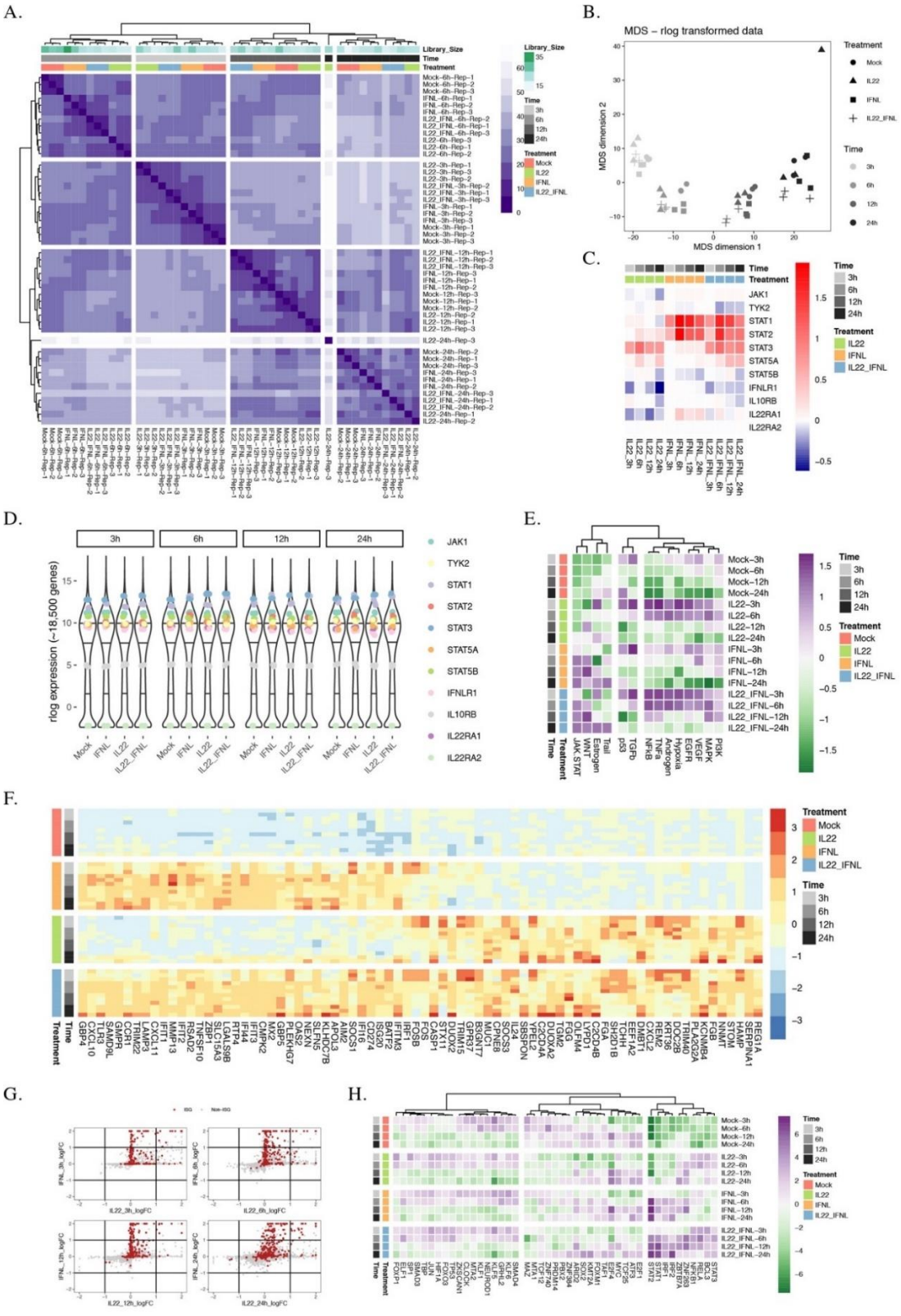

Figure 3-19. Antiviral activity mediated by IL-22 and IFN-λ in human intestinal epithelial cells. (A) Hierarchical clustering (heatmap) of sample similarity. (B) Multidimensional scaling (MDS) of global sample similarity. (C) Heatmap to show different expression levels of kinases, STATs and receptors involved in IFN-λ and IL-22-activating pathways. (D) Absolute expression levels of kinases, STATs and receptors involved in IFN-λ and IL-22-activating pathways. (E) PROGENy to show signalling pathways induced by IFN-λ and/or IL-22. (F) Hierarchical clustering (heatmap) of top 20 genes enriched by each treatment. (G) Volcano plot to compare ISGs expression between IFN-λ and/or IL-22 at different time points. (H) Transcriptional factor activity analysis through DoRothEA in different treatment samples.

2.3.6 IL-22 promotes stem cells proliferate in human intestinal organoids

The RNA-seq data showed that IL-22 promoted the EGFR pathway, which is involved in cell proliferation and differentiation. IL-22 also induced the expression of OLFM4 which is a well characterized stem cell marker. Previous studies showed that IL-22 can contribute to cell proliferation and tissue regeneration in mouse intestinal organoids (Lindemans, Calafiore et al. 2015). To determine if IL-22 treatment and co-treatment of IL-22 and IFN-λ would impact the cell proliferation of human intestinal cells, human intestinal organoids were treated with 300 ng/mL of IFN-λs and/or 100 ng/mL of IL-22. At 1-, 3-, 5- and 7-d post-treatment, organoids were analysed for their size, number, budding and cell proliferation. Results showed that IL-22 treatment triggered organoids to grow larger at day 3 and 7 (Figure 3-20A-B) but did not impact the number of organoids compared to mock treatment (Figure 3-20C). Furthermore, IL-22 could promote organoid budding after 3-day treatment, but this increase was only transient (Figure 3-20D). Importantly, IFN-λ did not impact the size, number and budding of intestinal organoids. Human intestinal organoids contain several types of cells, such as stem cells, goblet cells, enterocytes, and paneth cells. Therefore, human intestinal organoids were treated with IL-22 and collected after 3- day treatment and analysed by qRT-PCR for cell type-specific markers (stem cell marker, OLFM4; paneth cell marker lysozyme; goblet cell marker, mucin-2; enterocytes marker, Cyp450). Results showed that IL-22 increased the expression of stem cell marker, OLFM4 (Figure 3-20E) but could not increase other cell type markers, lysozyme (Figure 3-20F), mucin-2 (Figure 3-20G) and Cyp450 (Figure 3-20H), suggesting that IL-22 only promoted stem cell proliferation in human colon organoids.

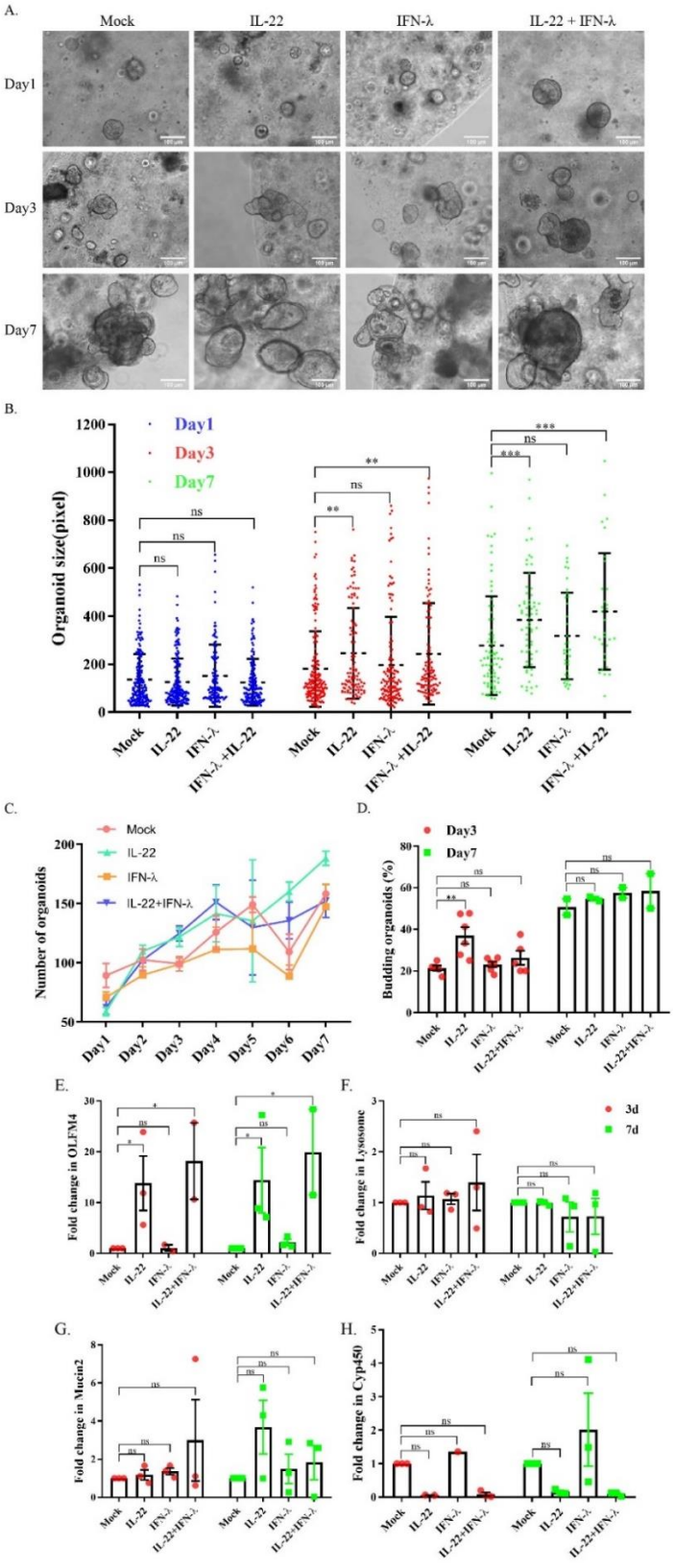

Figure 3-20. Effect of IL-22 and IFN-λ on human colon organoids. (A) The morphology of human colon organoids stimulated by IFN-λ and/or IL-22 at day1, 3 and 7. (B) The organoid size after stimulation by IFN-λ and/or IL-22 at day1, 3 and 7. (C) The number of human colon organoids stimulated by IFN-λ and/or IL-22 each day over one week. (D) The percentages of budding human colon organoids stimulated by IFN-λ and/or IL-22 at day 3 and 7. (E-H) Human colon organoids were treated with indicated concentrations of IFN-λ and IL-22 for 3 or 7 days. RNA samples were collected for q-PCR. Markers of different cell types, OLFM4, lysozyme, mucin-2 and Cyp450 were detected. Data represent the mean values of three independent experiments. Error bars indicate the SD. ns means no significant, $*P < 0.01$ (two-way ANOVA).

3.3.7 IL-22 promotes the percentage of stem cells in human intestinal organoids

My previous results suggested that IL-22 promoted human organoid proliferation by upregulating stem cells. To confirm this observation, I performed single molecule RNA-fluorescence in situ hybridization (smRNAFish) of OLFM4 in the organoids. Human colon organoids were treated with IFN-λ and IL-22 for 3 days and subsequently analysed by smRNAFish on OLFM4 expression. Results showed that organoids treated with IL-22 or combination of IL-22 and IFN-λ had a significantly higher ratio of stem cell than organoids without IL-22 treatment (Figure 3-21A-B). In contrast, IFN-λ did not impact the level stem cell ratio in human organoids. To further investigate whether IL-22 could also promote the proliferation of organoids, EdU (5-ethynyl-2'-deoxyuridine), a nucleoside analogue of thymidine and is incorporated into DNA during active DNA synthesis, was employed to measure cell proliferation. Human colon organoids were treated with IFN-λ and/or IL-22 for 3 days. Following cytokine treatment, organoids were fed with EdU for 6 h and collected for staining. Results showed that both IL-22 and/or IFN-λ could not change the ratio of proliferating cells in organoids (Figure 3-21C-D). All together these results showed that IL-22 promoted the number and ratio of stem cells but did not increase the ratio of proliferating cells in the organoids.

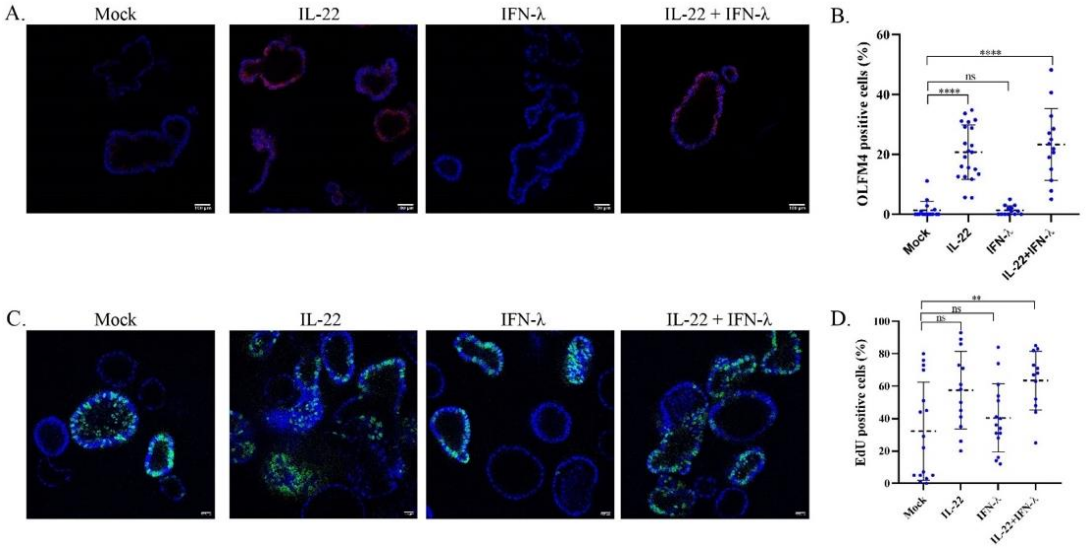

Figure 3-21. Effect of IL-22 and IFN-λ on stem cells and proliferation cells in human colon organoids. Human colon organoids were treated with indicated concentrations of IFN-λ and IL-22 for 3 days. Organoids were collected for smRNAFish and EdU staining. (A) OLFM4 (red) RNAFish staining on human colon organoids stimulated by IFN-λ and/or IL-22 at day3. (B) Quantification of OLFM4 in human colon organoids stained by OLFM4 RNAFish and DAPI in cell profiler software. (C) EdU staining on human colon organoids stimulated by IFN-λ and/or IL-22 at day 3. (D) Quantification of EdU in human colon organoids stained by EdU and DAPI in cell profiler software. Data represent the mean values of three independent experiments. Error bars indicate the SD. ns means not significant, $^{**}P < 0.01$, $^{****}P < 0.0001$ (two-way ANOVA).

3.3.8 The cytoplasmic domains of IFNLR1 and IL-22RA are responsible for downstream signaling pathway

To validate whether IFNLR1 is responsible for activating STAT2 and IL-22RA is responsible for activating STAT3, chimeric receptors of IFNLR1 and IL-22RA were designed and synthesised. It is known that both IFNLR1 and IL-22RA have three domains: extracellular domain, transmembrane domain, and cytoplasmic domain (Figure 3-22A). As the cytoplasmic domain of the two receptors oversees interacting with the downstream signaling components, this domain was targeted for swapping. Currently, two chimeric receptors were constructed: IFNLR1-IL22RA, consists of extracellular and transmembrane domains of IFNLR1 and cytoplasmic domain of IL-22RA, which will be transduced into IFNLR1.KO cells, is predicted to activate STAT3 and induce production of IL-22 related-genes following IFN-λ treatment. The second construct, IL22RA-IFNLR1, contains extracellular and transmembrane domains of IL-22RA and cytoplasmic domain of IFNLR1, which is supposed to express in T84 cells and is predicted to activate STAT2 and induce ISGs expression following IL-22 treatment (Figure 3-22B). To confirm these hypotheses, IFNLR1-IL22RA was transduced into IFNLR1.KO T84 cells. IFNLR1.KO cells were incubated with IFNLR1-IL22RA for 2 days and treated with IFN-λ or IL-22. Protein samples were harvested for western blot and RNA samples were harvested for qRT-PCR. The western blot results showed that IFN-λ could induce the phosphorylation of STAT3 in the presence of IFNLR1-IL22RA (Figure 3-22C), indicating that the cytoplasmic domain of IL22RA may be responsible for the activation of STAT3. Interestingly, p-STAT1 could be induced without treatment or with IFNLR1-IL22RA treatment, suggesting that p-STAT1 had basal expression and could be increased by stimulation. For the RNA expression, IFIT1 was chosen to test the stimulation of IFN-λ in cells; OLFM4 and SOCS3 were chosen to test whether IFN-λ can also induce the expression of IL-22-activated genes. Results revealed that IFN-λ induced the expression of OLFM4 and SOCS3 in the presence of IFNLR1-IL22RA (Figure 3-22E-F). IFIT1 was normally induced in the presence of IFN-λ (Figure 3-22D). The role of the second construct has not yet been tested.

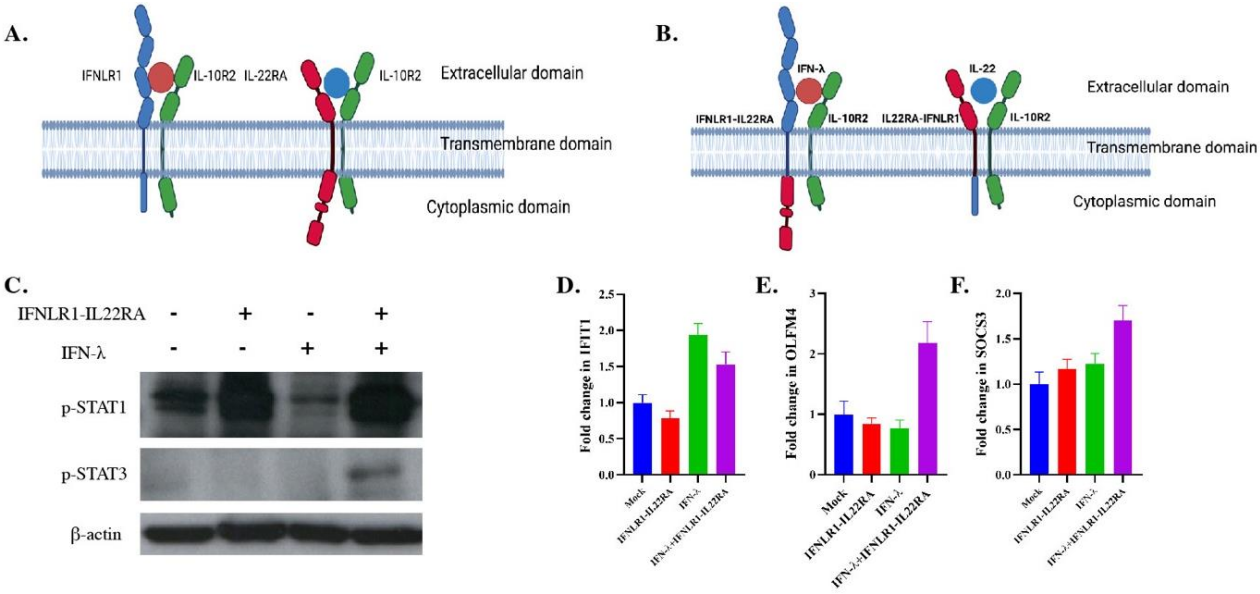

Figure 3-22. Effect of swap of IFN-λ receptor 1 and IL-22 receptor alpha. (A) IFNLR1 and IL-22RA consist of three domains, extracellular domain, transmembrane domain and cytoplasmic domain. (B) The swap of cytoplasmic domain of IFNLR1 and IL-22RA. (C-F) IFNLR1.KO T84 were incubated with plasmid IFNLR1-IL22RA and subsequently treated with indicated concentrations of IFN-λ. Lysates were harvested for Western blot or q-PCR. (C) Western blot for IFNLR1.KO T84 cells incubated with IFNLR1-IL22RA and IFN-λ. (D-F) Q-PCR for IFNLR1.KO T84 cells incubated with IFNLR1-IL22RA and IFN-λ; IFIT1, OLFM4 and SOCS3 were detected.

4 Discussion

4.1 Crosstalk of type I and III IFN signaling cascades

In this project, a crosstalk between type I and III IFN signaling pathways was investigated to test if they were interacting with each other. By employing human intestinal epithelial cells deficient in either IFNLR1 or IFNAR1, I showed that ISG expression was impacted when the cells were stimulated by the reciprocal IFN. Precisely, IFNLR1$^{-/-}$ cells showed increased ISGs with type I IFN treatment while IFNAR1$^{-/-}$ cells showed decreased ISGs with type III IFN treatment. These results were subsequently validated by using neutralizing antibodies against either the type I or III IFN receptors to inhibit IFN-mediated signaling. The results showed that the positive or negative crosstalk were independent of the levels of IFN receptors, but dependent on the activation of STAT1. Together, my results demonstrate that the type III IFN receptor downregulates type I IFN siganling while type I IFN receptor upregulates type III IFN signaling. By employing the IFNLR1$^{-/-}$ cell line and neutralizing antibodies against IFNLR1, results showed that type III IFN receptor downregulates the ISG induction and antiviral potency mediated by type I IFN (Figure 3-1 and 3-3).

Previous reports revealed that type III IFN led to a refractory state for IFN-β signaling in mice (François-Newton, Magno de Freitas Almeida et al. 2011, Makowska, Duong et al. 2011). These studies demonstrate that cells with either IFN-β or IFN-λ pre-treatment produce a negative regulator of IFN signaling, USP18. The production of USP18 decreased the ability of IFN-β to induce p-STAT1 and ISGs (François-Newton, Magno de Freitas Almeida et al. 2011, Makowska, Duong et al. 2011). Notably, IFN-β signaling was not influenced in these studies suggesting that both IFN-β and IFN-α employ the same IFN receptor and share the same downstream signaling cascade, but they respond to USP18 with different sensitivity. In addition, the function of USP18 appears more active in the liver and is less active in intestinal tissues, indicating the regulation activity of IFN signaling by USP18 is tissue dependent (Makowska et al., 2011). Here, it was clearly demonstrated that a negative regulatory loop downstream type III IFN receptor targets the type I IFN signalling cascade. However, the molecular origin of this negative regulatory mechanism remains unclear, but as it inhibits type I IFN signaling, USP18 may be involved in the process. Further studies constructing USP18 deficient cells are required to test this hypothesis. By contrast, my results also showed that type I IFN receptor upregulated type III IFN-mediated ISG induction and antiviral activity (Figure 3-1 and 3-3). Previous studies revealed that type I IFNs

displayed a positive feedback loop during viral infection. It was reported that Newcastle disease virus induced the IRF3-dependent production of IFN-α4 subtype (Marié, Durbin et al. 1998). The IFN-α4 was secreted from the cells and activated STAT1-dependent signalling pathway, driving the induction of other IFN-α subtypes and IRF7. The production of IRF7 promoted the induction of IFN-α in a positive feedback loop.

Similar positive feedback in type I IFN signaling was also found in vaginal tissue IFNAR$^{-/-}$ mice and splenocytes. Mice deficient of IFNAR show a reduced production of both type I and III IFN following virus infections compared to wild type mice (Ank, Iversen et al. 2008). The reduced IFN production in IFNAR$^{-/-}$ mice and splenocytes is consistent with the decreased ISG induction that is shown in my human IFNAR$^{-/-}$ intestinal epithelial cells (Figure 3-1). These results confirmed the positive feedback loop that type I IFN signaling not only promotes more type I IFN induction but also more production of type III IFN.

Interestingly, a recent study reported the differences in the ability of mouse intestinal cells responsive to IFN-β and IFN-λ (Schwerk, Köster et al. 2013). In this report, murine epithelial cells and organoids with a Mx2-RFP reporter were treated with either type I or III IFN and the induction of ISG was determined by fluorescence microscopy or FACS (Bhushal, Wolfsmüller et al. 2017). It was demonstrated that increasing amount of IFN-β upregulated the percentages of Mx2-RFP positive cells within the population (Bhushal, Wolfsmüller et al. 2017). Other studies also reported this phenomenon in human intestinal cells where increasing levels of IFN-β results in a continuous upregulation of ISGs whereas IFN-λ treatment shows a plateau in ISG induction at low doses (Saxena, Simon et al. 2017, Pervolaraki, Rastgou Talemi et al. 2018). My findings are in line with these studies, showing that type I IFN signaling cascade induces positive feedback while type III IFN does not.

Some studies have determined the effect of either the type I or III IFN receptor knock out in mice and explored how their absence influences enteric viruses (Pott, Mahlakõiv et al. 2011, Mahlakoiv, Hernandez et al. 2015, Nice, Baldridge et al. 2015, Lin, Feng et al. 2016). In the murine models, IFNLR1 is strictly expressed in intestinal epithelial cells lining the gastrointestinal tract and IFNAR1 expression spreads in the lamina propria of mature mice. In the intestine, IFN-λ is critical in inhibiting infections of multiple enteric viruses (e.g., rotavirus, reovirus, and mouse norovirus) in the epithelial cells whereas type I IFN controls systemic infections of these viruses (Pott et al., 2011; Mahlakõiv et al., 2015; Nice et al., 2015; Lin et al., 2016). Interestingly, these studies have found that the basal expression of IFNs is influenced in knock-out mice. Their results are in line with my results that basal levels

of IFN and ISGs were also impacted (Figure 3-1A-B). A possible explanation for reduced ISG induction upon type I IFN receptor knock out is that blockade of type I IFN signaling cascade prevents the induction of basal type I IFN. The ISGs in turn contributes to positive feedback on type III IFN signaling cascade. As many viruses have evolved to antagonize IFN signaling, it may be the reason why previous studies did not detect any differences in the ISG induction in the gut of $IFNAR^{-/-}$ and $IFNLR^{-/-}$ mice (Pott, Mahlakõiv et al. 2011, Mahlakoiv, Hernandez et al. 2015, Nice, Baldridge et al. 2015, Lin, Feng et al. 2016). For instance, reovirus, rotavirus and mouse norovirus express IFN antagonists targeting the IRF3/7 molecules, transcriptional factors for type I and IFN induction, the IFN receptors and downstream signaling molecules (Arnold, Barro et al. 2013, Arnold, Sen et al. 2013, Pervolaraki, Stanifer et al. 2017).

It was reported that mice are not responsive to type I IFN in their intestinal epithelial cells but show basal type III IFN induction. My results revealed that the type III IFN receptor negatively regulates type I IFN siganling, it is possible that the low level of type I IFN signaling attributes to the repression induced by type III IFN signaling. Notably, when intestinal cells are isolated from tissue, they are responsible to type I IFN *ex vivo* (Pott, Mahlakõiv et al. 2011, Schwerk, Köster et al. 2013, Bhushal, Wolfsmüller et al. 2017, Selvakumar, Bhushal et al. 2017). This indicates that either the signaling is repressed in the setting of an animal caused by other environmental factors or that the type I IFN receptor distributed is polarized thereby inhibiting its signaling in the setting of the gut epithelium (Pott, Mahlakõiv et al. 2011). In addition, it has been demonstrated human intestinal organoids favour type III IFN activation in response to enteric viruses even though they are responsive to both type I and III IFNs (Pervolaraki, Stanifer et al. 2017, Pervolaraki, Rastgou Talemi et al. 2018). When the type I IFN mRNA is expressed, it is still difficult to detect its secreted type I IFN form from intestinal cells both in mice and human intestinal organoids (Pott, Mahlakõiv et al. 2011, Mahlakoiv, Hernandez et al. 2015, Pervolaraki, Stanifer et al. 2017). This indicates that intestinal epithelial cells do not make type I IFN. Interestingly, murine studies found where type I IFN was secreted from the immune cells located in the lamina propria (Pott, Mahlakõiv et al. 2011, Mahlakoiv, Hernandez et al. 2015, Lin, Feng et al. 2016). As studies have shown that type I IFN positively regulates type III IFN signaling, it is proposed that a complex interaction between these immune cells and the intestinal epithelial cells where type I IFN derived from hematopoietic strengthen the type III IFN-induced protection of the mucosal barrier.

4.2 Conserved induction of distinct antiviral signalling kinetics by primate interferon lambda 4 proteins

Figuring out the molecular signaling pathways among IFN signaling is essential to comprehend immunity to virus infections and exploit more efficacious interventions. The pattern of antiviral signaling is increasingly important and studies have shown that type III IFNs exhibit slower but sustained signaling kinetics compared to type I IFNs (Marcello, Grakoui et al. 2006, Pervolaraki, Stanifer et al. 2017, Pervolaraki, Rastgou Talemi et al. 2018). However, most studies concentrated on comparing type I and III IFNs, very few studies addressed whether distinct members of the type III IFNs show a similar kinetics of ISG induction and STAT1 activation (Obajemu, Rao et al. 2017). Evidence has shown that human IFN-λ4 has non-redundant functions compared to other IFN-λs but the mechanism for this discrepancy remains unclear (Prokunina-Olsson, Muchmore et al. 2013, Terczyńska-Dyla, Bibert et al. 2014). In addition, several functional variants of IFN-λ4 are known to impact its potency (Hong, Schwerk et al. 2016, Bamford, Aranday-Cortes et al. 2018). In this work, I addressed whether IFN-λ4 and its variants (e.g., P70S and K154E) showed different antiviral kinetics compared to IFN-λ3. Using two cell lines from two distinct organs, I compared IFN-λ4 signaling and antiviral activity to determine conserved and variable features of IFN-λ4 and IFN-λ3 signaling exhibiting different antiviral kinetics, in line with recent work (Obajemu, Rao et al. 2017). In particular, the IFN-λ4 variants (P70S and K154E) influenced the magnitude of IFN siganling but not the kinetics. Furthermore, the kinetics are conserved outside of humans through using both non-human primate cell lines and IFN-λs.

It is notoriously challenging to compare IFN activity across variants considering the requirement for normalising input and processing. To solve the issues, input IFN-λs were normalised using a C-terminal “split luciferase” “HiBiT” tag and were produced in HEK-293T cells thereby preserving their appropriate glycosylation patterns. In addition, differential features were identified by comparing within a treatment group. Interestingly, different potencies of each IFN were determined using the normalized IFNs. Generally, WT IFN-λ3 was more effective compared to IFN-λ4 in both human colon cell line and hepatocytes. Precisely, IFN-λ3 induced higher magnitude of ISG production, more and prolonged p-STAT1, and stronger antiviral activity than WT IFN-λ4. However, the IFN-λ4 K154E variant’s potent was more like IFN-λ3. In addition, this mutant induced a stronger activation of p-STAT1 and ISG induction, and a more effective antiviral activity than WT IFN-λ4 whereas the P70S mutant exhibited the inverse phenotype, and its potency was weaker than WT IFN-λ4.

An important finding of this work is that the detected patterns were conserved in non-human species through using macaque and chimpanzee IFN-λ4 and macaque IFN-λ3 in human and macaque cell lines. This is vital because humans seem to have developed unique IFN-λ4 features associated with outcome of infectious diseases like HCV (Prokunina-Olsson, Muchmore et al. 2013). In addition, non-human primate IFN-λ4s showed antiviral potency similar to IFN-λ3. These results were complicated by the fact that the input cytokine levels could not be normalised as human primate IFN-λ3 and IFN-λ4 did not contain a split-luciferase tag but instead contained FLAG-tag. However, previous studies suggest that human and non-human primate IFN-λ4 share little difference in production and secretion.

The relationship between IFN-λs and their receptor complexes remains unclear even though some crystal structures of IFN-λ proteins in the absence and presence of its receptor complex IFNLR1 and IL10R2 are determined (Gad, Dellgren et al. 2009). The crystal structure of IFN-λ4 on its own or with receptors has not been solved. It is reasonable to speculate that IFN-λ4 differently interacts with its receptors considering amino acid sequence alignments. IFN-λ4 only has about 30% homology in common with IFN-λ1/2/3 and the homology are mostly located in the IFNLR1 binding site 'helix F'. Besides helix F, IFN-λ4 is different from the other IFN-λs, containing other receptor binding helices, for example D which binds IFNLR2. To check the contribution of varying IFN-λ4 receptor interactors in helices A, D and F, chimeras based on IFN-λ1 were created and cloned into IFN-λ4. Chimeric IFN-λs were efficiently produced and similar kinetic profiles were detected as IFN-λ1 (and IFN-λ3) even though different potencies were observed, suggesting that molecular determinants do not lie solely in the putative surface-exposed receptor-binding interfaces. IFN-λ4 differs in structural capacity to IFNλ1/3, which may not be captured in our chimeras, and further differences are observed in other helices that may play roles in signalling, such as 'helix' B. A possible explanation for these differences could also be due to changes in stability of IFN-λs. The stability of each IFN-λ has not yet been tested but could shed light onto how each family member reaches its activity. As most of our assays were performed in short time frames it seems unlikely that IFN stability played a role in this difference and is more likely that IFN-λ4 activates the receptor more rapidly, likely through binding more strongly analogous to type I IFNs.

My work revealed several significant findings, mainly focusing on the differences between IFN-λ3 and IFN-λ4, which were preserved between human and non-human primates and thereby functionally relevant. In comparison with type I IFNs, IFN-λs were defined partially

due to their slower and sustained signaling kinetics. IFN-λ4 was only found in 2013 and held a highly varying member of human IFN-λ family. IFN-λ4 contains several unique features, associating with certain diseases, transcriptional repression, and evolution in humans, suggesting a specific feature. Unlike other IFN-λs, IFN-λ4 signals more similar to type I IFNs even though it binds to IFNLR1 and IL10R2. Therefore, IFN kinetics may be dependent on not only receptor biology but also the interactions between cytokine and receptor. The continued studies into the reasons and results of such divergent signaling remain unexplored in human immune system.

4.3 Transient synergetic effect of IL-22 and IFN-λ in human intestinal cells and human intestinal organoids

In this work, I explored the synergetic effect of IFN-λ and IL-22 on the activation of STATs, the induction of ISGs, and antiviral activity. Results showed that co-treatment of IFN-λ and IL-22 activated more pSTAT1 but did not play a combinatorial role in the induction of ISGs and antiviral in human intestinal epithelial cells, which is different with the results in the mouse (Hernández, Mahlakoiv et al. 2015). Precisely, IL-22 enhanced the production of IFN-λ-mediated p-STAT1. Nevertheless, IL-22 could not help IFN-λ produce more ISGs in human intestinal epithelial cells, which is inconsistent with the finding in the mouse work (Hernández, Mahlakoiv et al. 2015). Luminex assay revealed that both IL-22 and IFN-λ induced the phosphorylation of STAT1, while only IFN-λ activated the production of p-STAT2 and only IL-22 activated the production of p-STAT3. Furthermore, IL-22 could not promote the IFN-λ-mediated antiviral activity. As IL-22 and IFN-λ share a common receptor IL-10R2 it is reasonable to speculate that IL-10R2 may be responsible for activating p-STAT1, while their independent receptors IFNLR1 and IL-22R make activate p-STAT2 and p-STAT3, respectively. To validate this hypothesis, two chimeric receptors: IFNLR1-IL-22RA and IL-22RA-IFNLR1, were constructed and transduced into IFNLR1.KO and WT T84 cell lines, separately, to determine the activation of STATs and production of ISGs or IL-22-induced genes. Further studies and IL-22 knock-out cells would be required to fully appreciate these signaling pathways.

My results showed that both IL-22 and IFN-λ activated p-STAT1 at the same phosphorylated site, but more p-STAT1 did not lead to more ISGs and antiviral. It is reasonable to speculate the difference of IL-22-induced p-STAT1 and IFN-λ-induced p-STAT1. The two kinds of p-STAT1 have the same phosphorylated site, Y701, but they may have other different

phosphorylated sites or modifications. To solve this hypothesis, phospho-proteomics can be employed to figure out the differences between them.

Whole transcriptome data analysis of T84 cells treated with IFN-λ and/or IL-22 revealed that IL-22 and IFN-λ activated independent signaling pathways. Notably, IL-22 could activate signaling pathways associated with cell proliferation and regeneration, especially the gene OLFM4 which acts as a marker for stem cells, whereas IFN-λ upregulates interferon stimulated genes. To confirm the proliferation phenotype, human colon organoids were treated with IFN-λ and/or IL-22. Following organoid growth overtime revealed that IL-22 can increase the size of organoids and increase stem cell gene markers. OLFM4 smRNAFish confirmed the IL-22-mediated stem cell proliferation.

Some other studies already reported the function of IL-22 in tissue homeostasis. IL-22 helps wound healing and recover tissue integrity and homeostasis by preventing cell death and tissue damage induced by inflammation and infection in tissue and organs with high IL-22RA expression (Sonnenberg, Fouser et al. 2011, Rutz, Wang et al. 2014, Sabat, Ouyang et al. 2014). It was reported that intestinal epithelial cells were preferentially responsive to IL-22 and did not response to any other IL-20 subfamily members (Ouyang, Kolls et al. 2008). IL-22 was also reported to promote intestinal stem cell-mediated epithelial regeneration (Lindemans, Calafiore et al. 2015).

Although IL-22 are advantageous in inducing epithelial cell proliferation and tissue homeostasis, uncontrolled IL-22 activity can also contribute to cancer in patients and mouse models (Huber, Gagliani et al. 2012, Hernandez, Gronke et al. 2018). The dual role of IL-22 may be due to the cellular source of IL-22. For example, Th17 cells-derived IL-22 was shown to play a pathogenic role in colorectal cancer (Perez, Kempski et al. 2020), while IL-22 derived from ILC3 appears to protect against genotoxic stress in the colon (Gronke, Hernández et al. 2019). Many studies showed that IL-22 promoted epithelial integrity and repair following pathogen infections in the lung (Alcorn 2020). My results showed that IL-22 has limited effects on uninjured cell in vitro. However, it is important to determine the effects of IL-22 on epithelial cells in inflammatory settings or pathogen-infected settings.

When exploring the antiviral activity of cytokines, it is also dependent on the model and species of viruses. In the mouse model, IL-22 cooperates with IFN-λ to clear rotavirus infection (Hernández, Mahlakoiv et al. 2015). In addition, IL-22 treatment increases the expression of IFN-λ to control replication of enteric coronavirus in intestinal porcine epithelial

cell line J2 (Xue, Zhao et al. 2017). Moreover, in an acute *Pseudomonas aeruginosa* pneumonia mouse model, neutralization of IL-22 resulted in vulnerable to infection and lung damage, whereas rIL-22 administration decreased mouse susceptibility and promoted epithelium protection (Broquet, Jacqueline et al. 2017). These studies indicate that IL-22 and IFN-λ work in concert in some infection models, especially in mice models.

It is also possible that one cytokine influences the differential kinetics of expression of another cytokine. In pneumonia caused by carbapenem-resistant ST258 *K. pneumoniae* (ST258), the expression kinetics of IL-22 and IFN-λ are different, IL-22 is upregulated at the start of infection and then again in the resolution phase, while the expression of IFN-λ steadily increases with infection (Ahn, Wickersham et al. 2019). Sometimes, one signaling pathway is upregulated when the other is absent. In a mouse model, IL-22 and its downstream induced genes RegIIIγ and NGAL are upregulated in the upper airways of mice when IFN-λ signaling is lost (Planet, Parker et al. 2016).

My results showed that IL-22 only promoted stem cell proliferation human colon organoids. The stem cells differentiate to different cell types depending on the culture media. Therefore, it is also necessary to split organoids treated with IL-22 for several days and culture in differentiated media to determine whether the ratio of different cell types is altered compared to unsplit organoids. Recent studies have shown that IL-22 is able to drive IEC proliferation and migration into villus tips, forming extrusion of differentiated IEC and serving as a site of rotavirus replication in a rotavirus infected mice model (Zhang, Zou et al. 2020). As my results revealed IL-22 barely helped IFN-λ-mediated antiviral activity in human intestinal epithelial cells, it is necessary to further explore the effects of IL-22 and IFN-λ on virus infected organoids.

Many studies have demonstrated the protective role of IL-22 in anti-inflammatory pathology, such as IBD model in mice (Andoh, Zhang et al. 2005, Zenewicz, Yancopoulos et al. 2007, Zenewicz, Yancopoulos et al. 2008). In mice, DSS is often used to induce inflammation in the gut. However, it is worthy creating a human organoid damage model using DSS and investigating the effects of IL-22 and IFN-λ in a DSS-induced organoid damage model. In addition, I can also combine the inflammatory model and virus infection model together to explore the effective of these cytokines. Given that these models are successfully made, effects of other cytokines can also be determined in the models.

5 Summary

During my PhD, I firstly explored the crosstalk of type I and III interferons (IFNs) signaling. Intestinal epithelial cells (IECs) are primarily responsive to enteric viruses in human intestine. The virus infection results in the induction of both type I and type III IFNs. Subsequently, the IFNs induce a series of antiviral molecules to prevent IECs from viral propagation. Currently, whether there is a crosstalk between these two cytokine pathways remains unsolved. Using either type I or type III receptor-deficient human intestinal epithelial cells, the results showed that the two cytokine pathways are interconnected at the level of ISG induction and potent of antiviral activity. Moreover, in human IECs, type I IFN receptor upregulates type III IFN siganling whereas type III IFN downregulates type I IFN signaling. These findings indicate that human intestinal cells are preferentially protected by type III IFN signaling.

Subsequently, I investigated how the newly discovered IFN-λ4 and its variants impact cytokine signaling and the conservation between them. Human IFN-λ4 is very divergent and only shares about 30% homology with IFN-λ1-3. Interestingly, IFN-λ4 variants are related to the outcome of HCV infection in humans. In this study, I determine whether human IFN-λ4 and its variants have differences in antiviral signalling compared to IFN-λ3. My results demonstrate that human IFN-λ4 and its variants P70S and K154E induce a distinct magnitude and kinetics of ISG production in human hepatocyte and intestinal cells. In addition, antiviral response induced by IFN-λ4 is faster yet transient compared to IFN-λ3. Furthermore, the distinct antiviral potency was also found in non-human primate IFN-λs and cell lines. Modifications in IFN-λ1 receptor-interacting interface do not alter its kinetic profile. Together, the results emphasis the possibility of IFN-λs in tissue specialisation.

My third project is to explore the interaction between interleukin-22 and IFN-λ. In this project, I employed human cell lines and human intestinal organoids to reveal several important findings about the interaction. I found that co-treatment of IL-22 and IFN-λ can induce more p-STAT1 than individual treatment of IL-22 or IFN-λ, but IL-22 cannot enhance IFN-λ-induced ISGs and antiviral activity *in vitro.* Using RNA-seq, I found signaling induced by IL-22 and IFN-λ are relatively independent even though they share a receptor and activate the same JAK/STAT pathways. Subsequently, I applied human intestinal organoids to validate the cell proliferation function induced by IL-22 which is found in the RNA-seq. I demonstrate IL-22 can promote the proliferation and regeneration of human intestinal organoids. Notably, IL-22 can promote stem cell proliferation marked by the increase in OLFM4 expression in the organoids. Subsequent smRNAFish in OLFM4 confirms the result in organoids. These

results indicate a new finding concerning IL-22 in human intestinal cells and intestinal organoids.

6 Zusammenfassung

Während meiner Doktorarbeit habe ich zunächst das Crosstalk von Typ-I- und Typ-III-Interferonen (IFNs) untersucht. Darmepithelzellen (IECs) reagieren hauptsächlich auf enterische Viren im menschlichen Darm. Die Virusinfektion führt zur Induktion sowohl von Typ-I- als auch von Typ-III-IFNs. Anschließend induzieren die IFNs eine Reihe von antiviralen Molekülen, um IECs an der viralen Vermehrung zu hindern. Ob es ein Crosstalk zwischen diesen beiden Zytokinwegen gibt, bleibt derzeit ungeklärt. Unter Verwendung von entweder Typ I- oder Typ III-Rezeptor-defizienten menschlichen Darmepithelzellen zeigten die Ergebnisse, dass die beiden Zytokinwege auf der Ebene der ISG-Induktion miteinander verbunden sind und eine starke antivirale Aktivität aufweisen. Darüber hinaus reguliert in humanen IECs der Typ-I-IFN-Rezeptor die Typ-III-IFN-Signalgebung hoch, während Typ-III-IFN die Typ-I-IFN-Signalgebung herunterreguliert. Diese Ergebnisse weisen darauf hin, dass menschliche Darmzellen bevorzugt durch Typ-III-IFN-Signalgebung geschützt werden.

Anschließend untersuchte ich, wie das neu entdeckte IFN-λ4 und seine Varianten die Zytokin-Signalübertragung und die Konservierung zwischen ihnen beeinflussen. Humanes IFN-λ4 ist sehr divergent und teilt nur 30% Homologie mit IFN-λ1-3. Interessanterweise hängen IFN-λ4-Varianten mit dem Ausgang einer HCV-Infektion beim Menschen zusammen. In dieser Studie bestimme ich, ob humanes IFN-λ4 und seine Varianten Unterschiede in der antiviralen Signalübertragung im Vergleich zu IFN-λ3 aufweisen. Meine Ergebnisse zeigen, dass humanes IFN-λ4 und seine Varianten P70S und K154E eine unterschiedliche Größenordnung und Kinetik der ISG-Produktion in humanen Hepatozyten und Darmzellen induzieren. Darüber hinaus ist die durch IFN-λ4 induzierte antivirale Reaktion im Vergleich zu IFN-λ3 schneller aber trotzdem noch transient. Darüber hinaus wurde die ausgeprägte antivirale Wirksamkeit auch in nicht-humanen Primaten-IFN-λs und -Zelllinien gefunden. Modifikationen in der IFN-λ1-Rezeptor-Wechselwirkungsschnittstelle ändern nicht ihr kinetisches Profil. Kurz gesagt weisen die Ergebnisse auf die Möglichkeit einer Gewebespezialisierung von IFN-λs hin.

Mein drittes Projekt besteht darin, die Interaktion zwischen Interleukin-22 und IFN-λ zu untersuchen. In diesem Projekt habe ich menschliche Zelllinien und menschliche Darmorganoide verwendet, um mehrere wichtige Erkenntnisse über die Interaktion zu gewinnen. Ich fand heraus, dass die gleichzeitige Behandlung von IL-22 und IFN-λ mehr p-STAT1 induzieren kann als die Einzelbehandlung von IL-22 oder IFN-λ, aber IL-22 kann die IFN-λ-induzierten ISGs und die antivirale Aktivität in vitro nicht verstärken. Unter

Verwendung von RNA-seq stellte ich fest, dass die durch IL-22 und IFN-λ induzierten Signalübertragungen relativ unabhängig sind, obwohl sie einen gemeinsamen Rezeptor haben und dieselben JAK/STAT-Signalwege aktivieren. Anschließend habe ich humane intestinale Organoide angewendet, um die Zellproliferationsfunktion zu validieren, die durch IL-22 induziert wird, das in der RNA-Seq. Ich zeige, dass IL-22 die Proliferation und Regeneration von menschlichen Darmorganoiden fördern kann. Insbesondere kann IL-22 die Stammzellproliferation fördern, die durch die Zunahme der OLFM4-Expression in den Organoiden gekennzeichnet ist. smRNAFish in OLFM4 bestätigt das Ergebnis in Organoiden. Diese Ergebnisse weisen auf einen neuen Befund bezüglich IL-22 in menschlichen Zelllinien und Darmorganoiden hin.

7 References

ABREU, M. T. 2010. Toll-like receptor signalling in the intestinal epithelium: how bacterial recognition shapes intestinal function. *Nature Reviews Immunology,* 10**,** 131-144. DOI: 10.1038/nri2707

ABT, M. C., OSBORNE, L. C., MONTICELLI, L. A., DOERING, T. A., ALENGHAT, T., SONNENBERG, G. F., PALEY, M. A., ANTENUS, M., WILLIAMS, K. L. & ERIKSON, J. 2012. Commensal bacteria calibrate the activation threshold of innate antiviral immunity. *Immunity,* 37**,** 158-170. DOI: 10.1016/j.immuni.2012.04.011

AHN, D. & PRINCE, A. 2020. Participation of the IL-10RB related cytokines, IL-22 and IFN-λ in defense of the airway mucosal barrier. *Frontiers in Cellular and Infection Microbiology,* 10**,** 300. DOI: 10.3389/fcimb.2020.00300

AHN, D., WICKERSHAM, M., RIQUELME, S. & PRINCE, A. 2019. The effects of IFN-λ on epithelial barrier function contribute to Klebsiella pneumoniae ST258 pneumonia. *American journal of respiratory cell and molecular biology,* 60**,** 158-166. DOI: 10.1165/rcmb.2018-0021OC

ALAM, M. S., MAEKAWA, Y., KITAMURA, A., TANIGAKI, K., YOSHIMOTO, T., KISHIHARA, K. & YASUTOMO, K. 2010. Notch signaling drives IL-22 secretion in CD4+ T cells by stimulating the aryl hydrocarbon receptor. *Proceedings of the National Academy of Sciences,* 107**,** 5943-5948. DOI: 10.1073/pnas.0911755107

ALBENBERG, L., ESIPOVA, T. V., JUDGE, C. P., BITTINGER, K., CHEN, J., LAUGHLIN, A., GRUNBERG, S., BALDASSANO, R. N., LEWIS, J. D. & LI, H. 2014. Correlation between intraluminal oxygen gradient and radial partitioning of intestinal microbiota. *Gastroenterology,* 147**,** 1055-1063. e8. DOI: 10.1053/j.gastro.2014.07.020

ALCORN, J. F. 2020. IL-22 Plays a critical role in maintaining epithelial integrity during pulmonary infection. *Frontiers in Immunology,* 11**,** 1160. DOI: 10.3389/fimmu.2020.01160

ALVAREZ, M. J., SHEN, Y., GIORGI, F. M., LACHMANN, A., DING, B. B., YE, B. H. & CALIFANO, A. 2016. Functional characterization of somatic mutations in cancer using network-based inference of protein activity. *Nature genetics,* 48**,** 838-847. DOI: 10.1038/ng.3593

AMANZADA, A., KOPP, W., SPENGLER, U., RAMADORI, G. & MIHM, S. 2013. Interferon-λ4 (IFNL4) transcript expression in human liver tissue samples. *PloS one,* 8**,** e84026. DOI: 10.1371/journal.pone.0084026

ANDOH, A., ZHANG, Z., INATOMI, O., FUJINO, S., DEGUCHI, Y., ARAKI, Y., TSUJIKAWA, T., KITOH, K., KIM–MITSUYAMA, S. & TAKAYANAGI, A. 2005. Interleukin-22, a member of the IL-10 subfamily, induces inflammatory responses in colonic subepithelial myofibroblasts. *Gastroenterology,* 129**,** 969-984. DOI: 10.1053/j.gastro.2005.06.071

ANK, N., IVERSEN, M. B., BARTHOLDY, C., STAEHELI, P., HARTMANN, R., JENSEN, U. B., DAGNAES-HANSEN, F., THOMSEN, A. R., CHEN, Z. & HAUGEN, H. 2008. An important role for type III interferon (IFN-λ/IL-28) in TLR-induced antiviral activity. *The Journal of Immunology,* 180**,** 2474-2485. DOI: 10.4049/jimmunol.180.4.2474

APARICIO-DOMINGO, P., ROMERA-HERNANDEZ, M., KARRICH, J. J., CORNELISSEN, F., PAPAZIAN, N., LINDENBERGH-KORTLEVE, D. J., BUTLER, J. A., BOON, L., COLES, M. C. & SAMSOM, J. N. 2015. Type 3 innate lymphoid cells maintain intestinal epithelial stem cells after tissue damage. *Journal of Experimental Medicine,* 212**,** 1783-1791. DOI: 10.1084/jem.20150318

ARNOLD, M. M., SEN, A., GREENBERG, H. B. & PATTON, J. T. 2013. The battle between rotavirus and its host for control of the interferon signaling pathway. *PLoS pathogens,* 9**,** e1003064. DOI: 10.1371/journal.ppat.1003064

AUJLA, S. J., CHAN, Y. R., ZHENG, M., FEI, M., ASKEW, D. J., POCIASK, D. A., REINHART, T. A., MCALLISTER, F., EDEAL, J. & GAUS, K. 2008. IL-22 mediates mucosal host defense against Gram-negative bacterial pneumonia. *Nature medicine,* 14**,** 275-281. DOI: 10.1038/nm1710

AWANE, M., ANDRES, P. G., LI, D. J. & REINECKER, H.-C. 1999. NF-κB-inducing kinase is a common mediator of IL-17-, TNF-α-, and IL-1β-induced chemokine promoter activation in intestinal epithelial cells. *The Journal of Immunology,* 162**,** 5337-5344. URL: http://www.jimmunol.org/content/162/9/5337

BALDRIDGE, M. T., LEE, S., BROWN, J. J., MCALLISTER, N., URBANEK, K., DERMODY, T. S., NICE, T. J. & VIRGIN, H. W. 2017. Expression of Ifnlr1 on intestinal epithelial cells is critical to the antiviral effects of interferon lambda against norovirus and reovirus. *Journal of virology,* 91**,** e02079-16. DOI: 10.1128/JVI.02079-16

BAMFORD, C. G., ARANDAY-CORTES, E., FILIPE, I. C., SUKUMAR, S., MAIR, D., FILIPE, A. D. S., MENDOZA, J. L., GARCIA, K. C., FAN, S. & TISHKOFF, S. A. 2018. A polymorphic residue that attenuates the antiviral potential of interferon lambda 4 in hominid lineages. *Plos Pathogens,* 14**,** e1007307. DOI: 10.1371/journal.ppat.1007307

BARBER, G. N. 2011. Cytoplasmic DNA innate immune pathways. *Immunological reviews,* 243**,** 99-108. DOI: 10.1111/j.1600-065X.2011. 01051.x

BEVINS, C. L. & SALZMAN, N. H. 2011. Paneth cells, antimicrobial peptides and maintenance of intestinal homeostasis. *Nature Reviews Microbiology,* 9**,** 356-368. DOI: 10.1038/nrmicro2546

BHUSHAL, S., WOLFSMÜLLER, M., SELVAKUMAR, T. A., KEMPER, L., WIRTH, D., HORNEF, M. W., HAUSER, H. & KÖSTER, M. 2017. Cell polarization and epigenetic status shape the heterogeneous response to type III interferons in intestinal epithelial cells. *Frontiers in immunology***,** 671. DOI: 10.3389/fimmu.2017.00671

BIANCHERI, P., DI SABATINO, A., CORAZZA, G. R. & MACDONALD, T. T. 2013. Proteases and the gut barrier. *Cell and tissue research,* 351**,** 269-280. DOI: 10.1007/s00441-012-1390-z

BLASCHITZ, C. & RAFFATELLU, M. 2010. Th17 cytokines and the gut mucosal barrier. *Journal of clinical immunology,* 30**,** 196-203. DOI: 10.1007/s10875-010-9368-7

BLEICHER, L., DE MOURA, P. R., WATANABE, L., COLAU, D., DUMOUTIER, L., RENAULD, J.-C. & POLIKARPOV, I. 2008. Crystal structure of the IL-22/IL-22R1 complex and its implications for the IL-22 signaling mechanism. *FEBS letters,* 582**,**

2985-2992. DOI: 10.1016/j.febslet.2008.07.046

BLUMER, T., COTO-LLERENA, M., DUONG, F. H. & HEIM, M. H. 2017. SOCS1 is an inducible negative regulator of interferon λ (IFN-λ)–induced gene expression in vivo. *Journal of Biological Chemistry,* 292**,** 17928-17938. DOI: 10.1074/jbc.M117.788877

BOEHM, T. & SWANN, J. B. 2013. Thymus involution and regeneration: two sides of the same coin? *Nature Reviews Immunology,* 13**,** 831-838. DOI: 10.1038/nri3534

BOLEN, C. R., DING, S., ROBEK, M. D. & KLEINSTEIN, S. H. 2014. Dynamic expression profiling of type I and type III interferon-stimulated hepatocytes reveals a stable hierarchy of gene expression. *Hepatology,* 59**,** 1262-1272. DOI: 10.1002/hep.26657

BONIFACE, K., GUIGNOUARD, E., PEDRETTI, N., GARCIA, M., DELWAIL, A., BERNARD, F., NAU, F., GUILLET, G., DAGREGORIO, G. & YSSEL, H. 2007. A role for T cell-derived interleukin 22 in psoriatic skin inflammation. *Clinical & Experimental Immunology,* 150**,** 407-415. DOI: 10.1111/j.1365-2249.2007.03511.x

BRAND, S., ZITZMANN, K., DAMBACHER, J., BEIGEL, F., OLSZAK, T., VLOTIDES, G., EICHHORST, S. T., GÖKE, B., DIEPOLDER, H. & AUERNHAMMER, C. J. 2005. SOCS-1 inhibits expression of the antiviral proteins 2′, 5′-OAS and MxA induced by the novel interferon-λs IL-28A and IL-29. *Biochemical and biophysical research communications,* 331**,** 543-548. DOI: 10.1016/j.bbrc.2005.04.004

BRESTOFF, J. R., KIM, B. S., SAENZ, S. A., STINE, R. R., MONTICELLI, L. A., SONNENBERG, G. F., THOME, J. J., FARBER, D. L., LUTFY, K. & SEALE, P. 2015. Group 2 innate lymphoid cells promote beiging of white adipose tissue and limit obesity. *Nature,* 519**,** 242-246. DOI: 10.1038/nature14115

BROGGI, A., TAN, Y., GRANUCCI, F. & ZANONI, I. 2017. IFN-λ suppresses intestinal inflammation by non-translational regulation of neutrophil function. *Nature immunology,* 18**,** 1084-1093. DOI: 10.1038/ni.3821

BROQUET, A., BESBES, A., MARTIN, J., JACQUELINE, C., VOURC'H, M., ROQUILLY, A., CAILLON, J., JOSIEN, R. & ASEHNOUNE, K. 2020. Interleukin-22 regulates interferon lambda expression in a mice model of pseudomonas aeruginosa pneumonia. *Molecular immunology,* 118**,** 52-59. DOI: 10.1016/j.molimm.2019.12.003

BROQUET, A., JACQUELINE, C., DAVIEAU, M., BESBES, A., ROQUILLY, A., MARTIN, J., CAILLON, J., DUMOUTIER, L., RENAULD, J.-C. & HESLAN, M. 2017. Interleukin-22 level is negatively correlated with neutrophil recruitment in the lungs in a Pseudomonas aeruginosa pneumonia model. *Scientific reports,* 7**,** 1-11. DOI: 10.1038/s41598-017-11518-0

CASTELEYN, C., REKECKI, A., VAN DER AA, A., SIMOENS, P. & VAN DEN BROECK, W. 2010. Surface area assessment of the murine intestinal tract as a prerequisite for oral dose translation from mouse to man. *Laboratory animals,* 44**,** 176-183. DOI: 10.1258/la.2009.009112

CASTELEYN, G., LELIAERT, F., BACKELJAU, T., DEBEER, A.-E., KOTAKI, Y., RHODES, L., LUNDHOLM, N., SABBE, K. & VYVERMAN, W. 2010. Limits to gene flow in a cosmopolitan marine planktonic diatom. *Proceedings of the National Academy of Sciences,* 107**,** 12952-12957. DOI: 10.1073/pnas.1001380107

CELLA, M., FUCHS, A., VERMI, W., FACCHETTI, F., OTERO, K., LENNERZ, J. K., DOHERTY, J. M., MILLS, J. C. & COLONNA, M. 2009. A human natural killer cell subset provides an innate source of IL-22 for mucosal immunity. *Nature,* 457**,** 722-725. DOI: 10.1038/nature07537

CELLA, M., OTERO, K. & COLONNA, M. 2010. Expansion of human NK-22 cells with IL-7, IL-2, and IL-1β reveals intrinsic functional plasticity. *Proceedings of the National Academy of Sciences,* 107**,** 10961-10966. DOI: 10.1073/pnas.1005641107

CHEN, X., BAROZZI, I., TERMANINI, A., PROSPERINI, E., RECCHIUTI, A., DALLI, J., MIETTON, F., MATTEOLI, G., HIEBERT, S. & NATOLI, G. 2012. Requirement for the histone deacetylase Hdac3 for the inflammatory gene expression program in macrophages. *Proceedings of the National Academy of Sciences,* 109**,** E2865-E2874. DOI: 10.1073/pnas.1121131109

CHEN, Y., CHOU, K., FUCHS, E., HAVRAN, W. L. & BOISMENU, R. 2002. Protection of the intestinal mucosa by intraepithelial γδ T cells. *Proceedings of the National Academy of Sciences,* 99**,** 14338-14343. DOI: 10.1073/pnas.212290499

CHOW, K. T., GALE JR, M. & LOO, Y.-M. 2018. RIG-I and other RNA sensors in antiviral immunity. *Annual review of immunology,* 36**,** 667-694. DOI: 10.1146/annurev-immunol-042617-053309

CLEMENTE, J. C., URSELL, L. K., PARFREY, L. W. & KNIGHT, R. 2012. The impact of the gut microbiota on human health: an integrative view. *Cell,* 148**,** 1258-1270. DOI: 10.1016/j.cell.2012.01.035

COLGAN, S. P. & TAYLOR, C. T. 2010. Hypoxia: an alarm signal during intestinal inflammation. *Nature reviews Gastroenterology & hepatology,* 7**,** 281-287. DOI: 10.1038/nrgastro.2010.39

COLLINS, J. T., NGUYEN, A. & BADIREDDY, M. 2017. Anatomy, abdomen and pelvis, small intestine. StatPearls Publishing, Treasure Island (FL). PMID: 29083773.

CROTTA, S., DAVIDSON, S., MAHLAKOIV, T., DESMET, C. J., BUCKWALTER, M. R., ALBERT, M. L., STAEHELI, P. & WACK, A. 2013. Type I and type III interferons drive redundant amplification loops to induce a transcriptional signature in influenza-infected airway epithelia. *PLoS pathogens,* 9**,** e1003773. DOI: 10.1371/journal.ppat.1003773

CURETON, D. K., MASSOL, R. H., SAFFARIAN, S., KIRCHHAUSEN, T. L. & WHELAN, S. P. 2009. Vesicular stomatitis virus enters cells through vesicles incompletely coated with clathrin that depend upon actin for internalization. *PLoS pathogens,* 5**,** e1000394. DOI: 10.1371/journal.ppat.1000394

DATE, S. & SATO, T. 2015. Mini-gut organoids: reconstitution of the stem cell niche. *Annual review of cell and developmental biology,* 31**,** 269-289. DOI: 10.1146/annurev-cellbio-100814-125218

DE WEERD, N. A., VIVIAN, J. P., NGUYEN, T. K., MANGAN, N. E., GOULD, J. A., BRANIFF, S.-J., ZAKER-TABRIZI, L., FUNG, K. Y., FORSTER, S. C. & BEDDOE, T. 2013. Structural basis of a unique interferon-β signaling axis mediated via the receptor IFNAR1. *Nature immunology,* 14**,** 901-907. DOI: 10.1038/ni.2667

DHIMAN, R., INDRAMOHAN, M., BARNES, P. F., NAYAK, R. C., PAIDIPALLY, P., RAO, L. V. M. & VANKAYALAPATI, R. 2009. IL-22 produced by human NK cells inhibits growth of Mycobacterium tuberculosis by enhancing phagolysosomal fusion. *The Journal of Immunology,* 183**,** 6639-6645. DOI: 10.4049/jimmunol.0902587

DIEFENBACH, A., COLONNA, M. & KOYASU, S. 2014. Development, differentiation, and diversity of innate lymphoid cells. *Immunity,* 41**,** 354-365. DOI: 10.1016/j.immuni.2014.09.005

DOISNE, J.-M., SOULARD, V., BÉCOURT, C., AMNIAI, L., HENROT, P., HAVENAR-DAUGHTON, C., BLANCHET, C., ZITVOGEL, L., RYFFEL, B. & CAVAILLON, J.-M. 2011. Cutting edge: crucial role of IL-1 and IL-23 in the innate IL-17 response of peripheral lymph node NK1. 1− invariant NKT cells to bacteria. *The Journal of Immunology,* 186**,** 662-666. DOI: 10.4049/jimmunol.1002725

DUDAKOV, J. A., HANASH, A. M., JENQ, R. R., YOUNG, L. F., GHOSH, A., SINGER, N. V., WEST, M. L., SMITH, O. M., HOLLAND, A. M. & TSAI, J. J. 2012. Interleukin-22 drives endogenous thymic regeneration in mice. *Science,* 336**,** 91-95. DOI: 10.1126/science.1218004

DUDAKOV, J. A., HANASH, A. M. & VAN DEN BRINK, M. R. 2015. Interleukin-22: immunobiology and pathology. *Annual review of immunology,* 33**,** 747-785. DOI: 10.1146/annurev-immunol-032414-112123

DUHEN, T., GEIGER, R., JARROSSAY, D., LANZAVECCHIA, A. & SALLUSTO, F. 2009. Production of interleukin 22 but not interleukin 17 by a subset of human skin-homing memory T cells. *Nature immunology,* 10**,** 857-863. DOI: 10.1038/ni.1767

DUMOUTIER, L., VAN ROOST, E., AMEYE, G., MICHAUX, L. & RENAULD, J.-C. 2000. IL-TIF/IL-22: genomic organization and mapping of the human and mouse genes. *Genes & Immunity,* 1**,** 488-494. DOI: 10.1038/sj.gene.6363716

EBERL, G., COLONNA, M., DI SANTO, J. & MCKENZIE, A. 2015. Innate lymphoid cells. Innate lymphoid cells: a new paradigm in immunology. Science. 348: aaa6566. DOI: 10.1126/science.aaa6566

EL KASMI, K. C., HOLST, J., COFFRE, M., MIELKE, L., DE PAUW, A., LHOCINE, N., SMITH, A. M., RUTSCHMAN, R., KAUSHAL, D. & SHEN, Y. 2006. General nature of the STAT3-activated anti-inflammatory response. *The Journal of Immunology,* 177**,** 7880-7888. DOI: 10.4049/jimmunol.177.11.7880

EMING, S. A., WYNN, T. A. & MARTIN, P. 2017. Inflammation and metabolism in tissue repair and regeneration. *Science,* 356**,** 1026-1030. DOI: 10.1126/science. aam7928

EWELS, P., MAGNUSSON, M., LUNDIN, S. & KÄLLER, M. 2016. MultiQC: summarize analysis results for multiple tools and samples in a single report. *Bioinformatics,* 32**,** 3047-3048. DOI: 10.1093/bioinformatics/btw354

FANG, T. C., SCHAEFER, U., MECKLENBRAUKER, I., STIENEN, A., DEWELL, S., CHEN, M. S., RIOJA, I., PARRAVICINI, V., PRINJHA, R. K. & CHANDWANI, R. 2012. Histone H3 lysine 9 di-methylation as an epigenetic signature of the interferon response. *Journal of Experimental Medicine,* 209**,** 661-669. DOI: 10.1084/jem.20112343

FEMINO, A. M., FAY, F. S., FOGARTY, K. & SINGER, R. H. 1998. Visualization of single RNA transcripts in situ. *Science,* 280**,** 585-590. DOI: 10.1126/science.280.5363.585

FORKOSH, E. & ILAN, Y. 2019. The heart-gut axis: New target for atherosclerosis and congestive heart failure therapy. *Open heart,* 6**,** e000993. DOI: 10.1136/openhrt-2018-000993

FOXALL, R. B. 2016. Profile of interleukin-22 in gut mucosal health and. *International Journal of Interferon, Cytokine and Mediator Research,* 8**,** 1-11. DOI https://doi.org/10.2147/IJICMR.S64856

FRANÇOIS-NEWTON, V., MAGNO DE FREITAS ALMEIDA, G., PAYELLE-BROGARD, B., MONNERON, D., PICHARD-GARCIA, L., PIEHLER, J., PELLEGRINI, S. & UZÉ, G. 2011. USP18-based negative feedback control is induced by type I and type III interferons and specifically inactivates interferon α response. *PloS one,* 6**,** e22200. DOI: 10.1371/journal.pone.0022200

FUCHS, S. Y. 2013. Hope and fear for interferon: the receptor-centric outlook on the future of interferon therapy. *Journal of Interferon & Cytokine Research,* 33**,** 211-225. DOI: 10.1089/jir.2012.0117

FUNG, K. Y., MANGAN, N. E., CUMMING, H., HORVAT, J. C., MAYALL, J. R., STIFTER, S. A., DE WEERD, N., ROISMAN, L. C., ROSSJOHN, J. & ROBERTSON, S. A. 2013. Interferon-ε protects the female reproductive tract from viral and bacterial infection. *Science,* 339**,** 1088-1092. DOI: 10.1126/science.1233321

GAD, H. H., DELLGREN, C., HAMMING, O. J., VENDS, S., PALUDAN, S. R. & HARTMANN, R. 2009. Interferon-λ is functionally an interferon but structurally related to the interleukin-10 family. *Journal of Biological Chemistry,* 284**,** 20869-20875. DOI: 10.1074/jbc.M109.002923

GALANI, I. E., TRIANTAFYLLIA, V., ELEMINIADOU, E.-E., KOLTSIDA, O., STAVROPOULOS, A., MANIOUDAKI, M., THANOS, D., DOYLE, S. E., KOTENKO, S. V. & THANOPOULOU, K. 2017. Interferon-λ mediates non-redundant front-line antiviral protection against influenza virus infection without compromising host fitness. *Immunity,* 46**,** 875-890. e6. DOI: 10.1016/j.immuni.2017.04.025

GARCIA, M. A., NELSON, W. J. & CHAVEZ, N. 2018. Cell–cell junctions organize structural and signaling networks. *Cold Spring Harbor perspectives in biology,* 10**,** a029181. DOI: 10.1101/cshperspect.a029181

GARCIA-ALONSO, L., HOLLAND, C. H., IBRAHIM, M. M., TUREI, D. & SAEZ-RODRIGUEZ, J. 2019. Benchmark and integration of resources for the estimation of human transcription factor activities. *Genome research,* 29**,** 1363-1375. DOI: 10.1101/gr.240663.118

GARCÍA-PEÑALVO, F. J. 2018. Technological ecosystems for enhancing the interoperability and data flows. Journal of Information Technology Research, 11(1), vi-x. URL: https://repositorio.grial.eu/bitstream/grial/1106/1/Jitr11-1-Editorial.pdf

GARCÍA-SASTRE, A. & BIRON, C. A. 2006. Type 1 interferons and the virus-host relationship: a lesson in detente. *Science,* 312**,** 879-882. DOI: 10.1126/science.1125676

GERBE, F., SIDOT, E., SMYTH, D. J., OHMOTO, M., MATSUMOTO, I., DARDALHON, V., CESSES, P., GARNIER, L., POUZOLLES, M. & BRULIN, B. 2016. Intestinal epithelial tuft cells initiate type 2 mucosal immunity to helminth parasites. *Nature,* 529**,** 226-230. DOI: 10.1038/nature16527

GESSANI, S., BELARDELLI, F., PECORELLI, A., PUDDU, P. & BAGLIONI, C. 1989. Bacterial lipopolysaccharide and gamma interferon induce transcription of beta interferon mRNA and interferon secretion in murine macrophages. *Journal of virology,* 63**,** 2785-2789. DOI: 10.1128/JVI.63.6.2785-2789.1989

GIBBERT, K., SCHLAAK, J., YANG, D. & DITTMER, U. 2013. IFN-α subtypes: distinct biological activities in anti-viral therapy. *British journal of pharmacology,* 168**,** 1048-1058. DOI: 10.1111/bph.12010

GODINEZ, I., RAFFATELLU, M., CHU, H., PAIXÃO, T. A., HANEDA, T., SANTOS, R. L., BEVINS, C. L., TSOLIS, R. M. & BÄUMLER, A. J. 2009. Interleukin-23 orchestrates mucosal responses to Salmonella enterica serotype Typhimurium in the intestine. *Infection and immunity,* 77**,** 387-398. DOI: 10.1128/IAI.00933-08

GOODRIDGE, H. S. & UNDERHILL, D. M. 2008. Fungal recognition by TLR2 and Dectin-1. *Toll-like receptors (TLRs) and innate immunity***,** 87-109. DOI: 10.1007/978-3-540-72167-3_5

GRIBBLE, F. M. & REIMANN, F. 2016. Enteroendocrine cells: chemosensors in the intestinal epithelium. *Annual review of physiology,* 78**,** 277-299. DOI: 10.1146/annurev-physiol-021115-105439

GRONKE, K., HERNÁNDEZ, P. P., ZIMMERMANN, J., KLOSE, C. S., KOFOED-BRANZK, M., GUENDEL, F., WITKOWSKI, M., TIZIAN, C., AMANN, L. & SCHUMACHER, F. 2019. Interleukin-22 protects intestinal stem cells against genotoxic stress. *Nature,* 566**,** 249-253. DOI: 10.1038/s41586-019-0899-7

GUO, C., REUSS, D., COEY, J. D., SUKUMAR, S., LANG, B., MCLAUCHLAN, J., BOULANT, S., STANIFER, M. L. & BAMFORD, C. G. G. 2021. Conserved Induction of Distinct Antiviral Signalling Kinetics by Primate Interferon Lambda 4 Proteins. *Front Immunol,* 12**,** 772588. DOI: 10.3389/fimmu.2021.772588

GUO, H. & TOPHAM, D. J. 2010. Interleukin-22 (IL-22) production by pulmonary Natural Killer cells and the potential role of IL-22 during primary influenza virus infection. *Journal of virology,* 84**,** 7750-7759. DOI: 10.1128/JVI.00187-10

HAMILTON, J. A., WHITTY, G. A., KOLA, I. & HERTZOG, P. J. 1996. Endogenous IFN-alpha beta suppresses colony-stimulating factor (CSF)-1-stimulated macrophage DNA synthesis and mediates inhibitory effects of lipopolysaccharide and TNF-alpha. *The Journal of Immunology,* 156**,** 2553-2557. URL: http://www.jimmunol.org/content/156/7/2553

HAMMING, O. J., TERCZYŃSKA-DYLA, E., VIEYRES, G., DIJKMAN, R., JØRGENSEN, S. E., AKHTAR, H., SIUPKA, P., PIETSCHMANN, T., THIEL, V. & HARTMANN, R. 2013. Interferon lambda 4 signals via the IFNλ receptor to regulate antiviral activity against HCV and coronaviruses. *The EMBO journal,* 32**,** 3055-3065. DOI: 10.1038/emboj.2013.232

HANASH, A. M., DUDAKOV, J. A., HUA, G., O'CONNOR, M. H., YOUNG, L. F., SINGER,

N. V., WEST, M. L., JENQ, R. R., HOLLAND, A. M. & KAPPEL, L. W. 2012. Interleukin-22 protects intestinal stem cells from immune-mediated tissue damage and regulates sensitivity to graft versus host disease. *Immunity,* 37**,** 339-350. DOI: 10.1016/j.immuni.2012.05.028

HASEGAWA, M., YADA, S., LIU, M. Z., KAMADA, N., MUÑOZ-PLANILLO, R., DO, N., NÚÑEZ, G. & INOHARA, N. 2014. Interleukin-22 regulates the complement system to promote resistance against pathobionts after pathogen-induced intestinal damage. *Immunity,* 41**,** 620-632. DOI: 10.1016/j.immuni.2014.09.010

HELANDER, H. F. & FÄNDRIKS, L. 2014. Surface area of the digestive tract–revisited. *Scandinavian journal of gastroenterology,* 49**,** 681-689. DOI: 10.3109/00365521.2014.898326

HERNANDEZ, P., GRONKE, K. & DIEFENBACH, A. 2018. A catch-22: Interleukin-22 and cancer. *European journal of immunology,* 48**,** 15-31. DOI: 10.1002/eji.201747183

HERNÁNDEZ, P. P., MAHLAKOIV, T., YANG, I., SCHWIERZECK, V., NGUYEN, N., GUENDEL, F., GRONKE, K., RYFFEL, B., HÖLSCHER, C. & DUMOUTIER, L. 2015. Interferon-λ and interleukin 22 act synergistically for the induction of interferon-stimulated genes and control of rotavirus infection. *Nature immunology,* 16**,** 698-707. DOI: 10.1038/ni.3180

HILL, D. A. & ARTIS, D. 2009. Intestinal bacteria and the regulation of immune cell homeostasis. *Annual review of immunology,* 28**,** 623-667. DOI: 10.1146/annurev-immunol-030409-101330

HOFFMANN, H.-H., SCHNEIDER, W. M. & RICE, C. M. 2015. Interferons and viruses: an evolutionary arms race of molecular interactions. *Trends in immunology,* 36**,** 124-138. DOI: 10.1016/j.it.2015.01.004

HONDA, M., SHIRASAKI, T., SHIMAKAMI, T., SAKAI, A., HORII, R., ARAI, K., YAMASHITA, T., SAKAI, Y., YAMASHITA, T. & OKADA, H. 2014. Hepatic interferon-stimulated genes are differentially regulated in the liver of chronic hepatitis C patients with different interleukin-28B genotypes. *Hepatology,* 59**,** 828-838. DOI: 10.1002/hep.26788

HONG, M., SCHWERK, J., LIM, C., KELL, A., JARRET, A., PANGALLO, J., LOO, Y.-M., LIU, S., HAGEDORN, C. H. & GALE JR, M. 2016. Interferon lambda 4 expression is suppressed by the host during viral infection. *Journal of Experimental Medicine,* 213**,** 2539-2552. DOI: 10.1084/jem.20160437

HOOPER, L. V. 2004. Bacterial contributions to mammalian gut development. *Trends in microbiology,* 12**,** 129-134. DOI: 10.1016/j.tim.2004.01.001

HOWITT, M. R., LAVOIE, S., MICHAUD, M., BLUM, A. M., TRAN, S. V., WEINSTOCK, J. V., GALLINI, C. A., REDDING, K., MARGOLSKEE, R. F. & OSBORNE, L. C. 2016. Tuft cells, taste-chemosensory cells, orchestrate parasite type 2 immunity in the gut. *Science,* 351**,** 1329-1333. DOI: 10.1126/science.aaf1648

HUBER, S., GAGLIANI, N., ZENEWICZ, L. A., HUBER, F. J., BOSURGI, L., HU, B., HEDL, M., ZHANG, W., O'CONNOR, W. & MURPHY, A. J. 2012. IL-22BP is regulated by the inflammasome and modulates tumorigenesis in the intestine. *Nature,* 491**,** 259-263. DOI: 10.1038/nature11535

HUGHES, T., BECKNELL, B., FREUD, A. G., MCCLORY, S., BRIERCHECK, E., YU, J., MAO, C., GIOVENZANA, C., NUOVO, G. & WEI, L. 2010. Interleukin-1β selectively expands and sustains interleukin-22+ immature human natural killer cells in secondary lymphoid tissue. *Immunity,* 32**,** 803-814. DOI: 10.1016/j.immuni.2010.06.007

HUGHES, T., BECKNELL, B., MCCLORY, S., BRIERCHECK, E., FREUD, A. G., ZHANG, X., MAO, H., NUOVO, G., YU, J. & CALIGIURI, M. A. 2009. Stage 3 immature human natural killer cells found in secondary lymphoid tissue constitutively and selectively express the TH17 cytokine interleukin-22. *Blood, The Journal of the American Society of Hematology,* 113**,** 4008-4010. DOI: 10.1182/blood-2008-12-192443

HUNTER, C. A. 2005. New IL-12-family members: IL-23 and IL-27, cytokines with divergent functions. *Nature Reviews Immunology,* 5**,** 521-531. DOI: 10.1038/nri1648

IIMURA, M., GALLO, R. L., HASE, K., MIYAMOTO, Y., ECKMANN, L. & KAGNOFF, M. F. 2005. Cathelicidin mediates innate intestinal defense against colonization with epithelial adherent bacterial pathogens. *The journal of immunology,* 174**,** 4901-4907. DOI: 10.4049/jimmunol.174.8.4901

ISAACS, A. & LINDENMANN, J. 1957. Virus interference. I. The interferon. *Proceedings of the Royal Society of London. Series B-Biological Sciences,* 147**,** 258-267. DOI: 10.1089/jir.1987.7.429

IVANOV, I. I., ATARASHI, K., MANEL, N., BRODIE, E. L., SHIMA, T., KARAOZ, U., WEI, D., GOLDFARB, K. C., SANTEE, C. A. & LYNCH, S. V. 2009. Induction of intestinal Th17 cells by segmented filamentous bacteria. *Cell,* 139**,** 485-498. DOI: 10.1016/j.cell.2009.09.033

IVASHKIV, L. B. & DONLIN, L. T. 2014. Regulation of type I interferon responses. *Nature Reviews Immunology,* 14**,** 36-49. DOI: 10.1038/nri3581

IWASAKI, A. 2012. A virological view of innate immune recognition. *Annual review of microbiology,* 66**,** 177-196. DOI: 10.1146/annurev-micro-092611-150203

JEWELL, N. A., CLINE, T., MERTZ, S. E., SMIRNOV, S. V., FLANO, E., SCHINDLER, C., GRIEVES, J. L., DURBIN, R. K., KOTENKO, S. V. & DURBIN, J. E. 2010. Lambda interferon is the predominant interferon induced by influenza A virus infection in vivo. *Journal of virology,* 84**,** 11515-11522. DOI: 10.1128/JVI.01703-09

JIA, D., RAHBAR, R., CHAN, R. W., LEE, S. M., CHAN, M. C., WANG, B. X., BAKER, D. P., SUN, B., PEIRIS, J. M. & NICHOLLS, J. M. 2010. Influenza virus non-structural protein 1 (NS1) disrupts interferon signaling. *PloS one,* 5**,** e13927. DOI: 10.1371/journal.pone.0013927

JILG, N., LIN, W., HONG, J., SCHAEFER, E. A., WOLSKI, D., MEIXONG, J., GOTO, K., BRISAC, C., CHUSRI, P. & FUSCO, D. N. 2014. Kinetic differences in the induction of interferon stimulated genes by interferon-α and interleukin 28B are altered by infection with hepatitis C virus. *Hepatology,* 59**,** 1250-1261. DOI: 10.1002/hep.26653

JONES, B. C., LOGSDON, N. J. & WALTER, M. R. 2008. Structure of IL-22 bound to its high-affinity IL-22R1 chain. *Structure,* 16**,** 1333-1344. DOI: 10.1016/j.str.2008.06.005

KASTELEIN, R. A., HUNTER, C. A. & CUA, D. J. 2007. Discovery and biology of IL-23 and IL-27: related but functionally distinct regulators of inflammation. *Annu. Rev. Immunol.,* 25**,** 221-242. DOI: 10.1146/annurev.immunol.22.012703.104758

KAU, A. L., AHERN, P. P., GRIFFIN, N. W., GOODMAN, A. L. & GORDON, J. I. 2011. Human nutrition, the gut microbiome and the immune system. *Nature,* 474**,** 327-336. DOI: 10.1038/nature10213

KELLY, D., CAMPBELL, J. I., KING, T. P., GRANT, G., JANSSON, E. A., COUTTS, A. G., PETTERSSON, S. & CONWAY, S. 2004. Commensal anaerobic gut bacteria attenuate inflammation by regulating nuclear-cytoplasmic shuttling of PPAR-γ and RelA. *Nature immunology,* 5**,** 104-112. DOI: 10.1038/ni1018

KIM, C. H., HASHIMOTO-HILL, S. & KIM, M. 2016. Migration and tissue tropism of innate lymphoid cells. *Trends in immunology,* 37**,** 68-79. DOI: 10.1016/j.it.2015.11.003

KISS, E. A., VONARBOURG, C., KOPFMANN, S., HOBEIKA, E., FINKE, D., ESSER, C. & DIEFENBACH, A. 2011. Natural aryl hydrocarbon receptor ligands control organogenesis of intestinal lymphoid follicles. *Science,* 334**,** 1561-1565. DOI: 10.1126/science.1214914

KLOSE, C. S., KISS, E. A., SCHWIERZECK, V., EBERT, K., HOYLER, T., D'HARGUES, Y., GÖPPERT, N., CROXFORD, A. L., WAISMAN, A. & TANRIVER, Y. 2013. A T-bet gradient controls the fate and function of CCR6−RORγt+ innate lymphoid cells. *Nature,* 494**,** 261-265. DOI: 10.1038/nature11813

KONISHI, H., MOTOMURA, T., MATSUMOTO, Y., HARIMOTO, N., IKEGAMI, T., YOSHIZUMI, T., SOEJIMA, Y., SHIRABE, K., FUKUHARA, T. & MAEHARA, Y. 2014. Interferon-lambda4 genetic polymorphism is associated with the therapy response for hepatitis C virus recurrence after a living donor liver transplant. *Journal of viral hepatitis,* 21**,** 397-404. DOI: 10.1111/jvh.12154

KONTSEK, P., KARAYIANNI-VASCONCELOS, G. & KONTSEKOVA, E. 2003. The human interferon system: characterization and classification after discovery of novel members. *Acta virologica,* 47**,** 201-216. URL: http://www.elis.sk/download_file.php?product_id=34&session_id=q76g50gobdeeaqjst0b4hdmap7

KOTENKO, S. V., GALLAGHER, G., BAURIN, V. V., LEWIS-ANTES, A., SHEN, M., SHAH, N. K., LANGER, J. A., SHEIKH, F., DICKENSHEETS, H. & DONNELLY, R. P. 2003. IFN-λs mediate antiviral protection through a distinct class II cytokine receptor complex. *Nature immunology,* 4**,** 69-77. DOI: 10.1038/ni875

KULESHOV, M. V., JONES, M. R., ROUILLARD, A. D., FERNANDEZ, N. F., DUAN, Q., WANG, Z., KOPLEV, S., JENKINS, S. L., JAGODNIK, K. M. & LACHMANN, A. 2016. Enrichr: a comprehensive gene set enrichment analysis web server 2016 update. *Nucleic acids research,* 44**,** W90-W97. DOI: 10.1093/nar/gkw377

LEONEL, A. J. & ALVAREZ-LEITE, J. I. 2012. Butyrate: implications for intestinal function. *Current Opinion in Clinical Nutrition & Metabolic Care,* 15**,** 474-479. DOI: 10.1097/MCO.0b013e32835665fa

LEUNG, S., QURESHI, S. A., KERR, I. M., DARNELL JR, J. E. & STARK, G. R. 1995. Role of STAT2 in the alpha interferon signaling pathway. *Molecular and cellular biology,*

15**,** 1312-1317. DOI: 10.1128/MCB.15.3.1312

LIANG, S. C., TAN, X.-Y., LUXENBERG, D. P., KARIM, R., DUNUSSI-JOANNOPOULOS, K., COLLINS, M. & FOUSER, L. A. 2006. Interleukin (IL)-22 and IL-17 are coexpressed by Th17 cells and cooperatively enhance expression of antimicrobial peptides. *The Journal of experimental medicine,* 203**,** 2271-2279. DOI: 10.1084/jem.20061308

LIAO, Y., SMYTH, G. K. & SHI, W. 2014. featureCounts: an efficient general purpose program for assigning sequence reads to genomic features. *Bioinformatics,* 30**,** 923-930. DOI: 10.1093/bioinformatics/btt656

LIAO, Y., SMYTH, G. K. & SHI, W. 2019. The R package Rsubread is easier, faster, cheaper and better for alignment and quantification of RNA sequencing reads. *Nucleic acids research,* 47**,** e47-e47. DOI: 10.1093/nar/gkz114

LIN, J.-D., FENG, N., SEN, A., BALAN, M., TSENG, H.-C., MCELRATH, C., SMIRNOV, S. V., PENG, J., YASUKAWA, L. L. & DURBIN, R. K. 2016. Distinct roles of type I and type III interferons in intestinal immunity to homologous and heterologous rotavirus infections. *PLoS pathogens,* 12**,** e1005600. DOI: 10.1371/journal.ppat.1005600

LINDEMANS, C. A., CALAFIORE, M., MERTELSMANN, A. M., O'CONNOR, M. H., DUDAKOV, J. A., JENQ, R. R., VELARDI, E., YOUNG, L. F., SMITH, O. M. & LAWRENCE, G. 2015. Interleukin-22 promotes intestinal-stem-cell-mediated epithelial regeneration. *Nature,* 528**,** 560-564. DOI: 10.1038/nature16460

LIU, S., YAN, R., CHEN, B., PAN, Q., CHEN, Y., HONG, J., ZHANG, L., LIU, W., WANG, S. & CHEN, J.-L. 2019. Influenza virus-induced robust expression of SOCS3 contributes to excessive production of IL-6. *Frontiers in immunology***,** 1843. DOI: 10.3389/fimmu.2019.01843

LOWES, M. A., BOWCOCK, A. M. & KRUEGER, J. G. 2007. Pathogenesis and therapy of psoriasis. *Nature,* 445**,** 866-873. DOI: 10.1038/nature05663

LUCI, C., REYNDERS, A., IVANOV, I. I., COGNET, C., CHICHE, L., CHASSON, L., HARDWIGSEN, J., ANGUIANO, E., BANCHEREAU, J. & CHAUSSABEL, D. 2009. Influence of the transcription factor RORγt on the development of NKp46+ cell populations in gut and skin. *Nature immunology,* 10**,** 75-82. DOI: 10.1038/ni.1681

MABBOTT, N. A., DONALDSON, D. S., OHNO, H., WILLIAMS, I. R. & MAHAJAN, A. 2013. Microfold (M) cells: important immunosurveillance posts in the intestinal epithelium. *Mucosal immunology,* 6**,** 666-677. DOI: 10.1038/mi.2013.30

MACMICKING, J. D. 2012. Interferon-inducible effector mechanisms in cell-autonomous immunity. *Nature Reviews Immunology,* 12**,** 367-382. DOI: 10.1038/nri3210

MAHLAKOIV, T., RITZ, D., MORDSTEIN, M., DEDIEGO, M. L., ENJUANES, L., MÜLLER, M. A., DROSTEN, C. & STAEHELI, P. 2012. Combined action of type I and type III interferon restricts initial replication of severe acute respiratory syndrome coronavirus in the lung but fails to inhibit systemic virus spread. *Journal of General Virology,* 93**,** 2601-2605. DOI: 10.1099/vir.0.046284-0

MAILLARD, I., FANG, T. & PEAR, W. S. 2005. Regulation of lymphoid development, differentiation, and function by the Notch pathway. *Annu. Rev. Immunol.,* 23**,** 945-

974. DOI: 10.1146/annurev.immunol.23.021704.115747

MAKOWSKA, Z., DUONG, F. H., TRINCUCCI, G., TOUGH, D. F. & HEIM, M. H. 2011. Interferon-β and interferon-λ signaling is not affected by interferon-induced refractoriness to interferon-α in vivo. *Hepatology,* 53**,** 1171-1180. DOI: 10.1002/hep.24189

MALAKHOVA, O. A., KIM, K., LUO, J. K., ZOU, W., KUMAR, K. S., FUCHS, S. Y., SHUAI, K. & ZHANG, D. E. 2006. UBP43 is a novel regulator of interferon signaling independent of its ISG15 isopeptidase activity. *The EMBO journal,* 25**,** 2358-2367. DOI: 10.1038/sj.emboj.7601149

MANGAN, P. R., HARRINGTON, L. E., O'QUINN, D. B., HELMS, W. S., BULLARD, D. C., ELSON, C. O., HATTON, R. D., WAHL, S. M., SCHOEB, T. R. & WEAVER, C. T. 2006. Transforming growth factor-β induces development of the TH17 lineage. *Nature,* 441**,** 231-234. DOI: 10.1038/nature04754

MANRY, J., LAVAL, G., PATIN, E., FORNARINO, S., ITAN, Y., FUMAGALLI, M., SIRONI, M., TICHIT, M., BOUCHIER, C. & CASANOVA, J.-L. 2011. Evolutionary genetic dissection of human interferons. *Journal of Experimental Medicine,* 208**,** 2747-2759. DOI: 10.1084/jem.20111680

MARCELLO, T., GRAKOUI, A., BARBA–SPAETH, G., MACHLIN, E. S., KOTENKO, S. V., MACDONALD, M. R. & RICE, C. M. 2006. Interferons α and λ inhibit hepatitis C virus replication with distinct signal transduction and gene regulation kinetics. *Gastroenterology,* 131**,** 1887-1898. DOI: 10.1053/j.gastro.2006.09.052

MARIÉ, I., DURBIN, J. E. & LEVY, D. E. 1998. Differential viral induction of distinct interferon-α genes by positive feedback through interferon regulatory factor-7. *The EMBO journal,* 17**,** 6660-6669. DOI: 10.1093/emboj/17.22.6660

MARTIN, J. C., BÉRIOU, G., HESLAN, M., CHAUVIN, C., UTRIAINEN, L., AUMEUNIER, A., SCOTT, C., MOWAT, A., CEROVIC, V. & HOUSTON, S. 2014. Interleukin-22 binding protein (IL-22BP) is constitutively expressed by a subset of conventional dendritic cells and is strongly induced by retinoic acid. *Mucosal immunology,* 7**,** 101-113. DOI: 10.1038/mi.2013.28

MCDERMOTT, A. J. & HUFFNAGLE, G. B. 2014. The microbiome and regulation of mucosal immunity. *Immunology,* 142**,** 24-31. DOI: 10.1111/imm.12231

MORDSTEIN, M., NEUGEBAUER, E., DITT, V., JESSEN, B., RIEGER, T., FALCONE, V., SORGELOOS, F., EHL, S., MAYER, D. & KOCHS, G. 2010. Lambda interferon renders epithelial cells of the respiratory and gastrointestinal tracts resistant to viral infections. *Journal of virology,* 84**,** 5670-5677. DOI: 10.1128/JVI.00272-10

MORRIS, R., KERSHAW, N. J. & BABON, J. J. 2018. The molecular details of cytokine signaling via the JAK/STAT pathway. *Protein Science,* 27**,** 1984-2009. DOI: 10.1002/pro.3519

MUENCHAU, S., DEUTSCH, R., DE CASTRO, I. J., HIELSCHER, T., HEBER, N., NIESLER, B., LUSIC, M., STANIFER, M. L. & BOULANT, S. 2019. Hypoxic environment promotes barrier formation in human intestinal epithelial cells through regulation of microRNA 320a expression. *Molecular and cellular biology,* 39**,** e00553-18. DOI: 10.1128/MCB.00553-18

MUÑOZ, M., HEIMESAAT, M. M., DANKER, K., STRUCK, D., LOHMANN, U., PLICKERT, R., BERESWILL, S., FISCHER, A., DUNAY, I. R. & WOLK, K. 2009. Interleukin (IL)-23 mediates Toxoplasma gondii–induced immunopathology in the gut via matrixmetalloproteinase-2 and IL-22 but independent of IL-17. *Journal of Experimental Medicine,* 206**,** 3047-3059. DOI: 10.1084/jem.20090900

MURANO, T., OKAMOTO, R., ITO, G., NAKATA, T., HIBIYA, S., SHIMIZU, H., FUJII, S., KANO, Y., MIZUTANI, T. & YUI, S. 2014. Hes1 promotes the IL-22-mediated antimicrobial response by enhancing STAT3-dependent transcription in human intestinal epithelial cells. *Biochemical and biophysical research communications,* 443**,** 840-846. DOI: 10.1016/j.bbrc.2013.12.061

NAGAO-KITAMOTO, H., LESLIE, J. L., KITAMOTO, S., JIN, C., THOMSSON, K. A., GILLILLAND, M. G., KUFFA, P., GOTO, Y., JENQ, R. R. & ISHII, C. 2020. Interleukin-22-mediated host glycosylation prevents Clostridioides difficile infection by modulating the metabolic activity of the gut microbiota. *Nature medicine,* 26**,** 608-617. DOI: 10.1038/s41591-020-0764-0

NICHOLSON, J. K., HOLMES, E., KINROSS, J., BURCELIN, R., GIBSON, G., JIA, W. & PETTERSSON, S. 2012. Host-gut microbiota metabolic interactions. *Science,* 336**,** 1262-1267. DOI: 10.1126/science.1223813

NIWA, M., FUJISAWA, T., MORI, K., YAMANAKA, K., YASUI, H., SUZUKI, Y., KARAYAMA, M., HOZUMI, H., FURUHASHI, K. & ENOMOTO, N. 2018. IL-17A attenuates IFN-λ expression by inducing suppressor of cytokine signaling expression in airway epithelium. *The Journal of Immunology,* 201**,** 2392-2402. DOI: 10.4049/jimmunol.1800147

O'BRIEN, T. R., THOMAS, D. L., JACKSON, S. S., PROKUNINA-OLSSON, L., DONNELLY, R. P. & HARTMANN, R. 2020. Weak induction of interferon expression by SARS-CoV-2 supports clinical trials of interferon lambda to treat early COVID-19. *Clin Infect Dis,* 71**,** 1410-1412. DOI: 10.1093/cid/ciaa453

OBAJEMU, A. A., RAO, N., DILLEY, K. A., VARGAS, J. M., SHEIKH, F., DONNELLY, R. P., SHABMAN, R. S., MEISSNER, E. G., PROKUNINA-OLSSON, L. & ONABAJO, O. O. 2017. IFN-λ4 attenuates antiviral responses by enhancing negative regulation of IFN signaling. *The Journal of Immunology,* 199**,** 3808-3820. DOI: 10.4049/jimmunol.1700807

O'HARA, A. M. & SHANAHAN, F. 2006. The gut flora as a forgotten organ. *EMBO reports,* 7**,** 688-693. DOI: 10.1038/sj.embor.7400731

O'NEILL, L. A., GOLENBOCK, D. & BOWIE, A. G. 2013. The history of Toll-like receptors—redefining innate immunity. *Nature Reviews Immunology,* 13**,** 453-460. DOI: 10.1038/nri3446

OTKJAER, K., KRAGBALLE, K., FUNDING, A., CLAUSEN, J., NOERBY, P., STEINICHE, T. & IVERSEN, L. 2005. The dynamics of gene expression of interleukin-19 and interleukin-20 and their receptors in psoriasis. *British Journal of Dermatology,* 153**,** 911-918. DOI: 10.1111/j.1365-2133.2005.06800.x

OUELLETTE, A. J. 2010. Paneth cells and innate mucosal immunity. *Current opinion in gastroenterology,* 26**,** 547-553. DOI: 10.1097/MOG.0b013e32833dccde

OUYANG, W., KOLLS, J. K. & ZHENG, Y. 2008. The biological functions of T helper 17 cell effector cytokines in inflammation. *Immunity,* 28**,** 454-467. DOI: 10.1016/j.immuni.2008.03.004

PAULI, E.-K., SCHMOLKE, M., WOLFF, T., VIEMANN, D., ROTH, J., BODE, J. G. & LUDWIG, S. 2008. Influenza A virus inhibits type I IFN signaling via NF-κB-dependent induction of SOCS-3 expression. *PLoS pathogens,* 4**,** e1000196. DOI: 10.1371/journal.ppat.1000196

PÈNE, J., CHEVALIER, S., PREISSER, L., VÉNÉREAU, E., GUILLEUX, M.-H., GHANNAM, S., MOLÈS, J.-P., DANGER, Y., RAVON, E. & LESAUX, S. 2008. Chronically inflamed human tissues are infiltrated by highly differentiated Th17 lymphocytes. *The Journal of Immunology,* 180**,** 7423-7430. DOI: 10.1371/journal.ppat.1000196

PEREZ, L. G., KEMPSKI, J., MCGEE, H. M., PELZCAR, P., AGALIOTI, T., GIANNOU, A., KONCZALLA, L., BROCKMANN, L., WAHIB, R. & XU, H. 2020. TGF-β signaling in Th17 cells promotes IL-22 production and colitis-associated colon cancer. *Nature communications,* 11**,** 1-14. DOI: 10.1038/s41467-020-16363-w

PERUSINA LANFRANCA, M., LIN, Y., FANG, J., ZOU, W. & FRANKEL, T. 2016. Biological and pathological activities of interleukin-22. *J Mol Med (Berl),* 94**,** 523-34. DOI: 10.1007/s00109-016-1391-6

PERVOLARAKI, K., GUO, C., ALBRECHT, D., BOULANT, S. & STANIFER, M. L. 2019. Type-specific crosstalk modulates interferon signaling in intestinal epithelial cells. *Journal of Interferon & Cytokine Research,* 39**,** 650-660. DOI: 10.1089/jir.2019.0040

PERVOLARAKI, K., RASTGOU TALEMI, S., ALBRECHT, D., BORMANN, F., BAMFORD, C., MENDOZA, J. L., GARCIA, K. C., MCLAUCHLAN, J., HÖFER, T. & STANIFER, M. L. 2018. Differential induction of interferon stimulated genes between type I and type III interferons is independent of interferon receptor abundance. *PLoS pathogens,* 14**,** e1007420. DOI: 10.1371/journal.ppat.1007420

PERVOLARAKI, K., STANIFER, M. L., MÜNCHAU, S., RENN, L. A., ALBRECHT, D., KURZHALS, S., SENÍS, E., GRIMM, D., SCHRÖDER-BRAUNSTEIN, J. & RABIN, R. L. 2017. Type I and type III interferons display different dependency on mitogen-activated protein kinases to mount an antiviral state in the human gut. *Frontiers in immunology,* 8**,** 459. DOI: 10.3389/fimmu.2017.00459

PESTKA, S., KRAUSE, C. D. & WALTER, M. R. 2004. Interferons, interferon-like cytokines, and their receptors. *Immunological reviews,* 202**,** 8-32. DOI: 10.1111/j.0105-2896.2004.00204.x

PICKERT, G., NEUFERT, C., LEPPKES, M., ZHENG, Y., WITTKOPF, N., WARNTJEN, M., LEHR, H.-A., HIRTH, S., WEIGMANN, B. & WIRTZ, S. 2009. STAT3 links IL-22 signaling in intestinal epithelial cells to mucosal wound healing. *Journal of Experimental Medicine,* 206**,** 1465-1472. DOI: 10.1084/jem.20082683

PLANET, P. J., PARKER, D., COHEN, T. S., SMITH, H., LEON, J. D., RYAN, C., HAMMER, T. J., FIERER, N., CHEN, E. I. & PRINCE, A. S. 2016. Lambda interferon restructures the nasal microbiome and increases susceptibility to Staphylococcus aureus superinfection. *MBio,* 7**,** e01939-15. DOI: 10.1128/mBio.01939-15

PODGORNY, O. V. & LAZAREV, V. N. 2017. Laser microdissection: A promising tool for exploring microorganisms and their interactions with hosts. *Journal of microbiological methods,* 138**,** 82-92. DOI: 10.1016/j.mimet.2016.01.001

PODOLSKY, D. K. 2002. The current future understanding of inflammatory bowel disease. *Best practice & research Clinical gastroenterology,* 16**,** 933-943. DOI: 10.1053/bega.2002.0354

PODOLSKY, D. K. 2002. Inflammatory bowel disease - Reply. *New England Journal of Medicine,* 347**,** 1983-1984. DOI: 10.1056/NEJM200212123472418

PORTER, E., BEVINS, C. L., GHOSH, D. & GANZ, T. 2002. The multifaceted Paneth cell. *Cellular and molecular life sciences CMLS,* 59**,** 156-170. DOI: 10.1007/s00018-002-8412-z

POTHLICHET, J., CHIGNARD, M. & SI-TAHAR, M. 2008. Cutting edge: innate immune response triggered by influenza A virus is negatively regulated by SOCS1 and SOCS3 through a RIG-I/IFNAR1-dependent pathway. *The Journal of Immunology,* 180**,** 2034-2038. DOI: 10.4049/jimmunol.180.4.2034

POTT, J., MAHLAKÕIV, T., MORDSTEIN, M., DUERR, C. U., MICHIELS, T., STOCKINGER, S., STAEHELI, P. & HORNEF, M. W. 2011. IFN-λ determines the intestinal epithelial antiviral host defense. *Proceedings of the national academy of sciences,* 108**,** 7944-7949. DOI: 10.1073/pnas.1100552108

PROKUNINA-OLSSON, L., MUCHMORE, B., TANG, W., PFEIFFER, R. M., PARK, H., DICKENSHEETS, H., HERGOTT, D., PORTER-GILL, P., MUMY, A. & KOHAAR, I. 2013. A variant upstream of IFNL3 (IL28B) creating a new interferon gene IFNL4 is associated with impaired clearance of hepatitis C virus. *Nature genetics,* 45**,** 164-171. DOI: 10.1038/ng.2521

QIU, J., HELLER, J. J., GUO, X., ZONG-MING, E. C., FISH, K., FU, Y.-X. & ZHOU, L. 2012. The aryl hydrocarbon receptor regulates gut immunity through modulation of innate lymphoid cells. *Immunity,* 36**,** 92-104. DOI: 10.1016/j.immuni.2011.11.011

RACHITSKAYA, A. V., HANSEN, A. M., HORAI, R., LI, Z., VILLASMIL, R., LUGER, D., NUSSENBLATT, R. B. & CASPI, R. R. 2008. Cutting edge: NKT cells constitutively express IL-23 receptor and RORγt and rapidly produce IL-17 upon receptor ligation in an IL-6-independent fashion. *The Journal of Immunology,* 180**,** 5167-5171. DOI: 10.4049/jimmunol.180.8.5167

RAJ, A., VAN DEN BOGAARD, P., RIFKIN, S. A., VAN OUDENAARDEN, A. & TYAGI, S. 2008. Imaging individual mRNA molecules using multiple singly labeled probes. *Nature methods,* 5**,** 877-879. DOI: 10.1038/nmeth.1253

RAUCH, A., KUTALIK, Z., DESCOMBES, P., CAI, T., DI IULIO, J., MUELLER, T., BOCHUD, M., BATTEGAY, M., BERNASCONI, E. & BOROVICKA, J. 2010. Genetic variation in IL28B is associated with chronic hepatitis C and treatment failure: a genome-wide association study. *Gastroenterology,* 138**,** 1338-1345. e7. DOI: 10.1053/j.gastro.2009.12.056

REINEKE, U., SCHNEIDER-MERGENER, J., GLASER, R. W., STIGLER, R. D., SEIFERT, M., VOLK, H. D. & SABAT, R. 1999. Evidence for conformationally different states of interleukin-10: binding of a neutralizing antibody enhances accessibility of a hidden

epitope. *Journal of Molecular Recognition,* 12**,** 242-248. DOI: 10.1002/(SICI)1099-1352(199907/08)12:4<242:AID-JMR461>3.0.CO;2-1

ROGLER, G. & ROSANO, G. 2014. The heart and the gut. *European heart journal,* 35**,** 426-430. DOI: 10.1093/eurheartj/eht271

ROUND, J. L. & MAZMANIAN, S. K. 2010. Inducible Foxp3+ regulatory T-cell development by a commensal bacterium of the intestinal microbiota. *Proceedings of the National Academy of Sciences,* 107**,** 12204-12209. DOI: 10.1073/pnas.0909122107

RUTZ, S., NOUBADE, R., EIDENSCHENK, C., OTA, N., ZENG, W., ZHENG, Y., HACKNEY, J., DING, J., SINGH, H. & OUYANG, W. 2011. Transcription factor c-Maf mediates the TGF-β-dependent suppression of IL-22 production in TH17 cells. *Nature immunology,* 12**,** 1238-1245. DOI: 10.1038/ni.2134

RUTZ, S., WANG, X. & OUYANG, W. 2014. The IL-20 subfamily of cytokines—from host defence to tissue homeostasis. *Nature reviews Immunology,* 14**,** 783-795. DOI: 10.1038/nri3766

SA, S. M., VALDEZ, P. A., WU, J., JUNG, K., ZHONG, F., HALL, L., KASMAN, I., WINER, J., MODRUSAN, Z. & DANILENKO, D. M. 2007. The effects of IL-20 subfamily cytokines on reconstituted human epidermis suggest potential roles in cutaneous innate defense and pathogenic adaptive immunity in psoriasis. *The Journal of Immunology,* 178**,** 2229-2240. DOI: 10.4049/jimmunol.178.4.2229

SABAT, R., OUYANG, W. & WOLK, K. 2014. Therapeutic opportunities of the IL-22–IL-22R1 system. *Nature reviews Drug discovery,* 13**,** 21-38. DOI: 10.1038/nrd4176

SALZMAN, N. H., HUNG, K., HARIBHAI, D., CHU, H., KARLSSON-SJÖBERG, J., AMIR, E., TEGGATZ, P., BARMAN, M., HAYWARD, M. & EASTWOOD, D. 2010. Enteric defensins are essential regulators of intestinal microbial ecology. *Nature immunology,* 11**,** 76-82. DOI: 10.1038/ni.1825

SATO, T., STANGE, D. E., FERRANTE, M., VRIES, R. G., VAN ES, J. H., VAN DEN BRINK, S., VAN HOUDT, W. J., PRONK, A., VAN GORP, J. & SIERSEMA, P. D. 2011. Long-term expansion of epithelial organoids from human colon, adenoma, adenocarcinoma, and Barrett's epithelium. *Gastroenterology,* 141**,** 1762-1772. DOI: 10.1053/j.gastro.2011.07.050

SATO, T., VRIES, R. G., SNIPPERT, H. J., VAN DE WETERING, M., BARKER, N., STANGE, D. E., VAN ES, J. H., ABO, A., KUJALA, P. & PETERS, P. J. 2009. Single Lgr5 stem cells build crypt-villus structures in vitro without a mesenchymal niche. *Nature,* 459**,** 262-265. DOI: 10.1038/nature07935

SAXENA, K., SIMON, L. M., ZENG, X.-L., BLUTT, S. E., CRAWFORD, S. E., SASTRI, N. P., KARANDIKAR, U. C., AJAMI, N. J., ZACHOS, N. C. & KOVBASNJUK, O. 2017. A paradox of transcriptional and functional innate interferon responses of human intestinal enteroids to enteric virus infection. *Proceedings of the National Academy of Sciences,* 114**,** E570-E579. DOI: 10.1073/pnas.1615422114

SCHAIBLE, B., SCHAFFER, K. & TAYLOR, C. T. 2010. Hypoxia, innate immunity and infection in the lung. *Respiratory physiology & neurobiology,* 174**,** 235-243. DOI: 10.1016/j.resp.2010.08.006

SCHRODER, K., HERTZOG, P. J., RAVASI, T. & HUME, D. A. 2004. Interferon-γ: an overview of signals, mechanisms and functions. *Journal of leukocyte biology,* 75**,** 163-189. DOI: 10.1189/jlb.0603252

SCHUBERT, M., KLINGER, B., KLÜNEMANN, M., SIEBER, A., UHLITZ, F., SAUER, S., GARNETT, M. J., BLÜTHGEN, N. & SAEZ-RODRIGUEZ, J. 2018. Perturbation-response genes reveal signaling footprints in cancer gene expression. *Nature communications,* 9**,** 1-11. DOI: 10.1038/s41467-017-02391-6

SCHULZ, S. M., KÖHLER, G., SCHÜTZE, N., KNAUER, J., STRAUBINGER, R. K., CHACKERIAN, A. A., WITTE, E., WOLK, K., SABAT, R. & IWAKURA, Y. 2008. Protective immunity to systemic infection with attenuated Salmonella enterica serovar enteritidis in the absence of IL-12 is associated with IL-23-dependent IL-22, but not IL-17. *The Journal of Immunology,* 181**,** 7891-7901. DOI: 10.4049/jimmunol.181.11.7891

SCHWERK, J., KÖSTER, M., HAUSER, H., ROHDE, M., FULDE, M., HORNEF, M. W. & MAY, T. 2013. Generation of mouse small intestinal epithelial cell lines that allow the analysis of specific innate immune functions. *PloS one,* 8**,** e72700. DOI: 10.1371/journal.pone.0072700

SELVAKUMAR, T. A., BHUSHAL, S., KALINKE, U., WIRTH, D., HAUSER, H., KÖSTER, M. & HORNEF, M. W. 2017. Identification of a predominantly interferon-λ-induced transcriptional profile in murine intestinal epithelial cells. *Frontiers in Immunology,* 8**,** 1302. DOI: 10.3389/fimmu.2017.01302

SEMENZA, G. L. 2012. Hypoxia-inducible factors in physiology and medicine. *Cell,* 148**,** 399-408. DOI: 10.1016/j.cell.2012.01.021

SEN, A., SHARMA, A. & GREENBERG, H. B. 2017. Rotavirus degrades multiple interferon (IFN) type receptors to inhibit IFN signaling and protects against mortality from endotoxin in suckling mice. *Journal of virology,* 92**,** e01394-17. DOI: 10.1128/JVI.01394-17

SEO, G.-Y., GILES, D. A. & KRONENBERG, M. 2020. The role of innate lymphoid cells in response to microbes at mucosal surfaces. *Mucosal immunology,* 13**,** 399-412. DOI: 10.1038/s41385-020-0265-y

SHAW, M. H., KAMADA, N., KIM, Y.-G. & NÚÑEZ, G. 2012. Microbiota-induced IL-1β, but not IL-6, is critical for the development of steady-state TH17 cells in the intestine. *Journal of Experimental Medicine,* 209**,** 251-258. DOI: 10.1084/jem.20111703

SHEAHAN, T., IMANAKA, N., MARUKIAN, S., DORNER, M., LIU, P., PLOSS, A. & RICE, C. M. 2014. Interferon lambda alleles predict innate antiviral immune responses and hepatitis C virus permissiveness. *Cell host & microbe,* 15**,** 190-202. DOI: 10.1016/j.chom.2014.01.007

SHEPPARD, P., KINDSVOGEL, W., XU, W., HENDERSON, K., SCHLUTSMEYER, S., WHITMORE, T. E., KUESTNER, R., GARRIGUES, U., BIRKS, C. & RORABACK, J. 2003. IL-28, IL-29 and their class II cytokine receptor IL-28R. *Nature immunology,* 4**,** 63-68. DOI: 10.1038/ni873

SIMPSON, S. J., HOLLÄNDER, G. A., MIZOGUCHI, E., ALLEN, D., BHAN, A. K., WANG, B. & TERHORST, C. 1997. Expression of pro-inflammatory cytokines by TCRαβ+ T

and TCRγδ+ T cells in an experimental model of colitis. *European journal of immunology,* 27**,** 17-25. URL: https://doi.org/10.1002/eji.1830270104

SINGHAL, R. & SHAH, Y. M. 2020. Oxygen battle in the gut: Hypoxia and hypoxia-inducible factors in metabolic and inflammatory responses in the intestine. *Journal of Biological Chemistry,* 295**,** 10493-10505. DOI: 10.1074/jbc.REV120.011188

SNOECK, V., GODDEERIS, B. & COX, E. 2005. The role of enterocytes in the intestinal barrier function and antigen uptake. *Microbes and infection,* 7**,** 997-1004. DOI: 10.1016/j.micinf.2005.04.003

SOMMEREYNS, C., PAUL, S., STAEHELI, P. & MICHIELS, T. 2008. IFN-lambda (IFN-λ) is expressed in a tissue-dependent fashion and primarily acts on epithelial cells in vivo. *PLoS pathogens,* 4**,** e1000017. DOI: 10.1371/journal.ppat.1000017

SONG, Q., WANG, X., WU, X., KANG, T. H., QIN, H., ZHAO, D., JENQ, R. R., VAN DEN BRINK, M. R., RIGGS, A. D. & MARTIN, P. J. 2021. IL-22-dependent dysbiosis and mononuclear phagocyte depletion contribute to steroid-resistant gut graft-versus-host disease in mice. *Nature communications,* 12**,** 1-19. DOI: 10.1038/s41467-021-21133-3

SONNENBERG, G. F., FOUSER, L. A. & ARTIS, D. 2011. Border patrol: regulation of immunity, inflammation and tissue homeostasis at barrier surfaces by IL-22. *Nature immunology,* 12**,** 383-390. DOI: 10.1038/ni.2025

SONNENBERG, G. F., MONTICELLI, L. A., ALENGHAT, T., FUNG, T. C., HUTNICK, N. A., KUNISAWA, J., SHIBATA, N., GRUNBERG, S., SINHA, R. & ZAHM, A. M. 2012. Innate lymphoid cells promote anatomical containment of lymphoid-resident commensal bacteria. *Science,* 336**,** 1321-1325. DOI: 10.1126/science.1222551

SPITS, H., ARTIS, D., COLONNA, M., DIEFENBACH, A., DI SANTO, J. P., EBERL, G., KOYASU, S., LOCKSLEY, R. M., MCKENZIE, A. N. & MEBIUS, R. E. 2013. Innate lymphoid cells—a proposal for uniform nomenclature. *Nature reviews immunology,* 13**,** 145-149. DOI: 10.1038/nri3365

STANIFER, M. L., CURETON, D. K. & WHELAN, S. P. 2011. A recombinant vesicular stomatitis virus bearing a lethal mutation in the glycoprotein gene uncovers a second site suppressor that restores fusion. *Journal of virology,* 85**,** 8105-8115. DOI: 10.1128/JVI.00735-11

STANIFER, M. L., PERVOLARAKI, K. & BOULANT, S. 2019. Differential regulation of type I and type III interferon signaling. *International journal of molecular sciences,* 20**,** 1445. DOI: 10.3390/ijms20061445

STARK, G. R. & DARNELL JR, J. E. 2012. The JAK-STAT pathway at twenty. *Immunity,* 36**,** 503-514. DOI: 10.1016/j.immuni.2012.03.013

STOJANOVIĆ, I., SAKSIDA, T., MILJKOVIĆ, Đ. & PEJNOVIĆ, N. 2021. Modulation of Intestinal ILC3 for the Treatment of Type 1 Diabetes. *Frontiers in Immunology,* 12**,** 2119. DOI: 10.3389/fimmu.2021.653560

SUTTON, C. E., LALOR, S. J., SWEENEY, C. M., BRERETON, C. F., LAVELLE, E. C. & MILLS, K. H. 2009. Interleukin-1 and IL-23 induce innate IL-17 production from γδ T cells, amplifying Th17 responses and autoimmunity. *Immunity,* 31**,** 331-341. DOI:

10.1016/j.immuni.2009.08.001

TAKAYANAGI, H., KIM, S. & TANIGUCHI, T. 2002. Signaling crosstalk between RANKL and interferons in osteoclast differentiation. *Arthritis Research & Therapy,* 4**,** 1-6. DOI: 10.1186/ar581

TERCZYŃSKA-DYLA, E., BIBERT, S., DUONG, F. H., KROL, I., JØRGENSEN, S., COLLINET, E., KUTALIK, Z., AUBERT, V., CERNY, A. & KAISER, L. 2014. Reduced IFNλ4 activity is associated with improved HCV clearance and reduced expression of interferon-stimulated genes. *Nature communications,* 5**,** 1-9. DOI: 10.1038/ncomms6699

TESCH, G. H., LAN, H. Y. & NIKOLIC-PATERSON, D. J. 2006. Treatment of tissue sections for in situ hybridization. *In situ hybridization protocols***,** 1-7. DOI: 10.1385/1-59745-007-3:1

THOMAS, D. L., THIO, C. L., MARTIN, M. P., QI, Y., GE, D., O'HUIGIN, C., KIDD, J., KIDD, K., KHAKOO, S. I. & ALEXANDER, G. 2009. Genetic variation in IL28B and spontaneous clearance of hepatitis C virus. *Nature,* 461**,** 798-801. DOI: 10.1038/nature08463

THOMPSON, A. J., MUIR, A. J., SULKOWSKI, M. S., GE, D., FELLAY, J., SHIANNA, K. V., URBAN, T., AFDHAL, N. H., JACOBSON, I. M. & ESTEBAN, R. 2010. Interleukin-28B polymorphism improves viral kinetics and is the strongest pretreatment predictor of sustained virologic response in genotype 1 hepatitis C virus. *Gastroenterology,* 139**,** 120-129. e18. DOI: 10.1053/j.gastro.2010.04.013

TREUTING, P. & DINTZIS, S. 2012. Lower gastrointestinal tract, in comparative anatomy and histology–a mouse and human atlas. In: Comparative anatomy and histology: a mouse and human atlas, *Elsevier, Amsterdam*, pg. 177-192. ISBN 978-0-12-381361-9

TRIVELLA, D. B. B., FERREIRA-JÚNIOR, J. R., DUMOUTIER, L., RENAULD, J.-C. & POLIKARPOV, I. 2010. Structure and function of interleukin-22 and other members of the interleukin-10 family. *Cellular and molecular life sciences,* 67**,** 2909-2935. DOI: 10.1007/s00018-010-0380-0

TURICCKI, J. 2021. Histology and Cellular Function of the Small Intestine. 01/27/2021 ed. TeachMePhysiology. URL: https://teachmephysiology.com/gastrointestinal-system/small-intestine/histology-and-cellular-function/

UETANI, K., HIROI, M., MEGURO, T., OGAWA, H., KAMISAKO, T., OHMORI, Y. & ERZURUM, S. C. 2008. Influenza A virus abrogates IFN-γ response in respiratory epithelial cells by disruption of the Jak/Stat pathway. *European journal of immunology,* 38**,** 1559-1573. DOI: 10.1002/eji.200737045

VAHEDI, G., TAKAHASHI, H., NAKAYAMADA, S., SUN, H.-W., SARTORELLI, V., KANNO, Y. & O'SHEA, J. J. 2012. STATs shape the active enhancer landscape of T cell populations. *Cell,* 151**,** 981-993. DOI: 10.1016/j.cell.2012.09.044

VAISHNAVA, S., BEHRENDT, C. L., ISMAIL, A. S., ECKMANN, L. & HOOPER, L. V. 2008. Paneth cells directly sense gut commensals and maintain homeostasis at the intestinal host-microbial interface. *Proceedings of the National Academy of Sciences,* 105**,** 20858-20863. DOI: 10.1073/pnas.0808723105

VELDHOEN, M., HIROTA, K., WESTENDORF, A. M., BUER, J., DUMOUTIER, L., RENAULD, J.-C. & STOCKINGER, B. 2008. The aryl hydrocarbon receptor links TH17-cell-mediated autoimmunity to environmental toxins. *Nature,* 453**,** 106-109. DOI: 10.1038/nature06881

VEREECKE, L., BEYAERT, R. & VAN LOO, G. 2011. Enterocyte death and intestinal barrier maintenance in homeostasis and disease. *Trends in molecular medicine,* 17**,** 584-593. DOI: 10.1016/j.molmed.2011.05.011

VICTOR, A. R., NALIN, A. P., DONG, W., MCCLORY, S., WEI, M., MAO, C., KLADNEY, R. D., YOUSSEF, Y., CHAN, W. K. & BRIERCHECK, E. L. 2017. IL-18 drives ILC3 proliferation and promotes IL-22 production via NF-κB. *The Journal of Immunology,* 199**,** 2333-2342. DOI: 10.4049/jimmunol.1601554

VON MOLTKE, J., JI, M., LIANG, H.-E. & LOCKSLEY, R. M. 2016. Tuft-cell-derived IL-25 regulates an intestinal ILC2–epithelial response circuit. *Nature,* 529**,** 221-225. DOI: 10.1038/nature16161

VONARBOURG, C. & DIEFENBACH, A. Multifaceted roles of interleukin-7 signaling for the development and function of innate lymphoid cells. Seminars in immunology, 2012. Elsevier, 165-174. DOI: 10.1016/j.smim.2012.03.002

VONARBOURG, C., MORTHA, A., BUI, V. L., HERNANDEZ, P. P., KISS, E. A., HOYLER, T., FLACH, M., BENGSCH, B., THIMME, R. & HÖLSCHER, C. 2010. Regulated expression of nuclear receptor RORγt confers distinct functional fates to NK cell receptor-expressing RORγt+ innate lymphocytes. *Immunity,* 33**,** 736-751. DOI: 10.1016/j.immuni.2010.10.017

WANG, H., BROWN, J., GARCIA, C. A., TANG, Y., BENAKANAKERE, M. R., GREENWAY, T., ALARD, P., KINANE, D. F. & MARTIN, M. 2011. The Role of Glycogen Synthase Kinase 3 in Regulating IFN-β–Mediated IL-10 Production. *The Journal of Immunology,* 186**,** 675-684. DOI: 10.4049/jimmunol.1001473

WANG, S., XIA, P., CHEN, Y., QU, Y., XIONG, Z., YE, B., DU, Y., TIAN, Y., YIN, Z. & XU, Z. 2017. Regulatory innate lymphoid cells control innate intestinal inflammation. *Cell,* 171**,** 201-216. e18. DOI: 10.1016/j.cell.2017.07.027

WEATHINGTON, N. M., SNAVELY, C. A., CHEN, B. B., ZHAO, J., ZHAO, Y. & MALLAMPALLI, R. K. 2014. Glycogen synthase kinase-3β stabilizes the interleukin (IL)-22 receptor from proteasomal degradation in murine lung epithelia. *Journal of Biological Chemistry,* 289**,** 17610-17619. DOI: 10.1074/jbc.M114.551747

WEBSTER, K., KIM, H., KYPARISSOUDIS, K., CORPUZ, T., PINGET, G., ULDRICH, A., BRINK, R., BELZ, G., CHO, J. & GODFREY, D. 2014. IL-17-producing NKT cells depend exclusively on IL-7 for homeostasis and survival. *Mucosal immunology,* 7**,** 1058-1067. DOI: 10.1038/mi.2013.122

WEHKAMP, J., FELLERMANN, K., HERRLINGER, K. R., BEVINS, C. L. & STANGE, E. F. 2005. Mechanisms of disease: defensins in gastrointestinal diseases. *Nature clinical practice Gastroenterology & hepatology,* 2**,** 406-415. DOI: 10.1038/ncpgasthep0265

WEISS, B., WOLK, K., GRÜNBERG, B., VOLK, H., STERRY, W., ASADULLAH, K. & SABAT, R. 2004. Cloning of murine IL-22 receptor alpha 2 and comparison with its

human counterpart. *Genes & Immunity,* 5**,** 330-336. DOI: 10.1038/sj.gene.6364104

WILSON, N. J., BONIFACE, K., CHAN, J. R., MCKENZIE, B. S., BLUMENSCHEIN, W. M., MATTSON, J. D., BASHAM, B., SMITH, K., CHEN, T. & MOREL, F. 2007. Development, cytokine profile and function of human interleukin 17–producing helper T cells. *Nature immunology,* 8**,** 950-957. DOI: 10.1038/ni1497

WOLK, K., KUNZ, S., WITTE, E., FRIEDRICH, M., ASADULLAH, K. & SABAT, R. 2004. IL-22 increases the innate immunity of tissues. *Immunity,* 21**,** 241-254. DOI: 10.1016/j.immuni.2004.07.007

WOLK, K., WITTE, E., HOFFMANN, U., DOECKE, W.-D., ENDESFELDER, S., ASADULLAH, K., STERRY, W., VOLK, H.-D., WITTIG, B. M. & SABAT, R. 2007. IL-22 induces lipopolysaccharide-binding protein in hepatocytes: a potential systemic role of IL-22 in Crohn's disease. *The Journal of Immunology,* 178**,** 5973-5981. DOI: 10.4049/jimmunol.178.9.5973

WU, J. & CHEN, Z. J. 2014. Innate immune sensing and signaling of cytosolic nucleic acids. *Annual review of immunology,* 32**,** 461-488. DOI: 10.1146/annurev-immunol-032713-120156

WU, P. W., LI, J., KODANGATTIL, S. R., LUXENBERG, D. P., BENNETT, F., MARTINO, M., COLLINS, M., DUNUSSI-JOANNOPOULOS, K., GILL, D. S. & WOLFMAN, N. M. 2008. IL-22R, IL-10R2, and IL-22BP binding sites are topologically juxtaposed on adjacent and overlapping surfaces of IL-22. *Journal of molecular biology,* 382**,** 1168-1183. DOI: 10.1016/j.jmb.2008.07.046

XIANG, X., FENG, D., HWANG, S., REN, T., WANG, X., TROJNAR, E., MATYAS, C., MO, R., SHANG, D. & HE, Y. 2020. Interleukin-22 ameliorates acute-on-chronic liver failure by reprogramming impaired regeneration pathways in mice. *Journal of hepatology,* 72**,** 736-745. DOI: 10.1016/j.jhep.2019.11.013

XU, H., FEELY, S. L., WANG, X., LIU, D. X., BORDA, J. T., DUFOUR, J., LI, W., AYE, P. P., DOXIADIS, G. G. & KHOSLA, C. 2013. Gluten-sensitive enteropathy coincides with decreased capability of intestinal T cells to secrete IL-17 and IL-22 in a macaque model for celiac disease. *Clinical Immunology,* 147**,** 40-49. DOI: 10.1016/j.clim.2013.02.012

XUE, M., ZHAO, J., YING, L., FU, F., LI, L., MA, Y., SHI, H., ZHANG, J., FENG, L. & LIU, P. 2017. IL-22 suppresses the infection of porcine enteric coronaviruses and rotavirus by activating STAT3 signal pathway. *Antiviral research,* 142**,** 68-75. DOI: 10.1016/j.antiviral.2017.03.006

YANG, S., ECKMANN, L., PANJA, A. & KAGNOFF, M. F. 1997. Differential and regulated expression of CXC, CC, and C-chemokines by human colon epithelial cells. *Gastroenterology,* 113**,** 1214-1223. DOI: 10.1053/gast.1997.v113.pm9322516

YANG, X., GAO, Y., WANG, H., ZHAO, X., GONG, X., WANG, Q. & ZHANG, X. 2014. Increased urinary interleukin 22 binding protein levels correlate with lupus nephritis activity. *The Journal of rheumatology,* 41**,** 1793-1800. DOI: 10.3899/jrheum.131292

ZENEWICZ, L. A., YANCOPOULOS, G. D., VALENZUELA, D. M., MURPHY, A. J., KAROW, M. & FLAVELL, R. A. 2007. Interleukin-22 but not interleukin-17 provides protection to hepatocytes during acute liver inflammation. *Immunity,* 27**,** 647-659. DOI:

10.1016/j.immuni.2007.07.023

ZHANG, Z., ZOU, J., SHI, Z., ZHANG, B., ETIENNE-MESMIN, L., WANG, Y., SHI, X., SHAO, F., CHASSAING, B. & GEWIRTZ, A. T. 2020. IL-22–induced cell extrusion and IL-18–induced cell death prevent and cure rotavirus infection. *Science immunology,* 5**,** eabd2876. DOI: 10.1126/sciimmunol.abd2876

ZHENG, L., KELLY, C. J. & COLGAN, S. P. 2015. Physiologic hypoxia and oxygen homeostasis in the healthy intestine. A review in the theme: cellular responses to hypoxia. *American Journal of Physiology-Cell Physiology,* 309**,** C350-C360. DOI: 10.1152/ajpcell.00207.2015

ZHENG, Y., DANILENKO, D. M., VALDEZ, P., KASMAN, I., EASTHAM-ANDERSON, J., WU, J. & OUYANG, W. 2007. Interleukin-22, a TH17 cytokine, mediates IL-23-induced dermal inflammation and acanthosis. *Nature,* 445**,** 648-651. DOI: 10.1038/nature05505

ZHENG, Y., VALDEZ, P. A., DANILENKO, D. M., HU, Y., SA, S. M., GONG, Q., ABBAS, A. R., MODRUSAN, Z., GHILARDI, N. & DE SAUVAGE, F. J. 2008. Interleukin-22 mediates early host defense against attaching and effacing bacterial pathogens. *Nature medicine,* 14**,** 282-289. DOI: 10.1038/nm1720

ZHOU, L., CHU, C., TENG, F., BESSMAN, N. J., GOC, J., SANTOSA, E. K., PUTZEL, G. G., KABATA, H., KELSEN, J. R. & BALDASSANO, R. N. 2019. Innate lymphoid cells support regulatory T cells in the intestine through interleukin-2. *Nature,* 568**,** 405-409. DOI: 10.1038/s41586-019-1082-x

ZHOU, Z., HAMMING, O. J., ANK, N., PALUDAN, S. R., NIELSEN, A. L. & HARTMANN, R. 2007. Type III interferon (IFN) induces a type I IFN-like response in a restricted subset of cells through signaling pathways involving both the Jak-STAT pathway and the mitogen-activated protein kinases. *Journal of virology,* 81**,** 7749-7758. DOI: 10.1128/JVI.02438-06

8 Personal contribution to data collection and evaluation

The small part of work in chapter 1.2 was adapted from a review paper. The review paper was partly funded by research grants from the Deutsche Forschungsgemeinschaft (DFG): project numbers 415089553 (Heisenberg program) to Steeve Boulant. I participated in draft writing and paper revision. The review paper was published in the following article: STANIFER, M. L., **GUO, C**., DOLDAN, P. & BOULANT, S. 2020. Importance of type I and III interferons at respiratory and intestinal barrier surfaces. *Frontiers in immunology,* 11**,** 3240. Publication 1

This work in chapter 3.1 was carried out as part of the SFB1129 project 14. The data was collected and analysed jointly by my co-doctoral student Dr. Kalliopi Pervolaraki. The results of the present work were published in the following article:
PERVOLARAKI, K., **GUO, C**., ALBRECHT, D., BOULANT, S. & STANIFER, M. L. 2019. Type-specific crosstalk modulates interferon signaling in intestinal epithelial cells*. Journal of Interferon & Cytokine Research,* 39**,** 650-660. Publication 2

The work in chapter 3.2 was funded by the UK Medical Research Council (https://mrc.ukri.org/) (MC_UU_12014/1) (JMcL) to Connor Bamford and China Scholarship Council (CSC) to Cuncai Guo. The data was mainly collected and analysed jointly by my colleague Dorothee Reuss. The results of the present work were published in the following article:
GUO, C., REUSS, D., COEY, J. D., SUKUMAR, S., LANG, B., MCLAUCHLAN, J., BOULANT, S., STANIFER, M. L. & BAMFORD, C. G. G. 2021. Conserved Induction of Distinct Antiviral Signalling Kinetics by Primate Interferon Lambda 4 Proteins. *Frontiers in Immunology,* 12. Publication 3

This work in chapter 3.3 was carried out as part of the SFB1129 project 14. It was also funded by Landesgraduiertenförderrung (LGF) from Heidelberg University to Cuncai Guo. The data was collected and analysed by me. The results of the present work were written in the following manuscript:
GUO, C., STANIFER, M. L., BOULANT, S. 2022. Transient synergetic effect of IL-22 and IFN-λ in human intestinal cells and organoids. Manuscript in preparation

Publication 1 is partly based on the dissertation chapter 1.2. My personal contribution to the publication extends to draft writing and paper revision.

Publication 2 is based on the results from the dissertation chapter 3.1. My personal contribution to the publication extends to performing experiments, data analysis and revision.

Publication 3 is based on the results from the dissertation chapter 3.2. My personal contribution to the publication extends to performing experiments, data analysis, part of draft writing and paper revision.

Manuscript in preparation is based on the results from the dissertation chapter 3.3. My personal contribution to the manuscript extends to performing experiments, data analysis and draft writing.

9 Personal publications

GUO, C., LIU, Y. & HUANG, Y. 2016. Inhibitory mechanism of host antiviral innate immunity by porcine epidemic diarrhea virus. *Chin J Biochem Mol Biol,* 32**,** 967-975. DOI: 10.13865/j.cnki.cibmb. 2016. 09. 01

PERVOLARAKI, K., GUO, C., ALBRECHT, D., BOULANT, S. & STANIFER, M. L. 2019. Type-Specific Crosstalk Modulates Interferon Signaling in Intestinal Epithelial Cells. *Journal of Interferon and Cytokine Research,* 39**,** 650-660. DOI: 10.1089/jir.2019.0040

STANIFER, M. L., GUO, C., DOLDAN, P. & BOULANT, S. 2020. Importance of type I and III interferons at respiratory and intestinal barrier surfaces. *Frontiers in immunology,* 11**,** 3240. DOI: 10.3389/fimmu.2020.608645

GUO, C., REUSS, D., COEY, J. D., SUKUMAR, S., LANG, B., MCLAUCHLAN, J., BOULANT, S., STANIFER, M. L. & BAMFORD, C. G. G. 2021. Conserved Induction of Distinct Antiviral Signalling Kinetics by Primate Interferon Lambda 4 Proteins. *Frontiers in Immunology,* 12. DOI:10.3389/fimmu.2021.772588

HE L, BOULANT S, STANIFER M, GUO C, NIEßEN A, CHEN M, FELIX K, BERGMANN F, STROBEL O, SCHIMMACK S., 2022. The link between menin and pleiotrophin in the tumor biology of pancreatic neuroendocrine neoplasms. Cancer Science, 00: 1-12. DOI: 10.1111/cas.15301.

METZ-ZUMARAN, C., KEE, C., DOLDAN, P., GUO, C., STANIFER, M.L. and BOULANT, S., 2022. Increased Sensitivity of SARS-CoV-2 to Type III Interferon in Human Intestinal Epithelial Cells. *Journal of Virology*, pp.e01705-21. DOI: https://doi.org/10.1128/jvi.01705-21

10 Appendix

List of Abbreviations

AhR	Aryl Hydrocarbon Receptor
aGVHD	Acute graft-versus-host diseases
AP-1	Activator protein 1
Anti-Anti	Antibiotic-Antimycotic
CK2	Casein kinase II
DC	Dendritic cell
DSS	Dextran sodium sulfate
EdU	5-ethynal-2'-deoxyuridine
EMCV	Encephalomyocarditis virus
FAE	Follicle-associated epithelia
GALTs	Gut-associated lymphoid tissues
GAS	Gamma activated sequence elements
GI	Gastrointestinal
GWAS	Genome-wide association studies
HAT	Histone acetyltransferases
HCV	Hepatitis C virus
HIE	Human intestinal enteroids
H3K9me2	Di-methylation of histone H3 at lysine 9
HIF	Hypoxia-inducible factor
HuNoV	Human norovirus
IAV	Influenza A virus
IBD	Inflammatory bowel disease
ICD	Intracellular domain
IECs	Intestinal epithelial cells
IELs	Intraepithelial lymphocytes
IFNs	Interferons
IFN-α	Interferon alpha
IFN-β	Interferon beta
IFN-ε	Interferon epsilon

IFN-κ	Interferon kappa
IFN-ω	Interferon omega
IFN-λ1	Interferon lambda 1
IFN-λ2	Interferon lambda 2
IFN-λ3	Interferon lambda 3
IFN-λ4	Interferon lambda 4
IFN-λ4-P70S	IFN-λ4 proline at position 70 to a serine
IFN-λ4- L79F	IFN-λ4 leucine to phenylalanine at position 79
IFN-γ	Interferon gamma
IFNAR	Interferon alpha receptor
IFNLR	Interferon lambda receptor
IL-1β	Interleukin-1 beta
IL-5	Interleukin-5
IL-7	Interleukin-7
IL-9	Interleukin-9
IL-10	Interleukin-10
IL-13	Interleukin-13
IL-17	Interleukin-17
IL-22	Interleukin-22
IL-22BP	Interleukin-22 binding protein
IL-23	Interleukin-23
IL-25	Interleukin-25
IL-33	Interleukin-33
ILCs	Innate lymphoid cells
ILC1s	Group 1 innate lymphoid cells
ILC2s	Group 2 innate lymphoid cells
ILC3s	Group 3 innate lymphoid cells
IRF3	Interferon regulatory transcription factor 3
IRF5	Interferon regulatory transcription factor 5
IRF7	Interferon regulatory transcription factor 7
ISG	Interferon stimulated gene
ISGF3	Interferon-stimulated gene factor 3

JAK	Janus kinases
KIR	Kinase inhibitory region
KGF	Keratinocyte growth factor
KO	Knock out
LD	Linkage disequilibrium
LGP2	Laboratory of genetics and physiology 2
LPS	Lipopolysaccharide
M cells	Microfold cells
MAPK	Mitogen-activated protein kinase
MAVS	Mitochondrial antiviral-signalling protein
MDA5	Melanoma differentiation association gene 5
miRNA-320a	microRNA 320a
MyD88	Myeloid differentiation primary response 88
NKT	Natural killer T
NF-κB	nuclear factor 'kappa-light-chain-enhancer' of activated B-cells
OLFM4	Olfactomedin 4
PAMPs	Pathogen-associated molecular patterns
PEI	Poly-ethylenimine
PHH	Primary human hepatocytes
PRR	Pattern-recognition receptors
PSA	Polysaccharide A
qRT-PCR	Quantitative real time polymerase chain reaction
REG3γ	Regenerating islet-derived protein 3γ
RLRs	Retinoic acid-inducible gene I like receptors
ROS	Reactive oxygen species
RT	Room temperature
SCFAs	Short chain-fatty acids
SDS-PAGE	Sodium dodecyl sulfate polyacrylamide gel electrophoresis
SFB	Segmented filamentous bacteria
sgRNA	Single-guide RNA

smRNAFish	Single-molecule RNA fluorescence in situ hybridization
SNP	Single nucleotide polymorphism
SOCS	suppressor of cytokine signaling proteins
STAT	Signal transducer and activator transcription
TGF	Tumor growth factor
Th2	Type 2 T helper
Th17	Type 17 T helper
TLR2	Toll-like receptor 2
TLR3	Toll-like receptor 3
TLR4	Toll-like receptor 4
TLR5	Toll-like receptor 5
TLR7	Toll-like receptor 7
TLR8	Toll-like receptor 8
TLR9	Toll-like receptor 9
TNF-α	Tumour necrosis factor-α
TRAF	TNF-receptor associated factor
Tregs	Regulatory T cells
TRIF	TIR-domain-containing adapter-inducing interferon-β
TSLP	Thymic stromal lymphopoitin
USP18	Ubiquitin carboxy-terminal hydrolase 18
VSV-luc	Vesicular stomatitis virus luciferase
WT	Wild type

Curriculum Vitae

Personal information

Name: Cuncai Guo
Gender: Male
Nationality: China
Mobile: +491731821350
E-mail: cuncaiguo@gmail.com
Address: Room 020, Im Neuenheimer Feld 344, 69120 Heidelberg

EDUCATION

- 2009.09-2013.06 Bachelor's degree in Veterinary Medicine, School of Veterinary Medicine at Huazhong Agriculture University, China
- 2013.09-2016.06 Master's degree in Molecular Immunology, School of Animal Sciences at Zhejiang University, China
- 2018.08-2022.08 PhD candidate in virology, Department of Infectious Diseases, Virology at Heidelberg University, Germany

AWARDS

- 2008-2009 Grade Achievement Award
- 2011-2012 Excellent Student Award
- 2012-2013 Excellent Graduate Award
- 2020-2021 Landesgraduiertenförderrung (LGF), Heidelberg University

RESEARCH EXPEERIENCE

- 2014.07-2016.06 Investigate inhibitory mechanisms of coronavirus nucleo-capsid proteins in the production of Type-I interferon, master project at Zhejiang University, China
- 2016.09-2017.09 Identify inhibitors for Respiratory Syncytial Virus interferon antagonistic protein NS2, visiting researcher project at University of St Andrews, Scotland
- 2018.08-2022.08 Transient synergetic effect of IL-22 and IFN-λ in human intestinal cells and organoids, PhD project at Heidelberg University Hospital, Germany

EXPERIMENTAL SKILLS

Organoid culture, 3D organoid, PCR, Cell Culture, Molecular Cloning, Western Blot, Real-time qPCR, Flow Cytometry, Confocal Laser Scanning Microscope, Animal experiment, Transfection, Tissue slice

Special thanks to my father, Chengxin Guo

Acknowledgements

This project is the outcome of a collaborative work and for this first of all I want to thank all the people who contributed with their work and ideas.

I would like to thank my supervisor and mentor Dr. Steeve Boulant for offering me an opportunity to study in his lab and for introducing me to the world of mucosal immunity. He was encouraging me by being always enthusiastic and passionate about science and fully supportive to my ideas and initiatives. Through our endless but very fruitful discussions, I have learned how to turn from a student into a scientist. Many special thanks go to my co-supervisor Dr. Megan Stanifer for her scientific, but also personal, support and advice. I am grateful to her for supporting me with all her knowledge on the project, the lab and the research world and for helping me developing my skills. Her guidance and scientific passion were very important for the fulfillment of my work. I really enjoyed the rich lab-out activities you organized.

Thanks to my TAC meeting members Dr. Alessia Ruggieri, Dr. Macro Binder and Dr. Bruno Galy for generous support in my PhD project. Your creative and critical thinking and advice made the project more solid and convincible.

I want to thank Prof. Hans-Georg Kräusslish for being my first referee for this thesis and for giving me the opportunity to present my data at his department.

I would like to thank my mom and dad, Ying Wang and Chengxin Guo, my sister Xiangxiang Guo. Thank you for your selflessness, endless love that keeps me flying higher. Thanks for giving continued love and support that helps me to be a better man.

To the Boulant family, it is awesome to spend four years with you. Dr. Markus Mukenhirn, Dr. Marta Fratini, Dr. Kalliopi Pervolaraki, Patricio Doldan, Carmon Kee, Camila Metz, Dr. Francesco Muraca, Jose Guzman, Dorothee Reuss and Dorothee Albrecht many thanks for your company and support in daily lab life. And staying with you, I really enjoyed the rich authentic life in Germany. Thanks for Dr. Beiping Miao, Dr. Xiaoying Liu, Peng Guo, Chaoyang Zhang and Qianyi Huang for your help in daily life and accompany during the

weekends and holidays. Thank Yaoling Dai, Dr. Zhaoju Deng, Wei Zhang, Jian Wang for your remote company and talking when I have pressure.

I am especially thankful to CSC and LGF for financial support and DKFZ for scientific support.

In the end, I also thank myself to insist in my dream step out from a small village in China to Europe.

EIDESSTATTLICHE VERSICHERUNG

1. Bei der eingereichten Dissertation zu dem Thema

……
handelt es sich um meine eigenständig erbrachte Leistung.

2. Ich habe nur die angegebenen Quellen und Hilfsmittel benutzt und mich keiner unzulässigen Hilfe Dritter bedient. Insbesondere habe ich wörtlich oder sinngemäß aus anderen Werken übernommene Inhalte als solche kenntlich gemacht.

3. Die Arbeit oder Teile davon habe ich bislang nicht an einer Hochschule des In- oder Auslands als Bestandteil einer Prüfungs- oder Qualifikationsleistung vorgelegt.*

4. Die Richtigkeit der vorstehenden Erklärungen bestätige ich.

5. Die Bedeutung der eidesstattlichen Versicherung und die strafrechtlichen Folgen einer unrichtigen oder unvollständigen eidesstattlichen Versicherung sind mir bekannt. Ich versichere an Eides statt, dass ich nach bestem Wissen die reine Wahrheit erklärt und nichts verschwiegen habe.

Ort und Datum Unterschrift

* Wenn dies nicht zutrifft, machen Sie folgende Angaben:
3. Die Arbeit oder Teile davon habe ich wie folgt an einer Hochschule des In- oder Auslands als Bestandteil einer Prüfungs- oder Qualifikationsleistung vorgelegt:

Titel der Arbeit:

Hochschule und Jahr:

Art der Prüfungs- oder Qualifikationsleistung: